
Black Holes
Dark Energy
Cosmic Feedback
Life Cycles of Matter

CHAPTER PAGE

CHAPTER PAGE

1. Introduction

The discovery of X-ray emitting sources beyond the solar system during the 1960s–80s gave rise to a new vibrant field of astrophysics, which was recognized by the 2002 Nobel Prize in Physics. With relatively modest space missions, the 1990s witnessed significant deepening of our understanding: an all-sky survey and excellent imaging by the U.S./German satellite Röntgensatellit (ROSAT); the discovery of rapidly variable phenomena with NASA's Rossi X-ray Timing Explorer (RXTE); and the beginnings of CCD imaging-spectroscopy with ASCA.

X-ray astronomy is now making huge strides with the Chandra and XMM-Newton missions of the 2000s. No longer restricted to a few exotic situations, we see virtually every class of celestial object, from the nearest planets to the most distant quasars. Complex diffuse structures of hot plasma, from the cosmic intergalactic medium to the most recent supernova ejecta, are studied. The phenomenon of accretion onto black holes, which may dominate the radiant energy of the Universe emitted since the Big Bang, has been identified.

But as Chandra and XMM-Newton results are being assimilated, we repeatedly encounter limits to their capabilities. Although they can localize and image structures with fluxes million of times times fainter than the brightest X-ray sources of the 1960s — producing many *astronomical* results — the limited collecting area of their high-spectral resolution systems (typically < 200 cm^2) prevents gathering sufficient photons for the spectroscopic analysis needed to understand the detailed physics of these astronomical sources. Many phenomena are transient, so longer exposures using smaller telescopes do not help.

Strong-signal, high-spectral-resolution spectroscopy has been the key to invaluable astrophysical insights throughout the past 150 years:

- The solar spectra of Fraunhofer led to the discoveries of helium and the mystery of the ionized corona. But the dominance of metal lines misled scientists about its composition of the Universe until Cecelia Payne, in her 1920 dissertation, applied quantum mechanics to show that the Sun was mainly hydrogen and helium.

- Optical astronomy was unable to penetrate the murky interstellar medium of the Milky Way, but high-resolution radio spectroscopy of the 21-cm line revealed its rotation around the hidden Galactic Center, its spiral structure, and the presence of Dark Matter.

- In more recent decades, millimeter and infrared spectroscopy have given us a detailed understanding of the molecular and solid state components of the Universe which comprise planets.

In the next decade when X-ray astronomy will leap into a deeper astrophysical understanding through high-throughput, high-spectral-resolution spectroscopy (see the recent review by Paerels & Kahn 2003). Doppler shifts from stellar flares, protostellar jets, quasar winds, and colliding galaxy clusters will tell us motions of hot gases that are inaccessible outside the X-ray band. Ratios of spectral lines will independently measure temperatures, densities and ionizations so that simplistic assumptions of local thermodynamic equilibrium and uniform structures can be replaced by realistic models of high-energy environments. Transient phenomena, such as clumps of material spiraling into the relativistic environment of spinning black holes, can finally be tracked. Spatially extended sources that are inaccessible to gratings instruments can be observed. These and many other accomplishments, can be made with NASA's planned mission, Constellation-X, which will have a large area and high-spectral resolution ($R=E/\Delta E$ of approximately 300 to 1500, see Table 1).

Constellation-X is one of the two flagship missions in NASA's Beyond Einstein program (for more details, see http://universe.nasa.gov). The three "Beyond Einstein questions" capture some of the biggest unsolved problems in astrophysics and cosmology: What happens at the edge of a black hole? What is the mysterious dark energy that is observed to be pulling the Universe apart? What powered the Big Bang? Together with the gravitational wave mission LISA, Constellation-X will address the first two of these fundamental questions. In addition, Constellation-X will allow us to understand a set of processes known as "cosmic feedback", which refers to the return, via outflows, of mechanical energy, radiation, and chemical elements from star formation and black holes to the interstellar and intergalactic medium. Feedback provides a form of self-regulation of processes of galaxy formation whereby objects on very small scales (i.e., nuclear black holes and starbursts)

Table 1

Baseline Mission Characteristics

Band Pass:	**0.25 to 40 keV**
Minimum effective area:	**1,000 cm² from 0.25 keV to 10 keV** **15,000 cm² at 1.25 keV** **6,000 cm² at 6.0 keV** **1,500 cm² from 10 keV to 40 keV**
Minimum telescope angular resolution:	**15 ″ HPD from 0.25 to 10 keV** **1 ′ HPD from 10 keV to 40 keV**
Goal Telescope Angular resolution:	**5″ from 0.25 keV to 10 keV** **30″ from 10 keV to 40 keV**
Spectral resolving power: (E/ΔE, FWHM)	**> 300 from 0.25 keV to 6.0 keV** **> 1,500 from 6.0 keV to 10 keV** **> 10 from 10 keV to 40 keV**
Fields of View:	**> 2.5 ′ (< 10 keV)** **> 8 ′ (> 10 keV)**
Mission Life:	**> 4 years (full capability)**

appear intimately connected with objects on the largest scales (i.e., galaxies and clusters of galaxies). Constellation-X is fully approved by NASA and is designated as a major priority by the Decadal Survey of the National Academy of Science, second only to JWST among large space missions.

During late 2004 the Constellation-X project asked its Facility Science Team and Science Panels, engendered by the spectacular new results of Chandra and XMM-Newton, to describe the science they consider to be the most important in the Constellation-X era. This document is condensed from the over 100 pages of text that were submitted. Please visit our website at http://constellation.gsfc.nasa.gov for the full text of the individual white papers. These teams judged the baseline mission parameters as sufficient to do breakthrough science and identified areas where modest improvements (such as angular resolution) would produce major scientific gains.

1.1 The *Constellation-X* Mission

Across the electromagnetic spectrum, larger collecting areas are needed to produce high signal-to-noise spectra at ever increasing spectral resolution. To illustrate the needs of X-ray astronomy, one may consider the "typical X-ray emitting source" that has the flux at which the vast majority of the diffuse X-ray background is resolved (for a recent review, see Brandt & Hasinger 2005). In the 0.5–2 keV band, ≈ 70–80% of the X-ray background is resolved at flux of 1×10^{-15} erg cm^{-2} s^{-1}, (incident photon flux of ~6.5×10^{-7} photons cm^{-2} s^{-1}). This X-ray flux value is taken as a target goal for a typical observation (100 ks). Requiring 1,000 counts per observation, this leads to an effective area requirement of 15,000 cm² at 1 keV (see above Table).

Figure 1 shows the collecting area of Constellation-X compared to the X-ray spectroscopic workhorses of this decade: the Chandra High Energy Transmission Gratings (HETG) and Low Energy Transmission Gratings (LETG), the XMM-Newton Reflection Grating Spec-

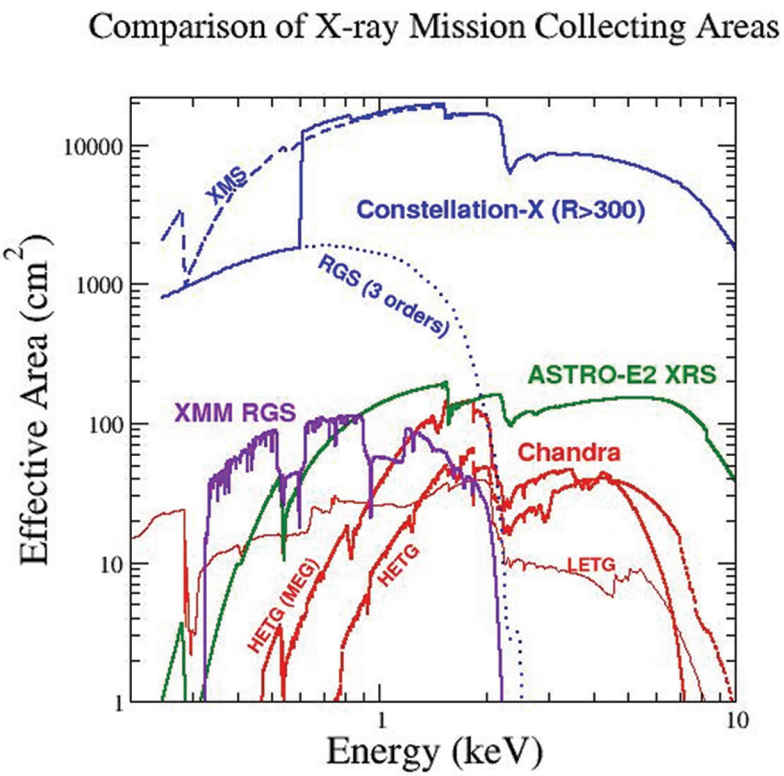

FIGURE 1. Effective area of Constellation-X in the 0.25-10 keV bandpass for both the calorimeter and gratings instruments where the resolution of either (or both) exceeds R=300. Note that the details of the X-ray Microcalorimeter Spectrometer (XMS) filter transmission below 1 keV will be strongly dependent upon the final mission configuration. The XMM and Chandra effective area curves are for the first order (both dispersion directions co-added).

trometer and the upcoming ASTRO-E2 XRS. The figure shows the total combined effective area from both XMM RGSs, and gives the first order effective area only for the LETG and HETG. Clearly Constellation-X will provide two orders of magnitude sensitivity increase over any of these high-resolution spectrometers.

The effective area shown in Figure 1 is for the two instruments operating in the 0.25–10 keV bandpass. Like Chandra and XMM-Newton, Constellation-X will have a grating spectrometer. The baseline Constellation-X gratings will have a $\Delta\lambda$ = 0.05 Å (in the first order, half-power width), and gratings are under study that will produce higher resolution values. The second component of high-resolution X-ray spectroscopy on Constellation-X is provided by an X-ray calorimeter with a nearly constant ΔE value of 2–4 eV (FWHM), reaching R=1500 in the Fe K band (see Figure 2).

What is not evident in Figure 1 is the tradeoff between collecting area, mirror figure (which affects the point-spread function; hereafter PSF), and the mass of the mirror assembly. Comparing the Chandra and XMM-Newton mirrors in terms of their effective area at 1 keV and their mass per square meter of effective area yields 18,500 kg/m^2 for Chandra and 2300 kg/m^2 for XMM-Newton. The half-power diameter (HPD) of the PSF, however, is 0.5″ for Chandra and 14″ for XMM-Newton. For the Chandra mission, great care was given to polishing the large surface area over the four mirror shells, whereas the XMM-Newton shells were mass-produced using replication, compromising mirror figure in exchange for a larger collecting area. Constellation-X has a requirement for a 15″ HPD PSF (similar to XMM-Newton) with a goal of 5″. Note that this spatial resolution goal is well-matched to a confusion limit at X-ray fluxes of a few times 10^{-16} erg cm^{-2} s^{-1}.

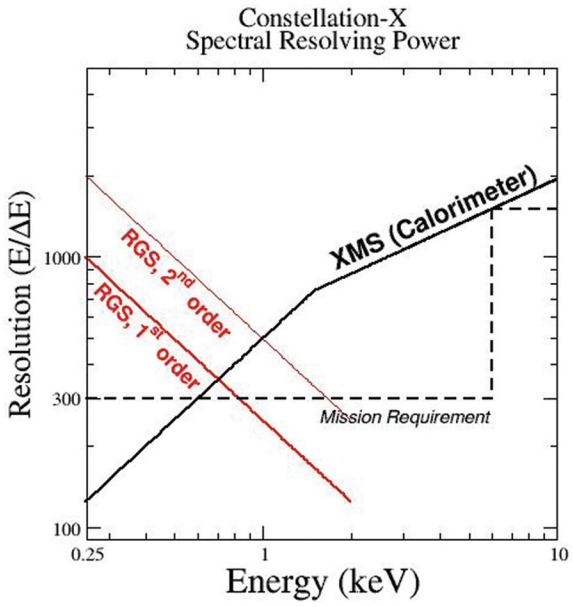

FIGURE 2. Spectral resolving power and requirements for the Constellation-X gratings and calorimeter instruments. Note that calorimeters have a fixed ΔE (presented as FWHM) so the calorimeter curve reflects the current detector requirements for the calorimeter, not the actual performance of the calorimeter (e.g., the resolution curve might be built up with different types of calorimeter pixels in different locations of the array). These curves will change as the mission design evolves. Note that the gratings have a fixed Δλ (presented as HEW).

1.2 Spectral Resolution Requirements

It is a truism that all else being equal, higher spectral resolution is always better. In optical wavebands, where large collecting areas are relatively easy to obtain, resolutions of 100,000 or higher are regularly used. Since the prime area for Constellation-X is high-spectral resolution in the X-ray bandpass, this section offers a very brief discussion of what is "high" spectral resolution at X-ray energies.

Thermal broadening in hot X-ray-emitting plasmas limits the resolution to $R \approx 410\sqrt{M/T}$ for an ion of mass M (in atomic mass units) and temperature T (in keV). This limits the "interesting" range of resolutions to a maximum of ~ 10,000; beyond this, the line profiles from hot X-ray-emitting plasmas are dominated by simple thermal broadening. Of course, absorption spectra of cool plasmas often contain complex velocity structure (see the NGC 3783 spectrum on the back cover of this booklet), and would benefit from higher resolutions, so ~ 10,000 is not a firm upper limit. Given the complexity of X-ray spectra, there is no prior reason why any particular lower resolution would be ideal for all tasks.

One way to quantify the advantages of improved resolution is by examining how it increases our ability to distinguish emission lines. The first question is: which emission lines need to be resolved? Density-dependent lines are often interesting, since their density-sensitivity is usually caused by a metastable level that can be collisionally (de)excited. As a result, the line may also be sensitive to radiative (de)excitation, or to non-equilibrium effects. Resolving the bright triplet of lines from the He-like iron provides density and temperature diagnostics, whereas additionally resolving the Li-like "q" line provides a robust ionization diagnostic. Using the Astrophysical Plasma Emission Code and Database (APEC/APED; Smith et al. 2001), spectral models were generated for a range of temperatures and densities, and then searched to find up to five bright lines (between 0.4–12.4 keV) from each ion that show at least 10% variation with density at particular temperatures. At 10^7 K, there are ~ 100 such lines; at $10^{6.5}$ K, ~ 50.

One can compare this list to *all* the lines emitted from a 10^7 K plasma, a "forest" of Fe-L lines and other transitions, and find how many would be "unblended" (see Figure 3). FWHM is used because this is a study of how well nearby lines can be separated. HEW better indicates the detectability of a weak feature against a strong continuum.

The number of resolvable lines rises almost linearly (in log space) with decreasing FWHM, except for resolution values below R ≈ 300 where only a few lines can be resolved. We have annotated Figure 3 to indicate resolution values at which particular diagnostics become available.

1.3 Mission Status

The Constellation-X mission plans to use four identical spacecraft launched two at a time with Atlas V or Delta IV launch vehicles. Each spacecraft has a 1.6m-diameter Spectroscopy X-ray Telescope (SXT) with a 10-m focal length, and Hard X-ray Telescope to extend the bandpass to 40 keV. Each of the SXT (0.25–10 keV)

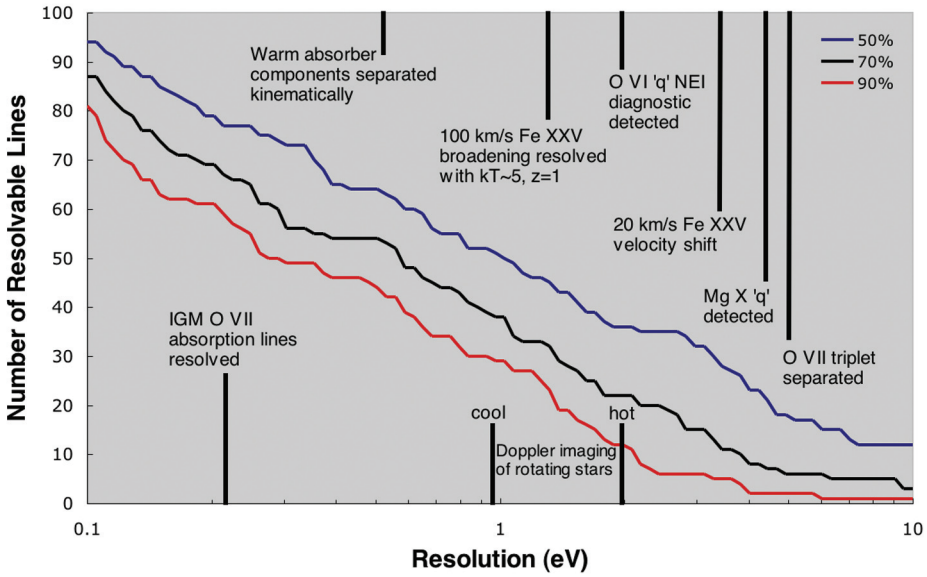

Figure 3: Number of "interesting" lines that can be resolved, as a function of resolution (E/ΔE, FWHM). The black line shows the number of lines if a purity of 70% is required; the red and blue lines bracket this with 50% at the top and 90% at the bottom. This figure and simulations were provided by Randall Smith.

mirror assemblies will have a mass of 675 kg (note that this translates to < 450 kg per m^2 of effective area at 1 keV). The mirrors will be Wolter-type nested, grazing-incidence X-ray mirrors, which will be manufactured using replication techniques.

The Constellation-X technology development effort has been aimed at large-area calorimeters and large area reflection gratings. In order to meet the 15″ HPD requirement the individual reflectors must have ~10″ HPD. This has recently been achieved on a subset of the reflectors. Future efforts will be directed at studying the mirror alignment system, and improving the figure in order to drive towards the goal of 5" HPD. Single-pixel X-ray calorimeters have now exceeded the Constellation-X goal of <4eV energy resolution at 6keV.

While the gratings can meet the required R=300 resolution, a substantial effort is underway to study alternate configurations that may allow very high resolution at low energies (R > 1000). The Hard X-ray Telescope (operating at 10–40 keV) system has benefited from a substantial balloon program pushing the energy range up to 60 keV, and a development effort is under way to extend this to larger-area detectors.

Alternate mission configurations are also under study, including one large, monolithic X-ray mirror with a 25 to 50m focal length. Such alternate configurations are feasible due to the newly anticipated availability of the Delta IV Heavy launch vehicle, which has higher lift capacity than the Atlas V.

2. Black Hole Science

2.1 Black Hole Accretion and Strong Gravity

While the predictions of General Relativity (GR) have been verified in the weak-field limit, it has not been possible to perform the necessary quantitative experiments in the strong-field regime. This is a fundamental physics problem as GR is not a unique solution for the physics of gravity: Until gravity can be studied experimentally in all of its applicable parameter space, alternatives cannot be eliminated.

Ever since the detection of rapid X-ray variability more than 20 years ago, it has been clear that X-ray observations of accreting black holes provide a window on the immediate vicinity of the black hole event horizon. In the Chandra/XMM-Newton era (the first decade of the 21st century), X-ray studies of black holes have been refined to the point where we finally have well-understood, quantitative probes of strong gravity and the inner, most highly energetic regions of their accretion flows. *The innermost regions of accretion disks require X-ray studies, since the last signal we receive from accreted matter is predominatnly emitted at X-ray wavelengths.*

The most powerful technique for inner accretion disk studies to date is the study of the broad iron fluorescence line seen in the X-ray spectrum of many accreting black holes (Tanaka et al. 1995; Reynolds & Nowak 2003). This line is emitted by the surface layers of the thin, Keplerian accretion disks believed to extend nearly down to the event horizon, and possesses a highly broadened and skewed energy profile sculpted by the effects of relativistic Doppler shifts and gravitational redshifts (see the Fe K line profile inset in Figure 1).

Iron line spectroscopy with Chandra and XMM-Newton has enabled dramatic progress in understanding black hole systems, and robust examples of extremely broadened iron lines have been found in both stellar-mass and supermassive black hole systems. The highest quality X-ray data of some systems reveal extreme gravitational redshifts indicative of rapidly rotating black holes (Fabian et al. 2002; Miller et al. 2004). In addition, the time variable, quasi-periodic substructure seen in iron lines of some systems is likely to be a first glimpse of orbiting non-axisymmetric features in the inner accretion disk (Iwasawa et al. 2004).

Despite the progress of recent years, we are hampered by the fact that several different models (e.g., with different black hole spin parameters) can fit the same line profile (Dovciak, Karas & Yaqoob 2004). Since the line profiles we can study are temporally averaged over at least a few orbital periods of the innermost disk, they do not contain sufficient information to uniquely constrain both the space-time geometry and the accretion disk physics.

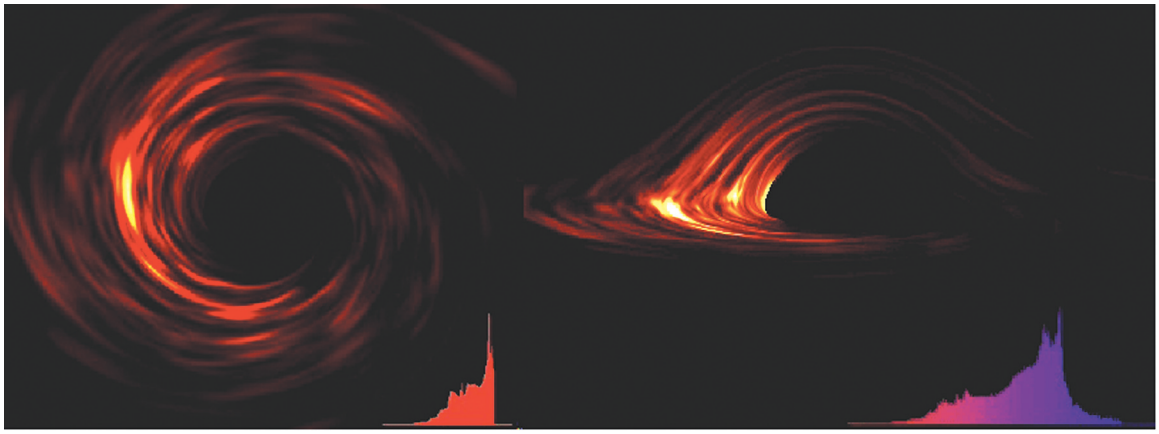

Figure 1: X-ray view of an accretion disk (Armitage & Reynolds 2003). View of the disk as seen by a distant observer at an inclination angle of 30° (left) and 80° (right). The inset in each panel shows the corresponding Iron K-shell spectral line profile that will be observed by Constellation-X.

By sweeping away these limitations, Constellation-X will trigger a major qualitative leap in our understanding of strong gravity and accretion physics. Constellation-X, with its extremely high effective area and spectral resolution, will measure iron line profiles of the brightest AGN in a fraction of an orbit, allowing us to track individual orbiting substructures within the disk. We can determine the line profile over the light-crossing time of the system for the more massive AGN systems, which will allow us to search for reverberation effects of dramatic X-ray flares across the disk surface. Such direct probing of the propagation of the X-ray signal provides a fundamental constraint on the nature of space-time around the black hole (Young & Reynolds 2000).

The space-time metric in the strong gravity regime can be qualitatively mapped using the constraints noted above. A similarly fundamental investigation of black hole spin will also be carried out. Theory predicts that accretion of matter onto a black hole causes it to spin up (up to a maximum angular momentum), spinning space-time along with it. A major goal of the Constellation-X mission is to observe and quantitatively measure these effects, in particular to measure the black-hole spin with sufficient precision to rule out competing theories and investigate the relation between the spin and the properties of the black hole system (for example, the relationship between the spin of a black hole and the existence of the relativistic jets).

Iron line studies by Constellation-X of the brightest AGN will allow us to calibrate time-averaged line profiles for measuring black hole spin. Further Constellation-X observations can then be used to measure the spin of any accreting black hole displaying this spectral feature, down to very faint flux levels. *The result will be an explosion of knowledge about the distribution and demographics of black hole spin, which is crucial if we are to understand the origin and evolution of black holes of all masses.*

In addition to exploring space-time geometry and black hole spin, Constellation-X observations of the innermost regions of black hole accretion flow will probe the behavior of matter as it undergoes its final plunge into the black hole's event horizon and will investigate the possibility that the spin energy of the black hole is energizing the inner accretion disk and/or a relativistic jet (Blandford & Znajek 1977).

From a General Relativity perspective, black holes have only two parameters: mass and angular momentum (significant charge cannot be sustained in a realistic astrophysical environment). While we cannot yet measure either of these with the precision that we can now measure cosmological parameters, *the two Beyond Einstein Great Observatories, LISA and Constellation-X, will allow precision measurements of the two crucial black hole parameters (mass and angular momentum) in complementary ways.* LISA will provide exquisite precision for a number of very special systems (stellar-mass black holes spiraling into 10^6 $M_\odot$ black holes and mergers of supermassive black holes with masses $< 10^7$ $M_\odot$). Constellation-X will measure mass and spin for a large number of accreting black holes, from stellar-mass systems to the multi billion-solar-mass black holes at the centers of giant elliptical galaxies. In addition, Constellation-X will further our understanding of how matter accretes onto a black-hole – a process which provides a huge, if not dominant, component of the radiant energy of the observable Universe (e.g., Brandt & Hasinger 2005).

2.1.1 Observatory Specifications

The strong gravity and inner accretion-disk physics presented here do not require large fields of view, and the 15" HPD baseline angular resolution requirement is more than sufficient. The main science driving parameters are collecting area and spectral resolution, which are all met by the current Constellation-X requirements.

Simulations suggest that relativistic iron line reverberation can be detected and studied in the brightest nearby Seyfert 1's by the baseline design for Constellation-X (0.6 m^2 at 6 keV). Both the mass and the signature of high (vs low) spin can be derived from time dependent variations of the iron line as measured with this baseline area. The simulations necessarily assume a source geometry, and unfortunate geometries could hamper determination of the mass and spin. However, recent work with XMM-Newton is indicating a geometry rather conducive to reverberation mapping (Miniutti, Fabian & Miller 2004). If the geometries are complex, or in order to do the full-up relativistic reverberation analysis of the type outlined in Young and Reynolds (2000) on a larger number of sources, a large effective area would be helpful.

2.2 Studies of Black Holes with Masses ~1-1,000 $M_\odot$

In addition to enabling new studies of supermassive black holes, Constellation-X will have unique capabilities for studying the stellar-mass black holes residing in binary systems in our own Milky Way and nearby galaxies. These objects become X-ray bright when matter is transferred to a black hole from its binary companion. A number of unique features make these black holes key sources for probing Einstein's theory of General Relativity. These objects are the nearest X-ray bright black holes that Constellation-X can study and are also the black holes about which we already know the most (McClintock & Remillard 2004). Many of these systems have been extensively observed at optical and other wavelengths, and their masses have been measured with good precision using the methods of dynamical astronomy. With precise mass measurements it becomes easier to constrain the other parameter that describes a black hole's structure, its spin. Perhaps most important, these are the only black holes for which X-ray spectroscopic and timing signatures of matter moving in the curved space-time near the event horizon have been detected. Constellation-X will be the first X-ray observatory with the capability to study both of these strong gravity signatures simultaneously.

Recent X-ray observations have shown that stellar-mass black holes are similar to their supermassive cousins in that they also show broad, relativistic iron K-shell emission lines (Miller et al. 2002, in 't Zand et al. 2002, Miniutti, Fabian & Miller 2004; Miller et al. 2004). The line profiles can be very similar to those seen from the supermassive black holes, indicating that, as in the Seyfert AGNs, they are likely produced in the innermost accretion flow near the black hole. Because these objects are bright, Constellation-X will be able to measure their relativistic line profiles with exquisite precision. Comparisons between lines detected in a number of stellar-mass black holes and Seyfert AGN will test the relative importance of mass accretion versus black hole formation in driving spin.

Observations of some of these same black hole binaries with NASA's Rossi X-ray Timing Explorer (RXTE) resulted in the discovery of high frequency quasi-periodic intensity oscillations (QPOs) with frequencies as high as 450 Hz (Remillard et al. 1999; Strohmayer 2001). These QPOs are the highest frequency flux variations seen from any black holes, and have frequencies characteristic of the orbital timescale near the event horizon. Four of these objects show a pair of QPOs with frequencies in a 3:2 ratio, which could be direct evidence of a resonance phenomenon associated with General Relativistic effects near the black hole (Abramowicz & Kluzniak 2001; Remillard et al. 2002). Interestingly, very recent work on the Galactic microquasar GRS 1915+105 using RXTE suggests that the strength of the broad iron K-shell line and the phase of maximum intensity of a lower frequency (1 – 2 Hz) QPO are correlated (Miller & Homan 2005). This suggests that simultaneous X-ray spectroscopy and fast timing measurements can provide new diagnostics of the space-time in the immediate vicinity of these black holes, particularly if Constellation-X can find a direct link between properties of the relativistic iron K-shell line and the high-frequency QPOs.

The presence of two different diagnostics provides determination of both the radial location of the X-ray emitting matter and its orbital frequency. If, for example, the black hole mass is known from optical observations, and the spin can be constrained using the observed relativistic line profile, then measurements of QPO frequencies could be used to test whether the orbital frequency at that radius is in agreement with the value predicted by General Relativity. Although such inferences require an understanding of the QPO production mechanism and this problem may not be fully solved by the time of the Constellation-X launch, the new data provided by Constellation-X will, at a minimum, greatly increase our understanding of how both the relativistic lines and QPOs are generated, and thus bring us closer to the goal of using them as fundamental probes of strong gravity.

Constellation-X may be able to crack one of the most intriguing mysteries confronting astronomers presently. The puzzle concerns the nature of a class of luminous, variable, point-like X-ray sources found in many nearby galaxies. Their observed variability confirms that they are compact objects, but they can have inferred isotropic luminosities hundreds of times larger than the expected maximum luminosity of a stellar mass black hole. This has led to speculation that these ultraluminous X-ray sources (ULX) may form a new class of black holes with masses in the range from about 100–2000 solar masses, so called intermediate-mass black holes (IMBH, Colbert & Mushotzky 1999).

Figure 2 shows a plot of X-ray luminosity versus implied accretion disk temperature for sources in the Milky Way, large Magellanic Cloud and nearby galaxies. Their location is consistent with that expected for ~1000 solar mass black holes with standard accretion disks in which the luminosity scales directly with the mass and the temperature scales inversely with the mass (Miller, Fabian, & Miller 2004).

Because these IMBH candidates are in external galaxies, it has not yet been possible to determine their masses with the same methods used to weigh Galactic black holes. Alternative models not requiring excessive masses have also been proposed, generally requiring that the observed X-ray emission is beamed (King et al. 2001). *It is imperative that astronomers clearly establish the existence or absence of intermediate-mass black holes: a population of intermediate-mass black holes may have profoundly affected early galaxy evolution (Madau & Rees 2001), and/or may affect the evolution of stellar clusters within galaxies (Miller & Hamilton 2002, Portegies-Zwart et al. 2004).*

Constellation-X will improve our understanding of these enigmatic objects in many ways. Constellation-X will spectroscopically confirm the presence of cool accretion disks in IMBH candidates, and perhaps more important, will detect relativistic iron K-shell emission lines if they are present. Detection of these lines would confirm the disk origin of the soft X-ray emission, and would strongly rule out beaming arguments for the high inferred luminosities. Measurement of relativistic line profiles would also provide information on the spins of these black holes. Indeed, if Constellation-X confirms the existence of IMBHs, then X-ray probes of General Relativity will be possible across an enormous range of black hole masses.

X-ray timing measurements can identify the characteristic timescales on which the objects are variable. By comparing studies of supermassive black holes with those of stellar mass black holes in our Galaxy, it has been shown that the characteristic variability times scale with black hole mass (Markowitz et al. 2003). The characteristic timescales may be evident either as breaks or QPOs in the power density spectrum. Indeed, recent work using XMM-Newton has led to the first detection of characteristic timescales in ULXs (Strohmayer & Mushotzky 2003; Cropper et al. 2004). The most compelling mass limits would come from sources for which more than one timing signature can be measured in the power spectrum. Exciting possibilities are that both a break in the power-law slope and a single QPO are detected, or that two (or more) QPOs are detected with or without a break. Indeed, if the pairs of 3:2 frequency ratio QPOs seen in Galactic systems are also present in truly more massive ULXs, then they would be expected to appear in the 1–10 Hz band (Abramowicz et al. 2004), and if found would convincingly establish at least some ULXs as IMBHs. Only Constellation-X will have the large collecting area necessary to obtain high-quality power spectra to search for such signatures.

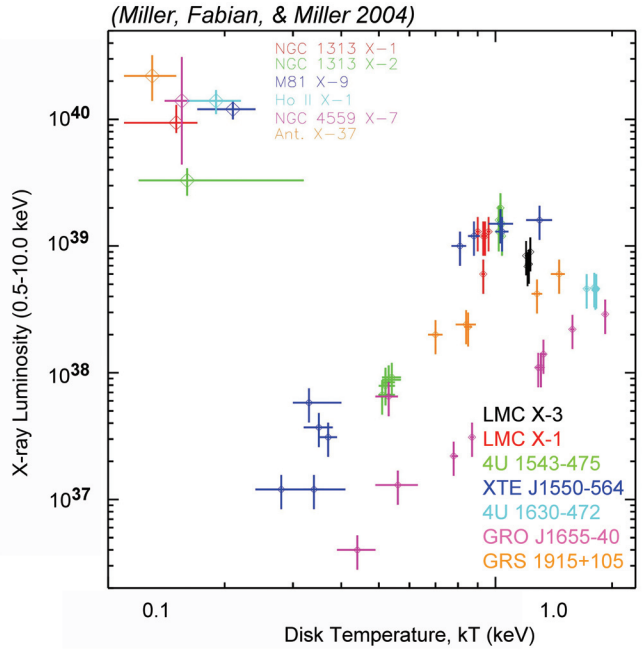

Figure 2: Black hole X-ray luminosity versus implied accretion disk temperature, for a number of stellar-mass black holes in the Milky Way and Large Magellanic Cloud, and a number of the brightest ultraluminous X-ray sources in nearby galaxies. The sources in the upper left hand corner are IMBH candidates. Constellation-X will make definitive spectroscopic and timing measurements to strongly confirm or reject the existence of intermediate-mass black holes.

2.2.1 Observatory Specifications

The spectral resolution requirements at 6.0 keV for stellar and IMBH studies are nearly identical to those for supermassive black holes described in Section 2.1. The large collecting area of Constellation-X will be critical for constraining the possible nature of the IMBH-candidates in external galaxies. The X-ray fluxes of the IMBH candidates in Figure 3 are typically in the range 10^{-12}–10^{-13} erg cm^{-2} s^{-1} so that with 6000 cm^2 of collecting area at 6 keV, Constellation-X should observe 1,000 counts at Fe-K in about 5–10 ks.

As described, one of the observatory requirements unique to this science is fast timing capability. The studies in this section require 400 microseconds (goal 200 microseconds) timing accuracy, which will easily be met by the baseline mission.

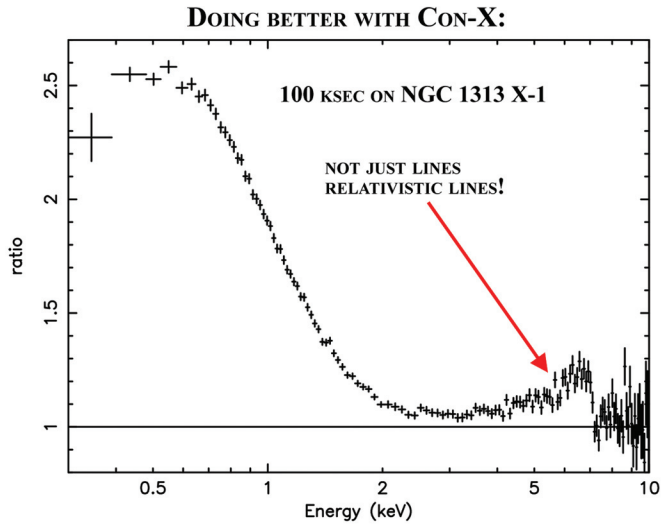

Figure 3: The plot above shows a simulated Constellation X spectrum of the intermediate-mass black hole candidate NGC 1313 X-1, plotted as a ratio to a simple power-law model. A 100 ksec exposure with Constellation-X will clearly reveal the cool accretion disk component glimpsed with XMM-Newton (Miller et al. 2003).

2.3 A Low-Luminosity Active Galactic Nucleus at the Center of the Milky Way

The Galactic Center harbors the nearest low-luminosity, accreting supermassive black hole. Surprisingly, the 2.6×10^6 $M_\odot$ black hole Sgr A* has an X-ray luminosity of only $L_x = 9 \times 10^{33}$ erg s^{-1} (0.5-8.0 keV), which is only 10^{-11} of the Eddington value. In fact, Sgr A* is the most under-luminous black hole yet identified; even quiescent black hole low-mass X-ray binaries produce $L_X \sim 10^{-8}$ L_{Edd}. This makes it the premier astrophysical target for understanding the physics of accretion at low rates.

The accretion that does occur is unstable. Chandra and XMM observations have revealed that Sgr A* flares by a factor of ten in X-rays for about an hour once a day (Baganoff et al. 2001). This time scale is tantalizingly close to the orbital period of the innermost stable orbit around Sgr A*. The nature of these flares is uncertain. They are accompanied by hour-long flares in the infrared (Eckart et al. 2004), and may be related to variability on hour time scales at millimeter wavelengths (Mauerhan et al. 2005) and the optical flares recently discovered from low-luminosity AGN in several distant galaxies (Totani et al. 2005). Constellation-X observations of Sgr A* will provide the signal required to study the spectra and time variability of these flares in great detail.

In order to achieve its current mass, Sgr A* must have accreted at higher rates in the past. Several features observed at X-ray wavelengths may be evidence of recent active phases from Sgr A*, including an arcminute-scale pair of lobes of X-ray emitting plasma centered on Sgr A* (Baganoff et al. 2003), a degree-scale radio and X-ray lobe above the Galactic plane that resembles a small version of the bubbles blown in the ISM by starburst activity (Bland-Hawthorn & Cohen 2003), and iron fluorescence nebulae associated with molecular clouds located within of Sgr A* (Murakami et al. 2001). Constellation-X will have the combination of spectral resolution to determine the emission mechanisms producing these features and the angular resolution (at it's goal of 5″) to separate these features from the other interesting X-ray objects in this crowded region.

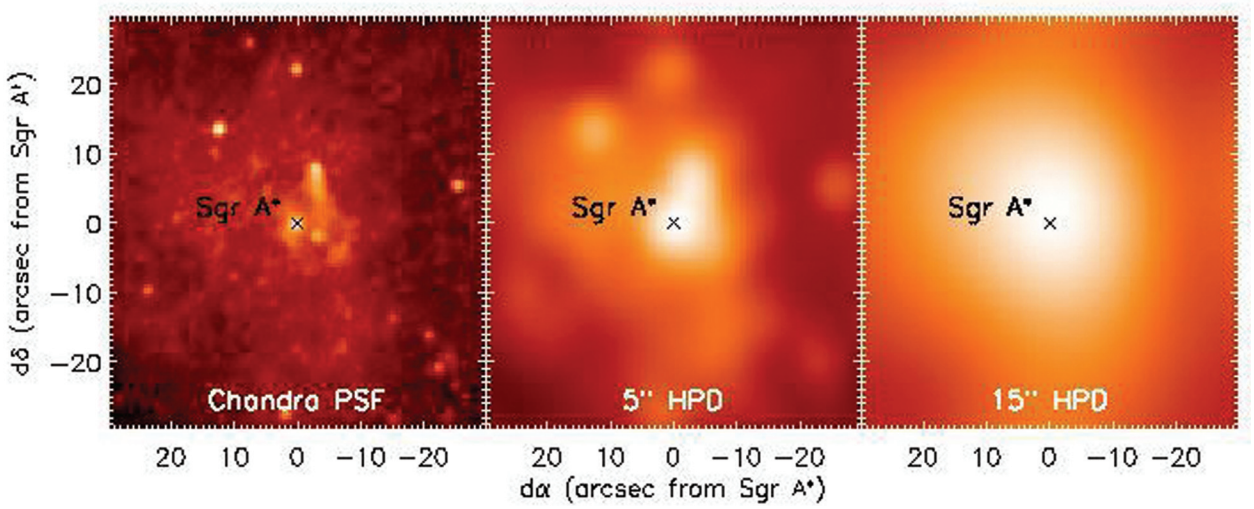

Figure 4: Chandra images of the central 2.5 × 2.5 pc around Sgr A*. We display the field assuming Gaussian PSFs with three different half-power diameters (HPDs): 0.5" to match the Chandra PSF, 5" to match the target resolution of Constellation-X, and 15" to match the minimum required performance of Constellation-X. We note that if the PSF has a sharp non-Gaussian core (like that for XMM-Newton, which has HPD=14" but FWHM=6"), then the middle image corresponds to the minimum required 15" HPD. Constellation-X will detect flares similar to those seen by Chandra even at its minimum required resolution, and its large effective area will allow detailed spectral and timing analysis.

3. Dark Energy, Dark Matter and Cosmology

3.1 Cosmology with Clusters and Groups of Galaxies

Recent studies of the baryonic mass fraction in clusters of galaxies, the evolution of clusters of galaxies, type Ia supernovae (SN), and the microwave background have revealed a "preposterous Universe" (Carroll 2005) in which ~70% of the energy density of the Universe today is in the form of "Dark Energy", 26% is in the form of Dark Matter, and the rest is the sum of normal matter and neutrinos. Strikingly, the observed value of the Dark Energy density today is many orders of magnitude smaller than the most natural values predicted by the standard model of particle physics.

These startling results have produced a revolution in cosmology and prompted the development of new cosmological models. *Understanding cosmic acceleration and the nature of Dark Energy is one of the most important goals in physics and astronomy today, and it is vital that these results be checked by a variety of precise cosmological tests over a wide range of astrophysical objects with small statistical and systematic errors. In the near term, there are several (non-X-ray) programs to study Dark Energy including cosmic microwave background (CMB) data, ground and HST-based SN studies, gravitational lensing studies, and studies of large-scale structure.*

One can define the equation of state of dark energy in terms of w, where w is the ratio of pressure to density. In combination, these multiwavelength data sets will place constraints on constant equation-of-state dark energy models at the level of σ_w~0.1–0.15. Each of these techniques has its own limits and systematic errors. For example, one of the major systematic uncertainties of the SN-based studies (see also Section 5.2 on SN Ia) is the unknown evolution of the standard candles with redshift. Other systematic concerns include the nature and subtraction of the host galaxy light and the effects of gravitational lensing. For an individual supernova event at z~1, the difference in SN Ia optical magnitude between a closed universe model and a ΛCDM model is only 0.25 mag. Thus, extreme care and precision are required in the analysis and interpretation of the SN Ia data.

In large-scale galaxy cluster surveys the difference between a closed model and a ΛCDM model is an order of magnitude (a much larger "signal" than SN Ia measurements, in the number of clusters above a fixed mass as a function of redshift). For this method, the major systematic uncertainty lies in connecting the observable, such as X-ray luminosity or optical number counts, to cluster masses. These surveys allow self-calibration of the data by taking advantage of redundant cosmological information in the spatial clustering of the sources and the evolution of the mass function with redshift (observed as a luminosity function). At the core, this technique relies on reliable and direct mass measurements, which are possible with the high resolution, high signal-to-noise spectroscopy of Constellation-X.

Two other longer-term projects to study Dark Energy—the Large Synoptic Survey Telescope (LSST) and the Joint Dark Energy Mission (JDEM) are complementary to Constellation-X. The LSST mission will focus on measuring cosmic shear and producing samples of 10^5 SN distances to z~0.8. One possible incarnation of JDEM will measure the distances to ~3,000 SN to z~1.7 and map cosmic shear over a small portion of the sky. These missions will be carried out on timescales similar to Constellation-X. Both claim to deliver constraints on the Dark Energy equation-of-state parameter at the level of a few percent, similar to that achievable with Constellation-X.

Constellation-X will be able to perform two independent sets of cosmological tests using X-ray measurements of clusters of galaxies. The first set of tests is measuring the absolute distances to clusters via direct and indirect means, thereby determining the transformation between redshift and true distance, d(z), which is a strong function of cosmological parameters. The second set of tests is measuring the growth of structure by using Constellation-X measurements together with theoretically informed models for how the baryon population changes with redshift. The number of and mass distribution of massive systems (clusters and groups of galaxies) is a very strong function of the cosmological parameters. The Constellation-X results will be limited only by systematics.

3.1.1 Dark Energy Constraints from Absolute Cluster Distances

It is now clear that relaxed, simple clusters of galaxies can be used as "standard candles" (Allen et al 2004) for relative distances using the observationally-verified prediction that the baryonic fraction of the cluster mass, in rich clusters, is independent of redshift. X-ray observations are crucial since ~90% of all the baryons are in the hot X-ray-emitting gas. The transformation from the observed X-ray temperature and surface brightness to gas mass depends on the absolute distance of the cluster, so its measure as a function of the constant baryonic mass fraction over redshift gives strong constraints on the amount and evolution of dark energy. With its large collecting area, Constellation-X will be able to observe the large samples (> 500 objects) over a wide redshift range (to z ~ 1) with the high precision required to use this distance determination method. Simulations show that Constellation-X data alone can obtain uncertainties on w to ±0.05 and, in combination with the microwave background data, constraints on w and its evolution that are substantially smaller.

To utilize this technique, Constellation-X must reach scales in the cluster where gravity is dominant, and have sufficient angular resolution to recognize merging clusters and separate out the complex physics in the centers of clusters. The first requirement results in the need for a large sample of objects and a big enough field of view so that clusters can be observed out to a significant fraction of the virial radius. A large sample of objects (~500) can be observed if the collecting area is large enough. The current collecting area projected for Constellation-X will allow measurements of accurate temperature profiles for massive clusters out to z~1 in a reasonable exposure (~25 ks).

The Sunyaev-Zeldovich (S-Z) effect provides another, independent method of obtaining absolute cluster distances. While this method has a long history, it is only with the advent of new microwave background detectors and the XMM-Newton and Chandra observatories that the first accurate results are being obtained. Currently, the method is limited by systematic errors to 15% uncertainty in distance. Constellation-X spectroscopic data and new S-Z measurements are expected to reduce this error significantly and produce precise distances. Distances with a precision of ~5% from joint X-ray and S-Z analysis would lead to measurements

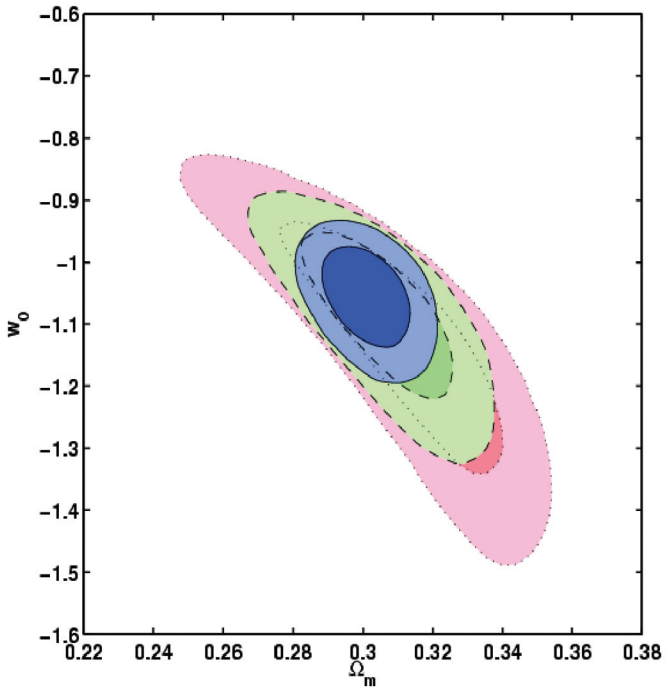

Figure 1:Anticipated Constellation-X constraints from cluster baryonic fraction measurements. The purple contours represent the 68 and 90% confidence errors on the cosmological parameters w and Ω_M if Constellation-X obtains 5% errors on f(gas) and assuming present uncertaintites in the Hubble constant and baryonic fraction of the Universe. The green and blue represent the 68 and 90% uncertainties if the errors on fgas can be reduced further by extending baryonic fraction measurements to a virial radius (R_{500}) and assuming some modest improvement in the errors on the priors for the universal baryonic fraction and the Hubble constant (anticipated by the time of the Constellation-X launch).

of cosmological parameters (Molnar et al 2004; Fox & Pen 2002) at a level of accuracy competitive with other techniques.

Another, very different technique for measuring cluster distances relies on X-ray resonance absorption against either background sources or the cluster itself compared to the cluster emission (Krolik & Raymond 1988; Sarazin 1989; David 2000). This method requires high-resolution spectroscopy at moderate spatial resolution, which is only possible with Constellation-X. Sarazin (1989) showed that there are over 1000 clusters whose distance can be determined by Constellation-X using this technique, allowing a large number of further, totally independent distances to be determined.

3.1.2 Constraining the Growth of Cosmic Structure via the Cluster Mass Function

Clusters of galaxies are the most massive systems in the Universe and are, therefore, very sensitive probes of the rate at which cosmic structure evolves. If one can measure the mass spectrum of clusters accurately at several well-separated redshifts, one can derive the growth parameter, G(z), that is the ratio of the amplitude of fluctuations at the same mass scale as a function of cosmic time. To obtain a measurement of **w** as a function of z using this technique requires a relatively small sample (~100 objects) but very high precision in the mass (~4%). This test requires the accurate Constellation-X mass measurements of clusters achievable only with calorimeter spectral resolution and can obtain limits on ω at the level of ±0.05.

While several ground-and space-based programs will get data before Constellation-X and claim high precision, Constellation-X is crucial to obtaining an accurate and reliable understanding of Dark Energy and cosmology due to the different physics, different parameter degeneracies, and different systematics. Constellation-X data will obtain the only other (besides SN Ia) direct measurements of the acceleration of the Universe and will sharpen and amplify cosmological constraints from current and upcoming X-ray and S-Z cluster surveys. Constellation-X constraints on cosmological parameters will have comparable accuracy to other tests (similar to SN Ia techniques) and a tight control of systematics. In some sense the Constellation-X studies of the physics of groups and galaxy clusters will provide these extraordinary cosmological constraints for free, if we target carefully selected cluster samples (which will exist by the time of the mission).

3.1.3 The Entropy Problem in Groups

The seminal work of White and Frenk (1991) showed that Cold Dark Matter models with hydrodynamics do not reproduce observations. Among the many observational problems is that of the excess entropy in groups. (Springel 2004). As pointed out by many authors, solutions to this problem require "feedback"- the injection of momentum, energy and/or heat into the gas, which serves to counteract the effects of over-cooling.

This "feedback" term has two currently known potential sources: star formation and active galaxies. While it seems clear that the effects of star formation will be visible as "galactic winds" (see figure 2), heating and ionizing the IGM as well as injecting metals, the effects of AGN energy injection are not so theoretically clear. However, almost all theoretical calculations seem to indicate that the energy from young stars and SN is not sufficient to provide the observed amount of feedback. As opposed to the multitude of techniques used to derive cosmological parameters, only X-ray astronomy can obtain the data needed to determine the forces that controlled the formation of clusters and galaxies.

Constellation-X can directly observe the injection of this "extra heat" into groups to z~1 by directly measuring the entropy of the gas as well as its dynamical state. Constellation-X observations will be able to directly measure the energy put out by AGN winds, quantifying the momentum and energy in the winds using high-resolution X-ray spectra of AGN.

In order to measure the spatially dependent gas turbulence and velocity structure necessary to constrain the amount and nature of the feedback in groups Constellation-X will need a spectral resolution adequate to measure velocities of 300 km/sec (corresponding to the ~1 keV/particle "extra" energy needed in the models) with sufficient spatial resolution to map the velocity

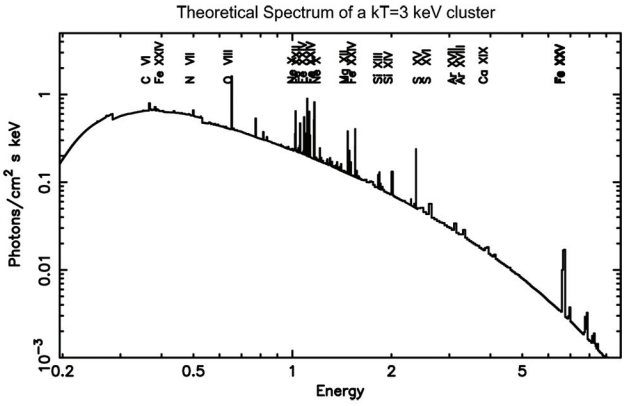

Figure 2: Theoretical spectrum of an isothermal plasma with kT ~ 3 keV, with many of the strong transitions labeled; however, many of the transitions from the same ion (e.g., multiple lines from Fe XXIV) have been suppressed. Note the strong lines from all the abundant elements. The data are plotted in the usual way for X-ray astronomers, photons cm^{-2} s^{-1} keV^{-1} vs. energy in keV, which emphasizes the dynamic range of X-ray spectroscopy.

field at z~0.5. This is equivalent to 2 eV resolution at ~ 0.38 keV (OVII at z ~ 0.5, assuming kT = 1 keV). Sufficient throughput is needed to obtain quality spectra in relatively short exposure times (< 100 ks).

3.1.4 Dark Matter

All dark energy measurements require an accurate knowledge of the dark matter distribution. The use of the baryonic mass fraction to derive the total mass of dark matter only works in the most massive systems where the "interesting physics" going on within clusters does not dominate the X-ray emission. To constrain dark matter in lower-mass systems and to decouple it from all the other physical processes going on in clusters, one requires high-spectral-resolution imaging detectors to constrain all the physics in these spatially extended systems.

Most of the baryons in groups and clusters of galaxies lie in the hot X-ray emitting gas ~ 2-100 × 10^6 K (velocity dispersions of 180–1200 km s^{-1}, which is in virial equilibrium with the dark matter potential well the ratio of gas to stellar mass is 2–10, Ettori & Fabian 1999). This gas is enriched in heavy elements (Mushotzky et al. 1978) and is thus the reservoir of stellar evolution in these systems (see Section 3.2 on abundances).

Since most of the baryons are in the gaseous phase and clusters are dark matter dominated, the detailed physics of cooling and star formation are less important than in galaxies. This makes clusters much more amenable to simulations. Detailed measurements of their density and temperature profiles (which requires high-spectral resolution) allow an accurate determination of the dark matter profile and total mass. While gravity is clearly dominant in massive systems, much of the entropy of the gas in low-mass systems may be produced by non-gravitational processes.

As discussed in detail by Evrard (2004), we now have a good understanding of the formation of the dark matter structure for clusters of galaxies. If gravity has completely controlled the formation of structure, the gas should be in hydrostatic equilibrium with the vast majority of the pressure due to gas pressure. If this is true, the density and temperature structure provide a detailed measurement of the dark matter distribution in the cluster. Recent theoretical work has also taken into account other important process such as cooling and turbulence. The fundamental form of the Navarro, Frenk, & White (1997; hereafter NFW) dark matter potential results in a prediction, both from analytic (Komatsu & Seljak 2001) and numerical modeling (Loken et al. 2002), that the cluster gas should have a declining temperature profile at a sufficiently large distance from the center (in units of R/R_{virial}). The size of the temperature drop in the outer regions is predicted to be roughly a factor of 2 by $R/R_{virial} \sim 0.5$, which is consistent with the ASCA results of Markevitch (1998). However, there is considerable controversy about this analysis. While XMM-Newton in principle should resolve this controversy, its high and variable background has so far precluded definititive results. Constellation-X will need to have an overall background significantly lower than previous X-ray missions in order to constrain dark matter profiles of clusters at the important length scales.

Recent numerical work seems to validate the NFW potential, and much has been made of the fact that low-mass and low-surface brightness galaxies do not seem to follow this form in their central regions. Recent Chandra and XMM-Newton observations (Allen et al. 2002; Arabadjis et al. 2002; Pratt & Arnaud 2002) have been able to determine extremely accurate mass profiles via spatially resolved X-ray spectroscopy and the assumption of hydrostatic equilibrium. Perhaps the best documented of these examples are the Chandra data for Abell 2029 (Lewis, Buote & Stocke 2003), in which the profile is determined over a factor of 100 in length scale, from 0.001–0.1 characteristic lengths of the NFW profile, with essentially no deviation from the NFW prediction. This striking result is also seen in other Chandra results in the cores of clusters. The data show that the central regions of clusters tend to have rather steep density profiles in the innermost radii, indicating that whatever causes the deviation of the form of the potential in dwarf galaxies does not occur in clusters. This results strongly constrains interacting dark matter models (e.g. Voit & Bryan 2001; Bautz & Arabadjis 2004).

3.1.5 Observatory Specifications

Because of the need for precise mass and baryonic fraction measurements for these cosmological tests, one must determine the cluster and group temperatures, densities and dynamical state (e.g. mass motion and turbulence) for a reasonable sample of objects to high accuracy. These precision measurements require

high spectral resolution (<4 eV over the 0.5–10 keV bandpass), in particular to obtain the electron and ion temperatures as well as the gas dynamics. In addition, high spectral resolution is required to measure the origin of the 'excess' entropy in groups and the direct effects of feedback on the cluster and group x-ray - emitting gas. A minimum field of view of 2.5′ on a side is highly desirable to obtain cluster mass profiles out to a significant fraction of the virial radius. However, we believe that this is a bare minimum, because at z~0.3 the virial radius of a massive cluster is approximately 5.3′, and thus a larger field of view is highly desirable especially to allow sufficient solid angle to determine local background. Spatial resolution of 10″ or better is required to effectively remove point-source emission and to derive the morphology of high-redshift clusters so that mergers can be recognized.

Chandra and XMM-Newton are unable to detect cluster X-ray emission to the virial radius because their particle backgrounds are too high. Once the cluster surface brightness falls below the particle background, the exposure time required to detect the cluster emission rises very rapidly. Putting a precise limit on the Constellation-X particle background is difficult, as the equivalent surface brightness of the particle background depends on the telescope focal length and effective area. Both Chandra and XMM-Newton have specific particle backgrounds of approximately 10^{-2} counts s^{-1} keV^{-1} cm^{-2} at 1 keV. An initial estimate indicates that if Constellation-X reaches values of 4 x 10^{-3} counts s^{-1} keV^{-1} cm^{-2} at 1 keV, then surface photometry to the virial radius will become straightforward for luminous clusters at moderate redshifts (z~0.3), but may still be challenging for more typical (less massive) systems at z~1.

3.2 Measurements of Cluster Abundances

A crucial constraint on the formation of structure is the determination of where and when the metals were created. While the latest optical and X-ray data on massive clusters indicate that most of the massive galaxies were in place and already old at z ~1, and that the Fe abundance at z~1 is similar to that at lower redshifts (Tozzi et al 2003), we have no direct knowledge of the oxygen abundance, which is crucial to determining the Type II SN contribution to the metallicity. We also have no knowledge of how the abundance in groups, the average place in the Universe, evolves. Only Constellation-X can give us this information.

Unlike galaxies, clusters apparently retain all the enriched material created in them. Being essentially closed boxes, they provide an unbiased record of nucleosynthesis in the Universe. *Thus, measurement of the elemental abundances in clusters and their evolution provide fundamental data about the origin of the elements.* The distribution of the elements in clusters also reveals how the metals were removed from stellar systems into the intergalactic medium (IGM see section 3.4).

While many of the emission lines from Fe, Mg, and Ne are blended with CCD resolution they are easily resolved with the 4 eV Constellation-X spectral resolution as are the He-like triplets of all the abundant elements (see Section 1.3). The combination of high spectral resolution and high collecting area will allow definitive measurements out to z~1 for O,Si and Fe over a wide mass range allowing a true measure of the metal formation in the universe.

Recent XMM, Chandra and ASCA analysis (Baumgartner et al 2004; Jones et al 2004; Ettori et al 2004) have improved our understanding of the elemental composition of the cluster gas and its evolution with redshift. While there appears to be a narrow range of cluster Fe abundances at low redshift, the ratios of Fe/Si/S/Ni are not consistent with simple supernova nucleosynthesis models nor with the abundances seen in the only two other samples of old material: the damped Lyman-alpha galaxies and the metal-poor halo stars in the Milky Way galaxy. Further, there is a variation of Fe/O by a factor of two from cluster to cluster with no simple relationship with cluster mass (e.g., Peterson et al 2003). No simple model of the superposition of Type I and Type II SN can explain these data (Finoguenov et al 2003), severely testing our understanding of metal formation in the universe and the nature of supernova metal enrichment.

XMM and Chandra have allowed the measurement of Fe abundances out to z~1.2 (Hashimoto et al 2004; Tozzi et al 2003), showing that there has been little evolution in the Fe abundance over the last nine billion years. Combined with the lack of star formation in massive galaxies in clusters at these redshifts (e.g. Rosati et al 2004), this shows that most of the Fe in clusters is produced at z>2, requiring a truly enormous star-formation rate at very early times. However, the

XMM and Chandra results are limited to the most luminous clusters at z>0.6, and it is not clear how representative these results are. To more fully comprehend the implication of these new data requires extension to lower-mass systems, a wider redshift range, and the measurement of elements other than Fe in order to understand these recent startling results. Constellation-X has the collecting area, angular resolution and sensitivity to probe the creation of the elements to early times.

While the recent results on cluster chemical abundances are exciting, they do not represent the bulk of the material in the Universe. Most of the cosmic baryons lie in groups of galaxies and to date we have little or no information on how their chemical abundance has evolved. Also because most of these systems have kT~1 keV, many of the emission lines are not resolved in CCD data, leading to a wide range in published abundances for the gas (e.g., Buote et al 2003). If we are to truly understand the evolution of most of the material in the Universe we must expand high-resolution X-ray spectroscopy to the groups allowing robust chemical abundance determinations out to z>0.3 for a wide range of elements. Since groups are much less luminous than clusters, it will require the large collecting area of Constellation-X to obtain a large sample at moderate to high redshift. The launch of Astro-E2 in 2005 will allow the first detailed spectrum of these objects and pave the way for the Constellation-X observations.

3.3 From Cooling Flows to "Cool Cores" in Massive Galaxy Clusters

Clusters of galaxies have very deep potential wells with virial velocities equivalent to temperatures of 10^7-10^8 K. Gravitationally driven processes like accretion shocks and adiabatic compression should therefore heat gas accumulating within a cluster to X-ray-emitting temperatures. Spectroscopic X-ray observations show that most of a cluster's gas is indeed near the virial temperature $T_{vir} = 7.1 \times 10^7 \sigma_{1000}^2$ K or 6.2 σ_{1000}^2 keV, where σ_{1000} is the line-of-sight velocity dispersion in units of 1,000 km s^{-1} (Sarazin 1986).

In roughly 30% of all clusters we find a significant fraction of the baryons at a temperature significantly less than the virial temperature (see Donahue & Voit 2004 for a recent review). This gas would be considered quite hot in other astrophysical context, but in order to to be cooler than the virial temperature today it must have avoided the gravitational heating experienced by the rest of the cluster or it must have significantly cooled after entering the cluster.

Because this gas is dense enough to radiate an energy equivalent to its thermal energy in less than a Hubble time, astronomers have long speculated that it cools and contracts, forming a "cooling flow" of condensing gas in the cluster core (e.g., Fabian & Nulsen 1977). All the stars in a cluster's galaxies are made of such gas, implying that at least some cooling and condensation must have occurred during the assembly of the cluster.

The primary question concerning cool gas in clusters is whether these pieces – cool X-ray gas, stars, nebulae, molecular clouds – all fit together into a single coherent picture of condensation and star formation. If so, then studies of cluster cores may have much to teach us about the processes that govern galaxy formation. *What we have learned in the Chandra and XMM-Newton era is that simple cluster cooling flows do not occur (Molendi & Pizzolato 2001; Peterson et al. 2001, 2003).* High-resolution spectroscopic observations with XMM-Newton and Chandra are now revealing a deficit of emission from gas below T_{vir} / 3, which is not predicted by cooling flow models (see Figure 3).

Observations from the present generation of X-ray telescopes have challenged the simple cooling flow hypothesis, but what will take its place? Star formation, radio jets, and conduction may all have important roles to play in the development of cluster cores. Looking for hallmarks of episodic feedback, from both AGNs and supernovae, may be more fruitful, at least in the short term.

If feedback is episodic, then the state of the central intracluster medium should be closely related to other goings-on in the cluster core. Thus, it would be interesting to test whether the T_{vir}/3 scaling of the minimum plasma temperature apparent in the early sample of XMM-Newton clusters from Peterson et al. (2003) holds for a large sample of cool core clusters with various levels of core activity. For Constellation-X this means taking the ambitious high-spectral resolution observations of Peterson et al. (2003) using the XMM RGS to a much larger sample (requiring much larger

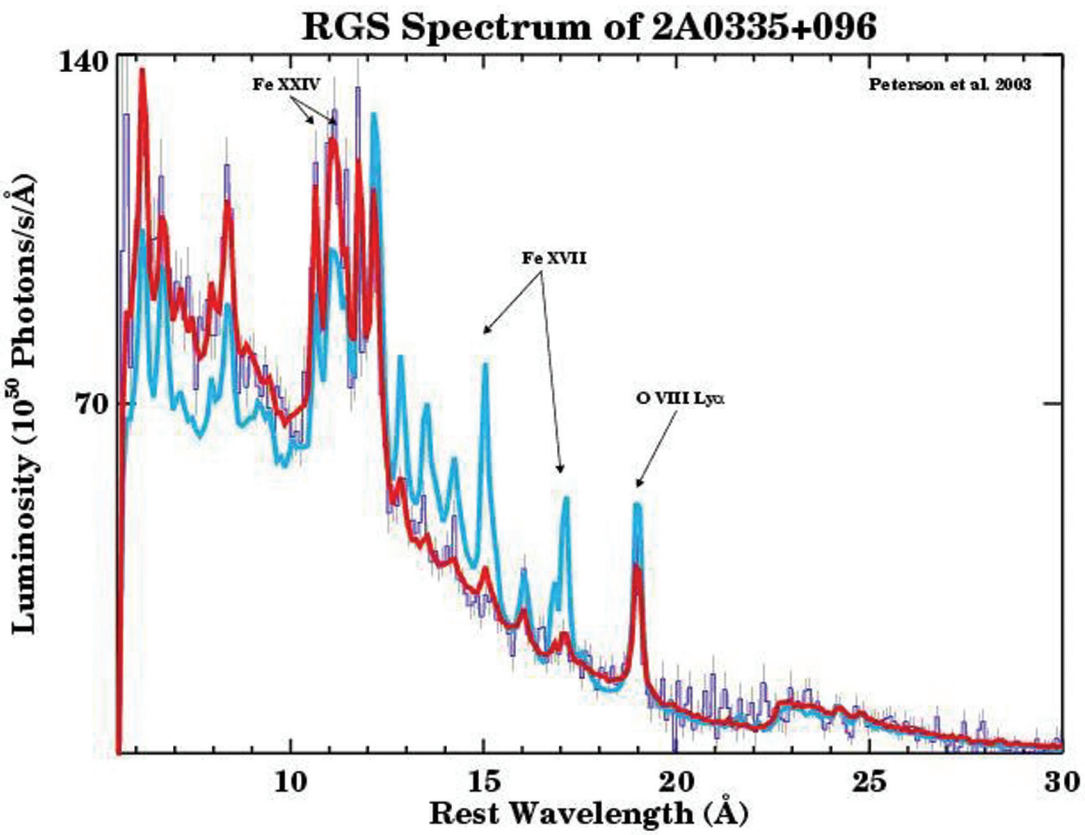

Figure 3: XMM-Newton RGS data for X-ray bright cluster 2A0335+096. The OVIII Lyα and Lyβ lines were detected, but no Fe XVII is apparent at the expected wavelengths of 15.014 Å or 16.78 Å. (Data courtesy J. Peterson; Peterson et al. 2003.)

mirror-collecting area). We will answer the questions of: How do the X-ray emission-line spectra of clusters with radio-loud nuclei differ from those of clusters with radio-quiet nuclei? Are there any correlations between X-ray line emission and the presence of obvious star formation or emission-line nebulae? Episodic heating also leads to a predictable pattern in the evolution of the core entropy distribution (Kaiser & Binney 2003). Thus, studying the core entropy distributions of a large sample of clusters may reveal a telltale pattern of entropy evolution with time.

3.4 The Warm Hot Intergalactic Medium (WHIM)

As mentioned at the beginning of this chapter, 96% of the energy density of the Universe is in dark energy and dark matter. Of the 4% of what remains, the "normal matter" or baryons, a significant fraction still remains to be accounted. This is a major astronomical puzzle: the location of the "missing baryons". At high redshift, much of this matter resides in the intergalactic medium (IGM; see Figure 4). Does intergalactic space provide a similar gaseous reservoir at low redshift ($z < 0.5$)?

Theoretical simulations (e.g., Cen & Ostriker 1999; Davè et al. 2001) of large-scale structure suggest that the IGM is a hierarchically structured, filamentary network (the commonly called "cosmic web", see Figure 4), shaped by processes of gravitational collapse, shock-heating from galactic outflows (see section 4.2), and photoionization by luminous AGN. The cosmic web therefore provides a rare opportunity to observe cosmological processes at work: gravitational instability of dark matter; baryonic infall and shocks; and radiative, mechanical, and chemical feedback from galaxy formation.

Detecting and measuring the cosmic web requires high-throughput spectrographs aboard both X-ray and ultraviolet telescopes. The warm phase (10^4 K) of the IGM has been detected by the Hubble Lyman-α survey (Penton, Shull, & Stocke 2004). Approximately 30% (+/- 4%) of the baryons reside in this photoionized

gas, and another 5–10% are in collapsed halos. This leaves 40–50% unaccounted for, perhaps residing in the theoretically predicted gas at $T > 10^6$ K. These hot baryons are only detectable in X-ray absorption from high ions of trace heavy elements.

With Chandra and XMM-Newton, X-ray astronomers have now found the first hints of this hot gas in the vicinity of the Milky Way galaxy and Local Group through $z = 0$ absorption lines in the spectra of background AGN (see Figure 5; Nicastro et al. 2002; Fang et al. 2003; McKernan et al. 2004). Good tracers of million-degree Galactic halo gas are the X-ray resonance lines of O VII (21.6019 Å) and O VIII (18.9689 Å), with additional nucleosynthetic information available in other lines such as N VI (28.787 Å), N VII (24.782 Å), Ne IX (13.337 Å), and C VI (33.736 Å).

Even more exciting cosmologically are the redshifted absorption lines from the WHIM – the Warm-Hot Intergalactic Medium. The first claimed detections of million-degree WHIM came from Chandra observations of two low-redshift O VII absorbers ($z = 0.011$ and $z = 0.027$) (Nicastro et al. 2005 a,b) toward Mrk 421. These detections are consistent with a large reservoir of WHIM at ~10^6 K.

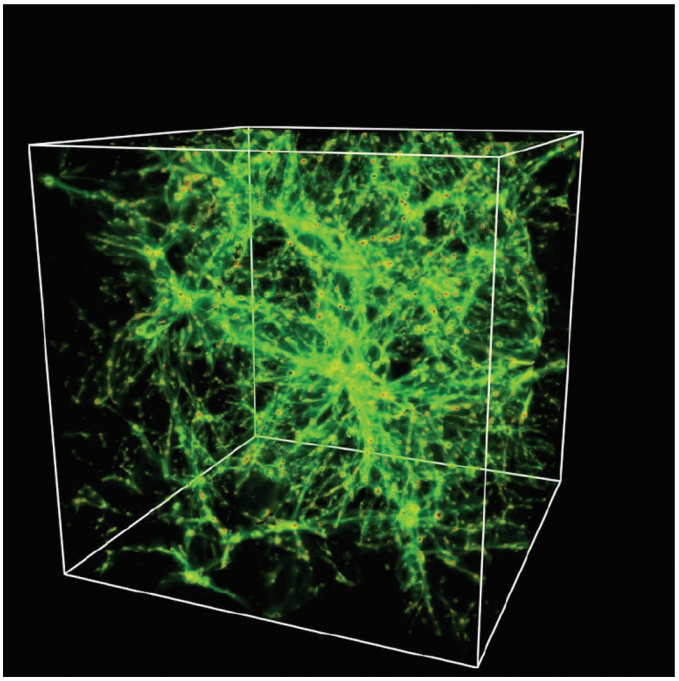

Figure 4: A simulated image of the filamentary netwrok of the WHIM by Cen & Ostriker (1999). It is commonly referred to as "the Cosmic Web".

The Constellation-X spectrographs will need to have much better spectroscopic throughput (collecting area, A_{eff}) and resolution ($R = E/\Delta E$; ΔE is FWHM) than the Chandra/LETG over the bandpass 0.3 - 1.0 keV. A critical tradeoff is between R and A_{eff} to maximize the number of AGN sightlines that can be surveyed down to critical column density limits in O VII and other ions (see Figure 5).

Constellation-X should be ideally suited to making a major improvement in X-ray absorption-line spectroscopy of the hot IGM and galactic halos. This improved capability will come from increased throughput (to at least 2,000 cm^2) and from better spectral resolution (R=600-1,200). Such capabilities would revolutionize X-ray IGM science, and could provide access to several observable AGN targets behind galaxy halos. It would allow astronomers to probe ~100 AGN sightlines in a census of "missing baryons" in the warm-hot IGM using X-ray absorption lines of O VII, O VIII, N VI, N VII, C VI, Ne IX, etc. (Nicastro et al. 2005a,b).

Several considerations suggest that a high-throughput X-ray spectrograph with the goal resolution of Constellation-X of R = 3,000 would provide a substantial increase in WHIM detectability. At the typical (1–2 mCrab) quiescent X-ray fluxes of low-z AGN, a 100 ksec exposure (with $A_{eff} = 2{,}000$ cm^2 and R = 1,500) will produce between 200-400 counts per 200 km/s resolution element at E = 500 eV. The brightest (X-ray flaring) AGN would yield very good spectra, and the WHIM surveys could be pushed to somewhat higher redshifts for the rare, brightest sources.

The goal Constellation-X spectral resolution of R=3,000 will also *resolve* the WHIM lines. The expected O VII and O VIII thermal line widths are $\Delta v = (53.5 \text{ km/s})(T_6)^{1/2}$ (FWHM) at temperatures of (10^6 K) T_6. Resolving thermal widths would therefore require $R = 5{,}600\ (T_6)^{-1/2}$. However, the lines are also broadened by IGM shock dynamics and shear flows. Comparative UV/X-ray absorption studies of H I, O VI, and O VIII using FUSE, HST, and Chandra (Fang et al. 2002; Shull et al. 2003) demonstrate that one needs resolution of 100–200 km/s (R = 1,500-3,000) to identify and separate kinematically the IGM absorbers and relate them to the nearest galaxies at distances of 0.2–1 Mpc. Such velocity resolution would also allow one to identify the absorbers with possible galaxy halos and infalling baryonic matter in small groups. These observations can also address

issues of chemical feedback and the extent of heavy-element transport from galaxy outflows into the IGM.

Thus, one can justify resolutions ranging from R = 1,500 for IGM absorber-galaxy kinematics up to R = 3,000 for line profile studies. These capabilities would allow Constellation-X spectra to be tied to the current state of moderate-resolution UV spectra (HST, FUSE) of H I, O VI, C III, C IV, and other metal ions. Constellation-X will be a powerful tool for studies of the missing baryons and large-scale structure in the hot, shocked IGM.

At even higher redshifts ($z > 0.5$), cosmological simulations predict a significant diminution in the baryon fraction of million-degree (WHIM) plasma, owing to a reduced rate of shock heating from gravitational structure formation (Davè et al. 2001). The slow chemical evolution of the IGM may also play a role; the high-z IGM is expected to have lower metallicities due to galaxy outflows and tidal stripping (Gnedin & Ostriker 1997).

Using the predicted strongest WHIM absorption features and the 40 Å cutoff, Constellation-X should be able to measure absorbers out to redshifts $z = 0.61$ (N VII), $z = 0.85$ (O VII), $z = 1.10$ (O VIII), and $z = 2.0$ (Ne IX) as long as a few X-ray bright AGN can be found. While the brightest AGN at $z = 0.1$-1.0 have quiescent soft X-ray fluxes of 1–2 mCrab (2×10^{-11} erg cm^{-2} s^{-1} at 0.5-2 keV), other AGN are fainter; a ROSAT survey of Sloan quasars (Shen et al. 2005) found 0.5-2.0 keV AGN fluxes ranging from 2×10^{-13} to 2×10^{-12} erg cm^{-2} s^{-1}, with a few at 10^{-11} . The Chandra WHIM detection (Nicastro et al. 2005 a,b) Mrk 421 came during a 10^{-9} erg cm^{-2} s^{-1} flare.

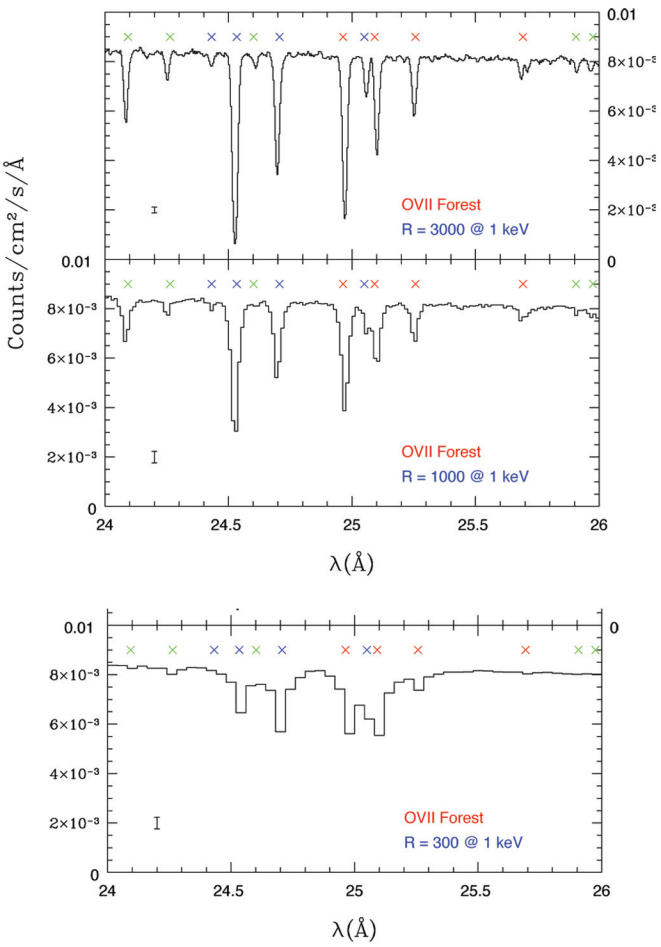

Figure 5: Simulated Constellation-X spectra of the WHIM (provided by Fabrizio Nicastro): This simulation is based on the density prediction for the OVII WHIM in the local Universe (z ~ 0) from Fang et al. 2002, including 48 OVII WHIM systems from z=0 to z=1. For the background source, a z=1 quasar, with a 0.5-2 keV (absorbed) flux of half-mCrab (10^{-11} erg cm^{-2} s^{-1}) was assumed. The spectral model consist of a simple power law with a photon spectral index of Gamma=1.8 (in energy), absorbed by a neutral column of Galactic hydrogen of 1.5×10^{20} cm^{-2}. All simulations have an exposure time of 100 ks.

4. Cosmic Feedback, The Growth of Structure

4.1 The Growth of Supermassive Black Holes at Early Times

Our understanding of the growth and evolution of massive black holes has undergone a revolution over the last few years. It now seems likely that the development of black holes and galaxies are intimately connected, possibly due to accretion-related outflows that regulate star formation (e.g., Silk & Rees 1998; King & Pounds 2003). This growth appears to undergo a curious evolutionary trend whereby black holes are built-up via accretion with the most massive black holes forming first, a process often referred to as cosmic downsizing (e.g., Cowie et al. 2003; Marconi et al. 2004). The number density of these accreting massive black holes [i.e., Active Galactic Nuclei (AGN)] changes dramatically over the history of the Universe; however, there is no clear observational evidence that AGNs of a given luminosity undergo substantial changes in their underlying accretion processes (e.g., Vignali, Brandt & Schneider 2003). Furthermore, it is apparent that a large (likely luminosity-dependent) fraction of AGNs are obscured at optical wavelengths but are detectable at hard X-ray energies (e.g., Mainieri et al. 2002; Ueda et al. 2003; Barger et al. 2005). These obscured sources are suspected to be the dominant AGN population in the Universe (outnumbering unobscured AGNs by factors of 3–10) and contribute the bulk of the cosmic X-ray background (CXRB) radiation.

With its high-resolution (R = 500–1,000) X-ray spectrometers, 100 times the collecting area of Chandra and XMM-Newton at 0.25–10 keV, and crucial sensitivity at hard (10–40 keV) X-ray energies, Constellation-X will probe the growth of black holes in the high-redshift Universe with unprecedented precision; see Figure 1.

Constellation-X will study $z \approx 1$ AGNs with the detail only currently possible for the ~10 brightest local AGN (such as NGC 5548); luminous $z > 6$ quasars will be more accessible to Constellation-X at high spectral resolution than $z \approx 1$ quasars are to Chandra and XMM-Newton at much lower spectral resolution. Coupled with current and future radio through hard X-ray data, these observations will provide comprehensive probes of the physics of accretion around high-redshift massive black holes. The large-scale AGN outflows (in absorption and emission) that likely regulate star formation in massive galaxies will be studied in detail, providing estimates of mass and energy outflow rates and chemical enrichment/heating of the IGM. The energetics and demographics of high-redshift obscured AGNs will be quantified and many luminous Compton-thick AGNs will be revealed with Constellation-X's high-energy sensitivity out to 40 keV.

Our basic picture of an AGN is an accretion disk funneling material into a supermassive black hole. AGNs emit X-rays as a result of Compton upscattering of ultraviolet photons from the accretion disk as they pass through a bath of high energy electrons in the accretion disk corona. This X-ray emission provides a unique window on the environment closest to the accreting black hole (to $R_g \approx 1.2$) which is inaccessible at other wavelengths. Constellation-X will provide X-ray spectroscopy of AGNs down to 0.5–8 keV flux levels of $\approx 10^{-15}$ erg s^{-1} cm^{-2} permitting constraints on the continuum shape, absorption, recombination emission, fluorescent iron K line emission, Compton reflection, and variability of accreting black holes out to and beyond $z = 6$; see Figures 1 and 2. At high redshift this emission gets shifted to lower observed energies, providing measurements at energies that may otherwise be inaccessible for studies of local AGNs.

Our understanding of the X-ray emission from high-redshift AGNs has advanced rapidly since the launches of Chandra and XMM-Newton and the advent of wide-field optical surveys (see Brandt et al. 2005 for a review); for example, the number of X-ray detections at $z > 4$ has increased from 6 in 2000 to ≈ 100 in the year 2005. No significant changes in the X-ray emission properties of AGNs at high and low redshift have yet been found, suggesting that the accretion disk environment of AGNs are insensitive to the dramatic evolution on larger scales that occurred over the last 12 billion years of cosmic history (e.g., Vignali, Brandt, & Schneider 2003; Strateva et al. 2005). However, our current Chandra and XMM-Newton detections of high-z AGNs are just that – detections. As a result of comparatively poor photon statistics we do not have sufficient data to study their detailed properties; existing studies have generally been restricted to broad comparisons of their spectral energy distributions (SEDs). Constellation-X will allow astronomers to take these analyses one

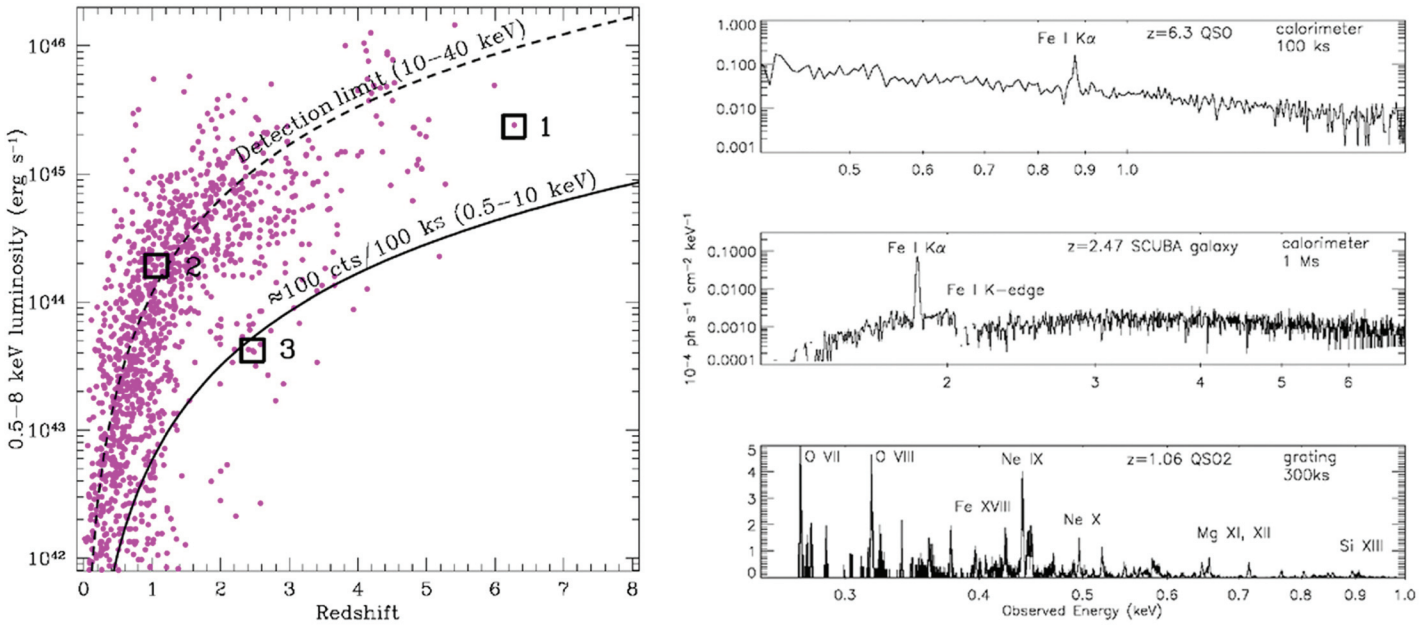

Figure 1 Left: X-ray luminosity versus redshift for some potential Constellation-X targets. The compiled sources are a heterogeneous combination of different samples in the literature, including wide and deep Chandra blank-field observations and X-ray targeted AGNs. The sources above the solid line can be studied by Constellation-X in the 0.5–10 keV band in < 100 ks exposures. The sources above the dashed line can be detected by Constellation-X in the 10–40 keV band. An X-ray spectral slope of Γ=2.0 was assumed when converting from the 0.5–8.0 keV band to the Constellation-X bands. Right: Simulated spectra demonstrating the capabilities of Constellation-X for the three highlighted sources (1) a z = 6.3 quasar, (2) a z = 2.47 Compton-thick AGN in a submillimeter-bright star-forming galaxy, and (3) a z = 1.06 obscured quasar. Interesting spectral features are highlighted.

step further, permitting comparisons of X-ray spectral features and emission regions and therefore providing direct astrophysical insight into the evolution of the environment around accreting massive black holes; see Figure 1.

Relativistically broadened iron Kα emission provides information on the physical conditions in the immediate vicinity of the black hole (see Chapter 2). A number of local AGNs have shown relativistic iron Kα emission, permitting measurements of the black hole spin and environment of the inner accretion disk (e.g., Reynolds & Nowak 2003). By comparison, luminous high-redshift AGN do not typically show these features (the weakness of iron Kα in luminous sources is known as the "X-ray Baldwin effect"); however, the stacked X-ray spectra of X-ray faint high-redshift AGN appear to show the signature of relativistically broadened iron Kα emission on average (Streblyanska et al. 2005). Constellation-X has the sensitivity to identify and study iron Kα emission lines in individual high-redshift AGN, providing insight into the conditions necessary to produce iron Kα emission and its evolution with redshift.

Beyond the iron Kα emission line and the reflection component (which peaks at 20–30 keV) the hard X-ray spectra of AGN are dominated by the Compton upscattered component. Since there are currently no reliable measures of the high-energy Compton cutoff in quasars, the sensitive 10–40 keV hard energy coverage of Constellation-X will provide new insights into our understanding of the state (via the cut-off temperature) and structure of the X-ray emitting accretion-disk coronae (e.g., Sobolewska, Siemiginowska, & Zycki 2004; Zdziarski & Gierlinski 2004). For high-redshift quasars where we can probe rest-frame energies of ~100–300 keV (and perhaps as high as 600 keV), we can expect to see the high-energy cutoff (50–200 keV) in some cases, thus allowing a determination of the electron temperature and optical depth of the Comptonizing plasma. This information is key to our understanding of the geometry of the corona, and, in turn, to the modeling of the accretion disk and disk-wind emission.

These studies of the central engine of high-redshift AGNs benefit significantly from Constellation-X's hard energy coverage, which for the highest-redshift quasars currently known will probe rest frame energies higher than 240 keV. However, the background must be lower than the expected 10–40 keV fluxes of typical $z \approx 4$ quasars of $\approx 10^{-14}$–10^{-15} erg $s^{-1}cm^{-2}$. Response at low energies is also important as crucial spectral features move with redshift; for example, iron Kα is observed at ≈ 1 keV at $z \approx 5$ and the presence of moderate absorption (i.e., $N_H \approx 2 \times 10^{22}$ cm^{-2}) becomes increasingly difficult to identify at high redshift without good low-energy response.

4.1.1 Accretion-disk Outflows and their Role in Galaxy Evolution

The study of AGNs has undergone a paradigm shift in recent years with considerable emphasis being placed on accretion-related outflows (e.g., Murray et al. 1995; Proga, Stone, & Kallman 2000). Over cosmic time a significant fraction of the energy from massive black hole accretion could be converted into kinetic energy by large-scale outflows, affecting the host galaxy by triggering star formation [e.g., shocking and compressing the interstellar medium (ISM)], or perhaps even shutting it down (e.g., clearing gas from the host; Fabian 1999). Indeed, current large scale-structure simulations require the presence of AGN "feedback" to regulate the growth of massive galaxies (e.g., De Lucia et al. 2004; Di Matteo et al. 2005). These high-velocity winds and jets are also an efficient means of distributing high-metallicity gas into the IGM (see Section 3.4), and could be important for disrupting cooling flows in the centers of massive galaxies and clusters (see Section 3.3). X-rays provide penetrating probes of all of the material in an outflow, from cool dust through to highly ionized gas, and only high-velocity X-ray photoionized outflows carry enough mass and kinetic energy to significantly affect the ISM and IGM. Constellation-X spectroscopy will provide the crucial information to quantify accretion-related mass-outflow rates and metallicities to determine their importance in massive galaxy evolution.

High spectral resolution studies of a few local AGN with Chandra and XMM-Newton have uncovered a forest of ionized absorption lines, indicating highly ionized outflows projected against the bright nucleus (e.g., Kaastra et al. 2000; Kaspi et al. 2002). However, Chandra and XMM-Newton only have the sensitivity to obtain low-resolution spectra of the more distant quasars (R=10–40 at 1–6 keV). Constellation-X's large effective area and high spectral resolution will permit detailed constraints on accretion-related outflows at $z \approx 1$–3, allowing their effect on the evolution of massive galaxies to be directly quantified. Figure 3 illustrates the potential of Constellation-X spectroscopy to reveal complex outflow structure in luminous high-redshift quasars for the first time. In the iron emission-line region (rest-frame energies > 6.4 keV), in-depth investigations of optically thick outflows will be readily accessible. However, as the low abundance of iron and fainter continuum will render less massive (and perhaps more typical) outflows harder to detect at high energies the spectral region at rest-frame energies < 2 keV where lighter elements dominate is also crucial.

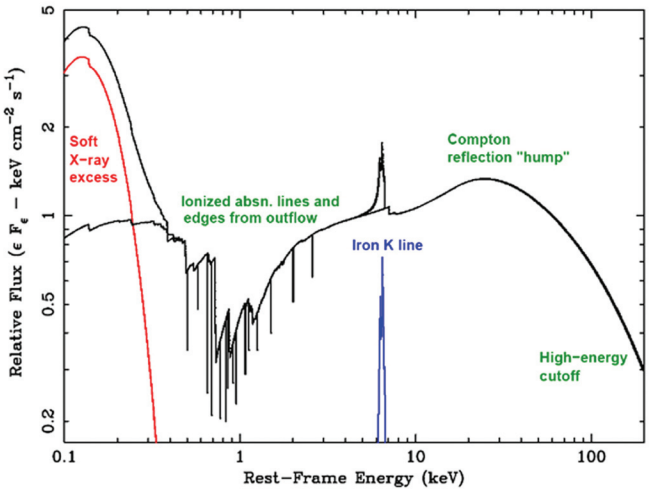

Figure 2: Typical soft X-ray through to hard X-ray spectral energy distribution of an AGN, showing the variety of spectral features that Constellation-X's resolution, throughput, and energy coverage will reveal. The broad Constellation-X bandpass covers an energy range equivalent to the far-ultraviolet—mid-infrared band at longer wavelengths. At z = 0, Constellation-X will sample 0.25–40 keV; at z = 6, Constellation-X will sample 1.75–280 keV.

In obscured AGNs the direct continuum from the central engine is hidden, thus hiding absorption signatures of outflows, but the outflows can still be seen as a forest of soft X-ray emission lines (e.g., Sako et al. 2000; Ogle et al. 2000). These emission-line spectra are as rich in diagnostic power as absorption-line spectra; and since obscured AGNs are more numerous than unobscured AGNs a larger fraction of the overall outflow energy might be present in emission-line outflows.

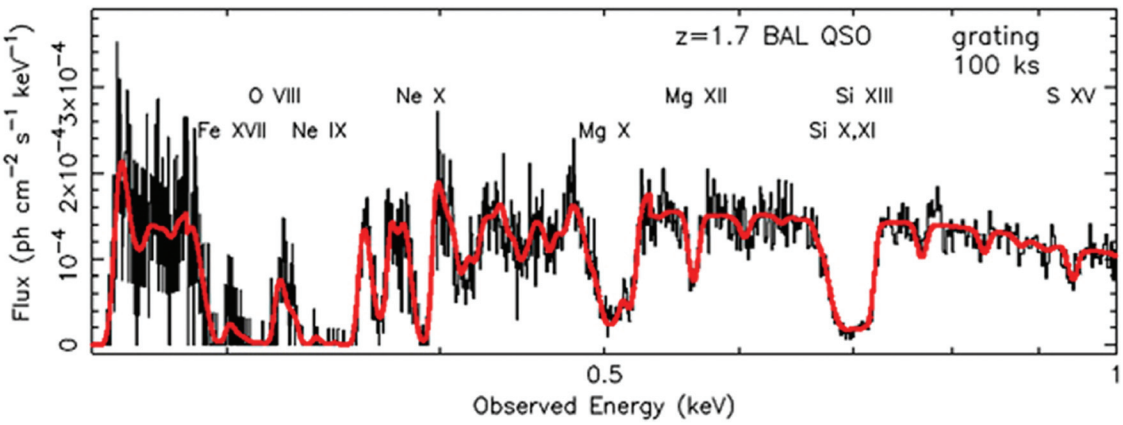

Figure 3: 100 ks Constellation-X simulation of a z = 1.7 quasar with an ionized, high velocity outflow and a flux comparable to PG1115+080 (Chartas et al. 2003). Substantial effective area at low energies (0.2–1 keV) is essential; crucial spectral features such as the resonance lines and edges of highly ionized O, Ne, Mg, and Si (E = 0.5–2.7 keV) move to lower energies with redshift. These spectral features provide important constraints on the physical conditions in moderate column density gas.

Only Constellation-X has the sensitivity and spectral resolution to observe emission-line dominated outflows over a wide range in redshift and luminosity and thus, for the first time, obtain a cosmic census of the mechanical energy from AGN activity. Emission from oxygen through iron can be used to measure the elemental abundances of high-redshift quasars, an essential constraint on early star formation. The column density of gas determines the ratio of recombination line strengths, while the temperature of the gas sets the width of the recombination continuum. The Doppler shifts and widths of emission lines yield the outflow and turbulent velocities, and together with the column densities, ionization parameter, and covering fraction, enables measurement of the kinematic power — the fundamental quantity for determining the impact of the AGN on its host galaxy and the IGM.

Each high-quality Constellation-X spectrum will reveal a wealth of physics integral to understanding the role of AGN feedback in galaxy formation as well as the interplay between massive black hole accretion and outflow. Extracting these physical diagnostics requires rest-frame spectral resolution of at least R~ 600 (250 km s^{-1} at z = 1) and high effective area (>1,000 cm^2) at energies down to 0.25 keV. With X-ray gratings spectroscopy, the constant $\Delta\lambda$ resolution allows source redshift to effectively improve the spectral resolution across a given transition by a factor of 1 + z.

4.1.2 The Energetics and Role of Obscured Accretion

The CXRB primarily probes the integrated accretion activity of the Universe over all of cosmic time. The deepest Chandra and XMM-Newton surveys have directly resolved ≈ 90% of the 0.5–6 keV CXRB and ≈ 50% of the 6–12 keV CXRB (Worsley et al. 2005), uncovering an order of magnitude higher AGN source density than found at other wavelengths (e.g., ≈ 7200 deg^{-2}; Bauer et al. 2004). Although it is apparent that many of these sources are previously undiscovered obscured AGN at z < 3 (e.g., Barger et al. 2003; Wilkes et al. 2002), their individual X-ray spectra, and therefore the properties of the primary X-ray emission, cannot be comprehensively characterized by Chandra and XMM-Newton. The black holes in many of the z > 1 obscured AGNs are likely to be undergoing a high accretion-rate growth phase (e.g., Marconi et al. 2004; Alexander et al. 2005) and Constellation-X will provide unique information on their environment and energetics.

The significant improvements in collecting area, spectral resolution, and high-energy bandpass that Constellation-X will bring over previous X-ray observatories will provide the first detailed understanding of the central engines of individual high-redshift obscured AGN; see Figure 1. This will lead to a greater understanding of the energetic output from obscured black hole growth and provide tighter constraints on the ratio

of obscured to unobscured accretion activity. Moderate-quality X-ray spectra of z ≈ 1–3 luminous obscured quasars will be possible in ≈ 100 ks exposures; however, X-ray spectra of more typical, and more heavily obscured AGNs, may require significantly longer, deep survey, exposures (e.g., ~1 Ms). These spectra will be of sufficient quality to constrain absorbing column densities, quantify the properties of any iron line emission, and determine the intrinsic X-ray luminosity of the AGN. Many of the X-ray sources detected in deep Chandra and XMM-Newton observations are X-ray bright but have counterparts too faint for optical spectroscopic redshift determination (e.g., Alexander et al. 2001; Barger et al. 2003). The identification of iron-K emission lines via Constellation-X spectroscopy may provide the most viable way to determine redshifts for these sources. In addition to the expected obscuration and outflow signatures expected in z >1 obscured AGNs (see Figure 1), many are also likely to be undergoing vigorous star formation. For a z ≈ 1 obscured quasar with the same star-formation characteristics as NGC 6240, Constellation-X would be able to obtain an X-ray spectrum of sufficient quality to be able to determine key star-formation properties in a typical 100 ks exposure. For example, this should allow for the detection of a star-formation related outflow with velocity of order 300 km s^{-1} and α process abundance enhancement relative to iron of a factor of two. Both of these would provide strong evidence for the enrichment of the IGM by starburst activity and the role of starburst feedback on galaxy formation.

The deepest >10 keV observations of the Universe have only resolved ≈ 3% of the CXRB at its ≈ 20–50 keV peak (Krivonos et al. 2005); see Figure 4. The undiscovered sources that contribute to the majority of the >10 keV background are likely to be heavily obscured, sometimes Compton-thick, AGN, and many may not be detectable at <10 keV; see Figure 1 for sensitivity constraints. With more than an order of magnitude improvement in both spectral and angular resolution, and a significant advance in collecting area, Constellation-X will be ≈ 100 times more sensitive than INTEGRAL at 40 keV, and will resolve approximately half of the CXRB at 10-40 keV.

Much of the potential high-redshift obscured AGN science with Constellation-X will require long exposures (>100 ks). The largest possible field of view will provide the best scientific return for these long exposures, enabling X-ray detections and X-ray spectra for many sources to be obtained in one Constellation-X observation. Minimizing the background level will maximize the scientific return of the HXT, permitting more sensitive 10–40 keV observations and resolving a larger fraction of the CXRB.

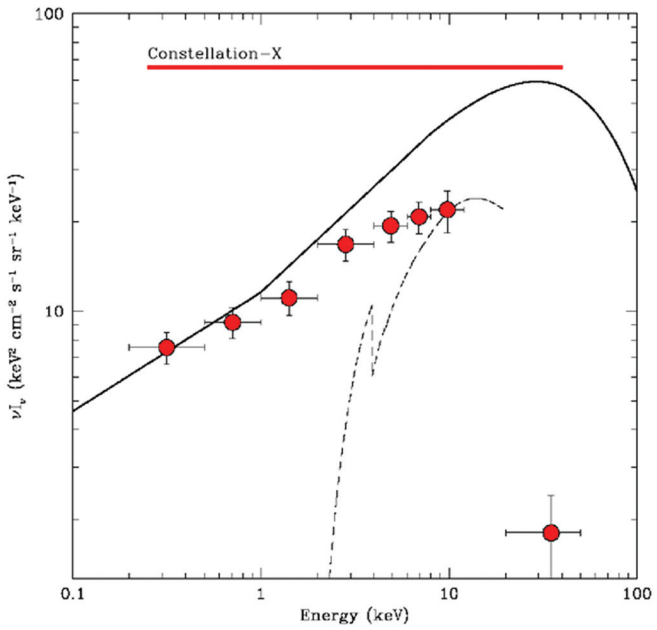

Figure 4: Energy density of the Cosmic X-ray Background (CXRB; solid line). The solid circles show the fraction of the CXRB resolved into sources by the deep XMM-Newton observation of the Lockman Hole up to 12 keV (Worsley et al. 2005) and at 20–50 keV by deep INTEGRAL observations of the Coma cluster (Krivonos et al. 2004). Constellation-X will directly observe the CXRB at the energy at which it peaks (≈ 30 keV) and will be several orders of magnitude more sensitive than previous missions. The dashed curve shows a moderate redshift (z = 0.8), obscured AGN (N_H = 4.5 x 10^{23} cm^{-2}); a large population of similar and more heavily obscured sources are most likely responsible for the 30 keV peak of the CXRB.

4.2 Black Hole Feedback in Cluster Cores

Both Chandra and XMM have provided tantalizing clues that accreting black holes affect their environments out to extremely large distances (a megaparsec or more) through the heating of intracluster or intergalactic medium (ICM/IGM). Dramatic progress has been made in determining the environmental impact of AGN in the cores of galaxy clusters. These are the monsters among the AGN wind sources, and theoretical calcu-

lations show that they may be the energetically most important factor in the evolution of the most massive galaxies in the Universe (e.g., White 2004; Benson et al. 2003).

As discussed in Section 3.3, Chandra and XMM observations show that the ICM in clusters that should display cooling flows only cool by a factor of about three between the outlying regions and the cluster core (Tamura 2001; Peterson 2001). Some agent must be heating the ICM core to prevent further cooling, and the prime candidate is an accreting supermassive black hole. Furthermore, the intracluster gas has appreciably more entropy than predicted by hierarchical clustering and gravitational collapse models, particularly in groups and small clusters (the "cluster entropy problem", see Section 3.1); the mostly likely solution to this is energy injection by growing black holes

The notion that black holes are heating the ICM is more compelling from the fact that black hole/ICM interactions are clearly seen in Chandra data (see Figure 5). The nature of these interactions is surprising, however. First, energy often seems to be added in a quiescent manner; evidence of strong shocks is lacking. For example, the rims surrounding the X-ray "cavities" in the Perseus cluster are colder than the ambient material, hence are not shocks driven by the expanding radio-lobes of Perseus-A (Fabian 2003). Second, the existence of the cavities in the X-ray surface brightness suggests that the hot (possibly relativistic) fluid injected by the AGN does not mix well with the cluster gas. Rather than occurring via direct particle-particle interactions, the heating could occur through dissipation of the sound waves generated by the buoyant bubbles of relativistic fluid. These waves may already have been seen in Chandra observations Perseus and M87.

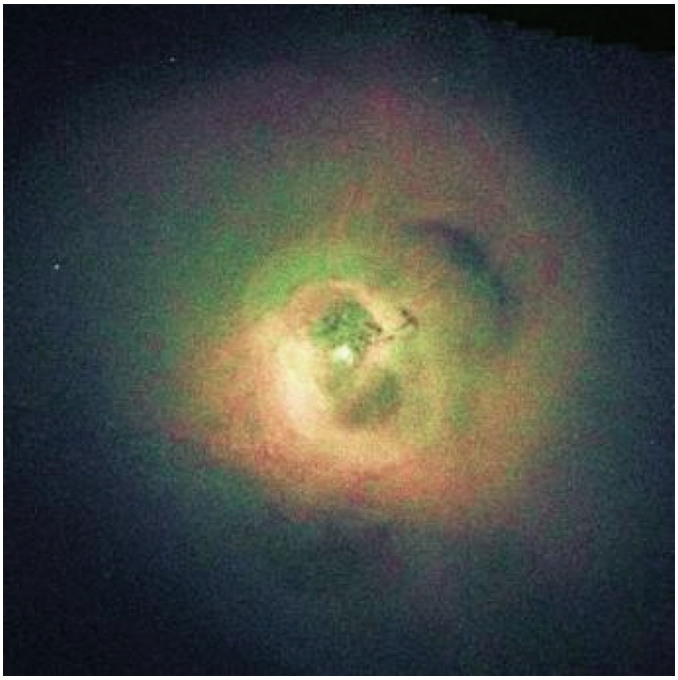

Figure 5: Chandra X-ray image of the cluster Perseus-A (Fabian et al. 2003). The central galaxy in this cluster, NGC 1275, is a radio source blowing radio "bubbles" into the intracluster medium. The image is 5.8' on a side. The Constellation-X field of view is quite important for this science, combined with ≈ 5" HPD PSF.

Can Constellation-X provide the "smoking gun" confirming AGN feedback on cluster scales? To image a large enough dynamic range of bubble structures at the distance of the Perseus cluster and map the innermost regions of nearby cluster cores requires a spatial resolution of approximately 5″ . A large collecting area is necessary, since the bubbles and related substructure have low contrast. In addition, a large field of view or scanning mode is needed to image bubbles and seek evidence of AGN-driven turbulence on the scales of the entropy problem (from a few hundred kiloparsecs to megaparsecs).

Velocity measurements will be important for establishing a connection between the mechanical heating phenomena and the AGN. With the spectral resolution (<4 eV), we can probe the ICM's velocity field to 200 km/s or less. We can also map the bubbles' velocity field and determine whether they are rising or expanding. AGN-induced turbulence in the ICM can be detected and spatially mapped. In addition, spectroscopy will offer measurements of abundance gradients, which can show the extent of entrainment by the rising bubbles, and information about the ionization mechanisms in the cluster gas that may reveal the role of, for example, cosmic rays in the ICM.

To date, cluster-heating studies emphasize radio galaxies that produce relativistic, collimated, low-density jets. But similar, perhaps larger, amounts of energy could emerge via denser, less collimated, subrelativistic winds —the same winds producing broad absorption line troughs in quasar spectra. Such winds are suspected to be more energetic than once thought, thanks to XMM observations of deep X-ray absorption.

For the radio galaxy/cluster studies, the field of view requirement is > 3 × 3 arcminutes, and PSF requirement is ≈ 5" HPD, which is driven by the scale of interaction between the radio jets and the intracluster medium.

4.3 Hot Gas in Star-Forming Galaxies

4.3.1 Starburst-Driven Superwinds

The previous two sections have focused on how AGN, via "feedback" (outflows) affect their environments. This section describes feedback driven by star formation. A significant fraction of all the heavy elements created by stars in galaxies are ejected by some process into the inter-galactic medium (IGM), with dwarf galaxies losing 80% of their metals and even massive galaxies like our own losing 10% of their metals (Tremonti et. al 2004).

Hot metal-enriched superwinds from starburst galaxies show the clear kinematic evidence for galaxy-scale outflows in both the local and high redshift Universe (e.g. Heckman et al 2000; Adelberger et. al 2003) of any of these classes of outflow. Such outflows have been observed in star-forming galaxies of all masses and environments, (see Figure 6) from dwarf starbursts such as NGC 1705 and NGC 1569, through moderate and high-mass disk galaxies such as M82, NGC 253 and NGC 3628, to ultraluminous merging galaxies, as is required to explain the observed galaxy mass-metallicity (M-Z) relationships. Almost all starburst galaxies show some evidence for outflow (Lehnert & Heckman 1995), and a substantial fraction (25%) of all (massive) star formation occurs in starbursts within the local universe. Starburst activity was more common in the past. The local space-density of starburst-driven winds of a given size and apparent power is approximately an order of magnitude greater than similar large-scale uncollimated winds from AGN.

Superwinds are driven by merged core-collapse supernova ejecta and stellar winds, which initially create a 10^8 K metal-enriched plasma within the starburst region. This over-pressured gas expands and breaks out of the disk of the host galaxy, converting thermal energy into kinetic energy in a bi-polar outflow, which can potentially reach a velocity of 3000 km/s. This tenuous wind-fluid sweeps up, entrains, accelerates and possibly shock-heats cooler, denser ambient disk and halo. Theoretical models predict that the entrained, cool gas is accelerated to lower velocities than the hot metal-enriched gas (e.g. Chevalier & Clegg 1985; Strickland & Stevens 2000). These models also predict that the majority of the energy (90%) and metal content in superwinds exists in the hot 10^6 K phases, with the kinetic energy of such gas being several times the thermal energy. X-ray observations are thus of singular importance in studying this phenomenon, as they provide a probe of the most energetic phases in these outflows, in particular of the metal-enriched phases most likely to escape into the IGM. Yet all existing observational velocity measurements of superwinds are of entrained cooler material, e.g. warm neutral and ionized gas with measured outflow velocities in the range 200 to 1000 km/s. Whether this material escapes into the IGM is uncertain, as $v_{obs} \sim v_{escape}$ for the host galaxy (see Heckman et. al 2000).

Despite a wealth of multi-wavelength data on starburst-driven outflows, the fundamental parameters of the absolute element abundances and velocity of the hot gas have not been measured. Observations with Chandra and XMM-Newton detects thermal X-ray emission from hot gas in superwinds extends out to 5–30 kpc from the plane of edge-on starburst galaxies (see Figure 7 and e.g. Strickland et. al 2004a,b), but these observations lack the spectral resolution (ΔE = 100 eV at E = 1 keV) to robustly determine the metal abundance and kinematics of this hot gas. High-resolution X-ray spectroscopy (with $\Delta v \approx 400$ km/s or ΔE = 1 eV at 0.65 keV) is the only method by which these parameters can be measured and by which the efficiency of winds in ejecting metals can be quantified.

4.3.2 Hot Halos Around Normal Spiral Galaxies

The properties of hot gas in the halos around more normal galaxies like our own are even less well understood than starbursts, yet they have the potential to reveal important clues about cosmology, galaxy formation and evolution. *By measuring the elemental abundances and composition of the very faint halos of hot gas around normal galaxies we can test theoretical cosmological models that predict this gas is pristine gas accreting from the IGM* (see Benson et. al 2000; Toft et. al 2002; Sommer-Larsen et. al 2003), or see if it is enriched, processed gas ejected from the disk of the galaxy by supernova explosions (galactic "fountains", e.g. Bregman 1980; Avillez 1999; Norman & Ikeuchi 1989). Current X-ray observatories have only

just reached the sensitivities needed to detect these extended galactic atmospheres (see Figure 6), but lack the spectral resolution to measure its composition.

Determining the properties of million-degree gas within the disks of star-forming galaxies is also of great importance. On galactic-scales it has long been known that the heavy elements created in stars and released in supernova explosions do not immediately appear (i.e. within a few million years) in the cool, dense gas from which new stars and planets form (Kobulnicky 1998). It has been suspected that these elements initially enter the hot-X-ray-emitting gas phase, before eventually cooling and condensing into denser clouds (if they are not ejected completely and lost to the IGM in a superwind or galactic fountain). As in the case of superwinds, measurements of the composition and abundances of the diffuse hot gas have been ambiguous with current or previous X-ray telescopes.

High-resolution dispersion-less X-ray spectroscopy is the only way of determining the temperature and ionization state (and hence the energy) of hot 10^6 to 10^8 K gas that has either been recently heated by supernova, or has accreted into the gravitational potential well of massive galaxies such as our own. Current X-ray spectroscopy must assume the gas is in ionization equilibrium, at one or a few well-defined temperatures. This is unlikely to be the truth. The absolute metal abundances (i.e. with respect to hydrogen) of the hot gas around normal spiral galaxies will be a strong diagnostic of its physical origin: metal-poor gas accreted from the IGM, or element-enriched by supernova activity. High α/Fe ratios are expected if massive stars are the heating source, while lower α/Fe ratios are expected if supernova type Ia can drive the winds (e.g. Wang 2004).

With the Constellation-X calorimeter we can determine the velocities of the diffuse hot gas, andand hence its kinetic energy. This is especially important for superwinds, the hot, metal-enriched gas is thought to have the most energy and is most likely to escape the host galaxy.

4.3.3 Star Formation and the ISM at the Center of the Milky Way

The central region of the Milky Way galaxy allows us to study the impact of star formation on the ISM with a factor of 100 higher spatial resolution. The region also provides exhibits an intriguing regime of star formation: the rate within the central 150 pc of the Galaxy is 0.04 $M_\odot$ yr^{-1}, which is several hundred times higher than the volume density of star formation in the Galactic disk, and a similar factor lower than that in starburst galaxies (Figer et al. 1999). This on-going star formation has dramatic manifestations in the Constellation-X bandpass (see Figure 9).

A hot, 10^8 K plasma is observed through emission lines from helium and hydrogen-like Fe (Muno et al. 2004 a,b). The high temperature of this plasma is surprising, because it is much hotter than that seen in supernova remnants. Moreover, any hydrogen with T ≈ 10^8 K would be too hot to be bound to the Galactic center, so if the plasma is indeed thermal, then it must be composed largely of helium and heavier ions (Belmont, et al. 2005). Constellation-X measurements of the elemental abundances could confirm this hypothesis. Alternatively, the plasma could be produced as a by-product of cosmic-ray acceleration (Dogiel et al. 2005). In this case, Constellation-X should observe ra-

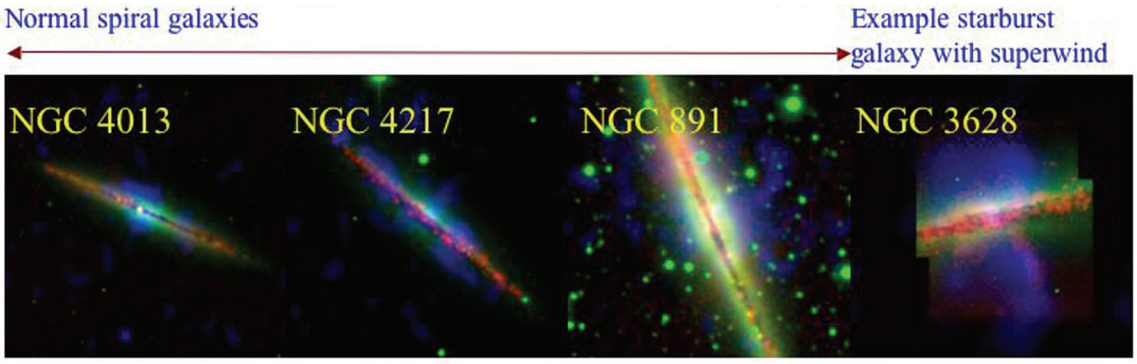

Figure 6: Hot gas around normal disk galaxies - Red: H-α (WIM), Green: R-band (starlight), Blue: Diffuse soft X-ray (3 million° gas). The region covered by each image is 20 x 20 kpc. Intensity scale in square-root.

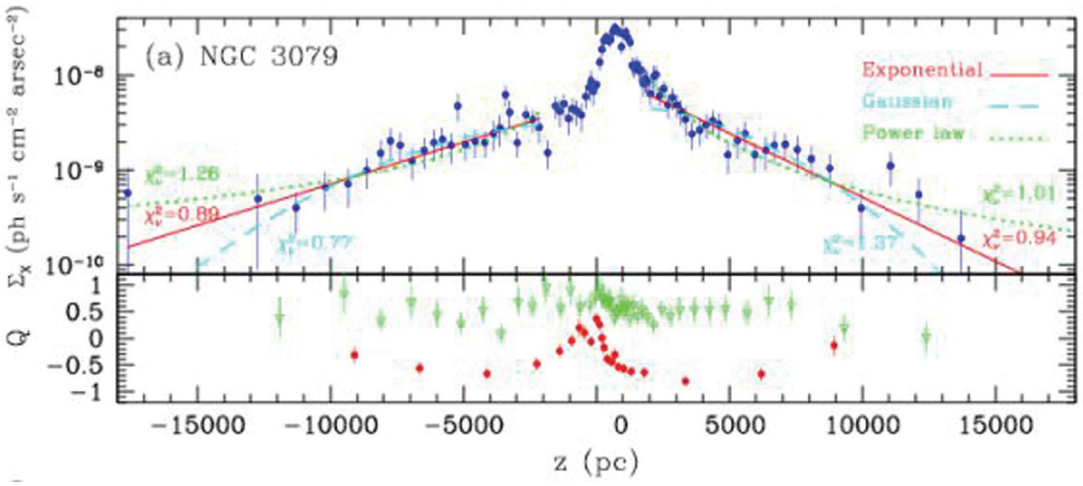

Figure 7: X-ray surface brightness profiles. We observe exponential X-ray surface brightness profiles with scale height ~ 2 – 4 kpc. Spectral hardness Q varies only weakly in halo, at z > 2 kpc. These observations are consistent with the wind hitting and shocking pre-existing exponential halo medium.

diative recombination continua from ions in the plasma and will be able to study the above spectral features on spatial scales of tens of arcseconds, determining where the plasma is accelerated.

Young star clusters at the Galactic center have been identified through the X-ray emission from shocks formed both when winds of binary Wolf-Rayet and O (WR/O) stars collide, and when the collective winds encounter the surrounding ISM (Law & Yusef-Zadeh 2004). The Arches cluster is the brightest such object, and exhibits diffuse line emission from neutral iron (Yusef-Zadeh et al. 2002). The presence of neutral iron suggests that the cluster wind is accelerating low-energy cosmic rays, which in turn bombard iron in nearby molecular clouds and cause it to fluoresce. Constellation-X has the right combination of spatial and spectral resolution to study these processes in detail.

The detection of X-ray emission from several synchrotron-emitting radio filaments is one of the most surprising Chandra results on the Galactic center. The filaments have been explained as magnetic instabilities formed in the wakes of in-falling molecular clouds (Shore & Larosa 1999), or shocks in outflows produced by massive stars (Yusef-Zadeh & Königl 2004). The first model assumes that ~1 mG fields are present in the Galactic Center, whereas the latter two assume $<$ 0.1 mG fields. The larger fields also are expected if the gas fed into the Galactic center carries with it magnetic fields. So distinguishing between these models is crucial for understanding whether fields build up or are destroyed in the nuclei of galaxies.

4.3.4 Observatory Specifications

The X-ray spectral energy distribution of the diffuse thermal X-ray emission in superwinds and normal spiral galaxies peaks between E= 0.5–1.1 keV. Spatial resolution, and the shape of the PSF, does affect the study of diffuse X-ray emission in starburst and normal spiral galaxies. Removal of the majority of point-source emission is a real requirement for exploiting high-resolution spectroscopy, in that we are trying to measure line strengths and shapes with respect to their continuum. Any additional source of continuum (e.g. unresolved binaries, or contamination from the PSF-wings of bright point source just outside of the field of view) makes the measurement ambiguous. The higher the spatial resolution, and the smaller the wings of the PSF, the less of a problem point-source contamination of diffuse-region spectra will be.

Even in Chandra data, where point sources are detected down to 10^{37} erg/s (10 Mpc, 50 ks Chandra), unresolved point source emission is almost certainly present in the disk of edge-on or face-on star-forming galaxies. Effectively complete point-source removal (with a 5″–10″ PSF) is possible for observations of the halo regions of edge-on starbursts and normal spirals, in that we know from Chandra observations where the bright sources are and that the region is effectively a subset of the extra-galactic background (and hence can be modeled reasonably well).

A small or medium FOV would make it more difficult to fully map out the nearest winds, but it is unlikely that

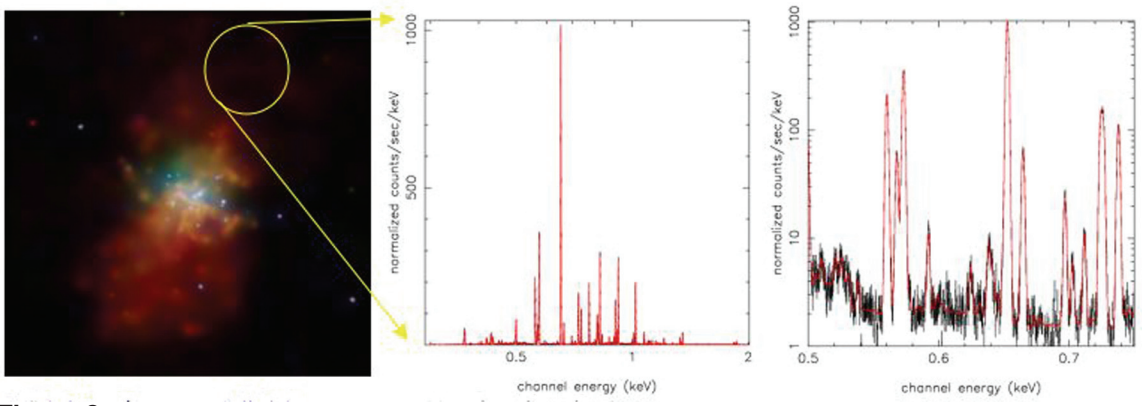

Figure 8:
M82 Chandra central 5x5 kpc
red: 0.3-1.1 keV,
green: 1.1-2.8 keV
blue: 2.8-9.0 keV

Simulated 20 ks Constellation-X northern halo observation, 0.3-2.0 keV.

O VII and O VIII region. Well resolved triplet, high S/N in continuum.

that would be done even with a large FOV (assuming that the trade off for higher angular resolution is a smaller field of view). For the study of star-forming galaxies, a field of view 2' on a side with good to moderate angular resolution (5″–10″) would be ideal.

The true outflow velocity of the X-ray-emitting gas could range from that of optically-emitting material (range of 200–1,000 km/s in various starbursts, up to a maximum of 3,000 km/s (raw merged supernova ejecta in free expansion). In edge-on starbursts only the projected velocity components would be seen, e.g. 150 km/s line shifts and 300 km/s line splitting for M82 for (true $v_{H\alpha}$ = 600 km/s. For reference , 1 eV (FWHM) spectral resolution would be adequate at 1.8 keV (170 km/s) but marginal at 0.65 keV (460 km/s).

The sensitivity of the Constellation-X calorimeter should be such that moderate-to-high quality spectra can be obtained of the faint diffuse halo-region X-ray emission, well away from the disk. Spectra would be accumulated over moderately large regions (e.g. 1'×1') after removing regions contaminated by point-source emission. Simulations show that at least 8,000 counts per spectrum are needed to meaningfully constrain the abundances and velocities of the hot gas. With current estimates of the calorimeter effective area, regions 8 kpc above the disks of the starbursts NGC 3079 or NGC 3628 (see Figures 6 and 7), or 3 kpc above the plane of the normal spiral NGC 891, would produce 270 counts s^{-1} arcmin^{-2} (27,000 counts arcminute^{-2} in a 100 ks).

4.4 The Interstellar Media of the Milky Way

Studying the interstellar medium (ISM) of galaxies is a vital component in understanding their evolution, and the ISM of our own Milky Way galaxy is particularly rich for detailed study. Stars form from cold ISM, evolve, and may end their lives as SNe. SNe produce heavy elements, distributing them into the ISM as hot plasma, which emits radiation observed from radio to X-rays as it expands and evolves. Eventually the plasma cools, coalesces into clouds, and the process begins again.

The composition and physical state of the ISM reflects the overall star formation properties of the Milky Way (past and present), but quantitative understanding of ISM properties remains poor. Traditional observational techniques are restrictive: mm lines trace only specific molecular species; IR continuum emission shows only grey body radiation; and optical/UV extinction curves do not respond strongly to specific properties of individual ISM components. Further, it is difficult to combine these to learn, for example, the total carbon abundance of the ISM (cf., Dwek 1997; Zubko et al. 2004).

Soft X-ray absorption spectroscopy is the only technique sensitive to all ISM constituents simultaneously, including dust and all molecular and atomic species. In the soft X-ray band, the K shell absorption spectra of the elements carbon through silicon are located between 0.28 and 1.8 keV, and the L shell spectrum of Fe is near 800 eV. For typical values of the Galactic column density, 10^{20}– 3 × 10^{21} cm^{-2}, the opacity at the

photoelectric edges makes them readily detectable in a bright high-resolution spectrum.

In response to small changes in the valence shell (ionization, chemical binding), the photoelectric absorption edges and lines exhibit small shifts, typically on the order of a few eV. A single sensitive X-ray absorption spectrum with a few eV-resolution can therefore address all of the physical chemistry of the major constituents of the ISM. In addition, the absorption spectrum is sensitive to the presence of dust, because in solids the X-ray absorption cross-section above the ionization threshold shows a characteristic "undulation" with energy due to quantum interference between the photoelectron and neighboring atoms. This effect is also sensitive to the precise crystalline composition and structure of the absorbing material. X-ray absorption spectroscopy can therefore provide unique information on the physical properties of astrophysical dust that cannot be obtained in any other way.

The validity of absorption spectroscopy has been successfully demonstrated with high resolution grating spectra of selected bright sources with Chandra and XMM-Newton. High-signal high-resolution X-ray spectroscopy showing individual absorption edges can give precision total abundances of individual elements (e.g., Crab pulsar, Weisskopf et al. 2004). The increased sensitivity of Constellation-X will extend this work to a larger number of lines-of-sight, and will allow more finely detailed studies of subtle features in the brightest objects.

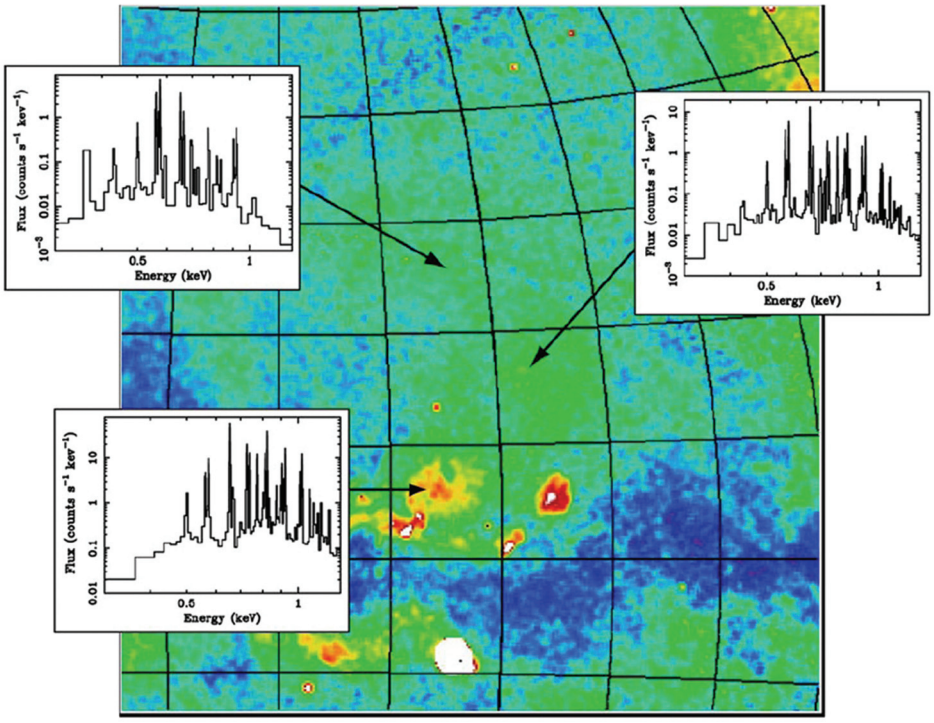

Figure 9: Chimneys connecting the galactic plane to the halo in spiral galaxies provide a mechanism for hot plasma with enhanced abundances to escape the disk. Such plasma, the result of supernovae and the winds of massive stars, heat and enrich the halo. This figure shows a possible example of such a chimney in the Milky Way, with a trail of enhanced X-ray emission from a number of energetic regions in the plane to a plume into the lower halo. The color image shows the ROSAT All-Sky Survey data at ¾ keV where red indicates high intensity and blue indicates low. The three panes show model Constellation-X spectra, based on the ROSAT data, from three points in the chimney. The cooling of the plasma as it progresses out of the disk can clearly be seen by the shifting of the emission to lower energies. However, Constellation-X observations will allow a much deeper study than what can currently be achieved with a considerably greater sensitivity to changes in ionization structure and abundances. With this additional information greater insight into the Galactic halo environment can be achieved.

5. Life Cycles of Matter

5.1 High-Energy Stellar, Protostellar and Protoplanetary Physics

The processes at work in the X-ray-emitting outer atmospheres of stars affect star and planet formation, the evolution of planetary atmospheres, magnetic dynamo processes at work in stellar interiors, the angular momentum evolution of stars, and the origin and acceleration of stellar winds and mass loss. High-energy phenomena in non-degenerate stars and protostars offer examples of processes that occur on much larger scales in the more distant cosmic X-ray sources—including magnetic reconnection and flares illuminating accretion disks of black holes and the radiatively-driven winds and outflows of these accretion disks. Our current ideas and understanding of these aspects of X-ray astronomy stand on the shoulders of our knowledge of stars, and are advanced by understanding the basic plasma processes that we can study in their unusually well-understood environments.

5.1.1 The Formation of Stars and Planets and their High-Energy Environments

Recent research points to protostellar and pre-main sequence X-ray and energetic particle activity as crucial aspects of star and planet formation (see Figure 1.) These produce the ionization necessary for accretion to proceed in stellar systems throughout protostar evolution, and mediate both terrestrial and Jovian planet formation (Glassgold et al, 2004). X-rays from large flares reprocessed into cold iron K lines by circumstellar disks have been detected in several protostars (Imanishi et al, 2001; Tsujimoto et al, 2004). The time-dependence of the Fe K flux can be used for "reverberation mapping" of the structure of gas and dust in inner protoplanetary disks revealing gaps at the locations of inner planets in the process of formation (see Figure 1).

Chandra and XMM-Newton grating spectra have detected shock-heated plasma from magnetospheric accretion from two out of the five or so CTTS studied at high resolution to date: in TW Hya (Kastner et al, 2002; Stelzer & Schmitt 2004) and BP Tau (Schmitt et al. 2005). The soft X-ray accretion signatures are high densities seen in the lines of He-like O and Ne and are completely missed at low resolution. Only a small handful of the very nearest CTTS are accessible to Chandra and XMM-Newton gratings. Constellation-X will instead probe accretion signatures at high resolution in stars up to 500 pc away, including those in the nearest regions of copious star formation such as Orion.

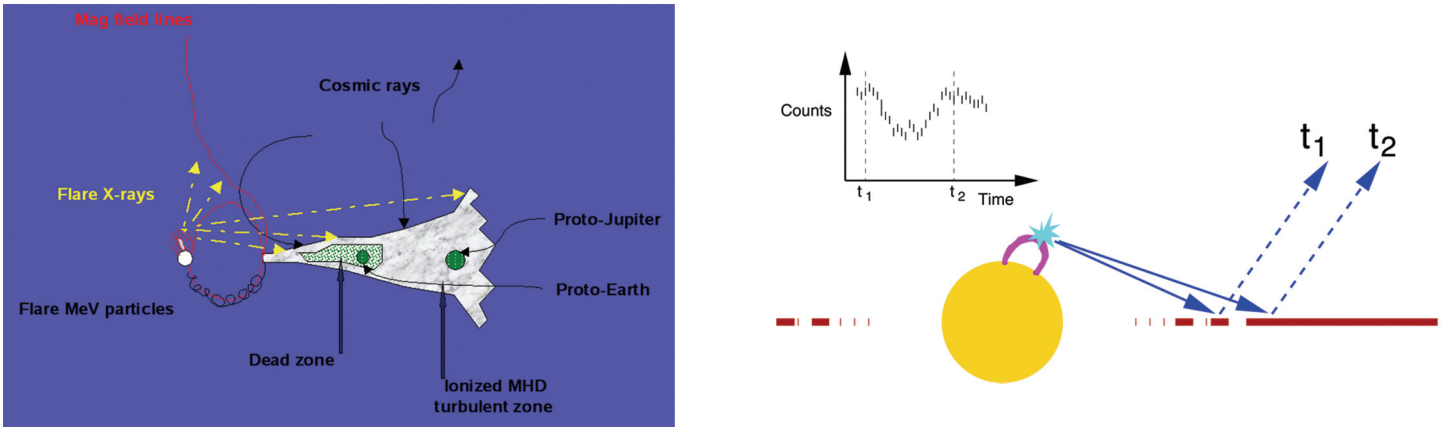

Figure 1 Left: A schematic illustrating the influence of stellar activity on protoplanetary disks through magnetically driven high-energy photon and particle emission. Ionizing X-rays penetrates deeply into disks, inducing MHD turbulence, which affects accretion, Jovian planet formation and migration. Terrestrial planets are believed to be formed in a disk "dead zone", which is sufficiently obscured by overlying material that ionizing X-ray photons and energetic particles cannot penetrate (From Feigelson 2003). Right: An illustration of the technique of reverberation mapping of protoplanetary disks. Bright flares on the central star are reprocessed by the disk and this signal is revealed in spectra in the light of the cold iron K-shell fluorescence line. The variations of the flux from this line with time can reveal the location of gaps in the disk where planets are forming.

5.1.2 *Hot Magnetized Plasmas in Brown Dwarfs, Main Sequence and Evolved Stars*

The Sun can be imaged in X-rays in fine detail, yet we currently know very little about how other stars can generate huge flares and sustain coronae up to 10,000 times brighter than that of the Sun, and how these coronae are structured.

While some spatial inference is possible from line shifts and broadening seen in Chandra spectra of nearby active stars (Hassain et al. 2005), full Doppler imaging requires both very high throughput and spectral resolution. A minimum resolving power that would allow study of the most rapidly rotating nearby systems is $\lambda / \Delta\lambda$ 2000 (FWHM). Stars such as AB Dor will provide up to 10^6 counts in a day long observation, allowing for quite detailed coronal images. A few hundred counts in the He-like λ 1.85 resonance line of Fe XXV, and substantially more in H-like and He-like lines of S (λ 4.73, 5.04), Si (λ 6.18, 6.65) and Mg (λ 8.42, 9.17) can be acquired in only a few ks, enable imaging of the very high temperature (10^7 K) plasma separately to that at lower temperatures (several 10^6 K). Doppler imaging of classical T-Tauri stars will allow the location of the X-ray emitting region to be determined, which initial indications suggest are in loops up to 10 stellar radii in size and may have footprints connecting the stellar surface to the accretion disk (Favata et al. 2005).

5.1.3 *Magnetic Flares: Prototypes of Energy Lifecycles and Release in the Universe*

Throughout the Universe—in stars, accretion disks, interstellar and intergalactic media, for example—magnetic fields store energy imparted by mechanical turbulent or convective plasma motions. This energy can be released again through magnetic reconnection events, whereby the plasma is spontaneously heated and accelerated. Our Sun provides dramatic examples of this process through solar flares. Solar flares and CMEs

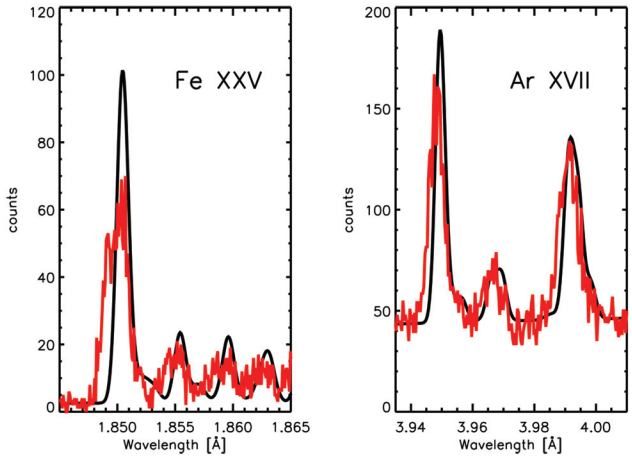

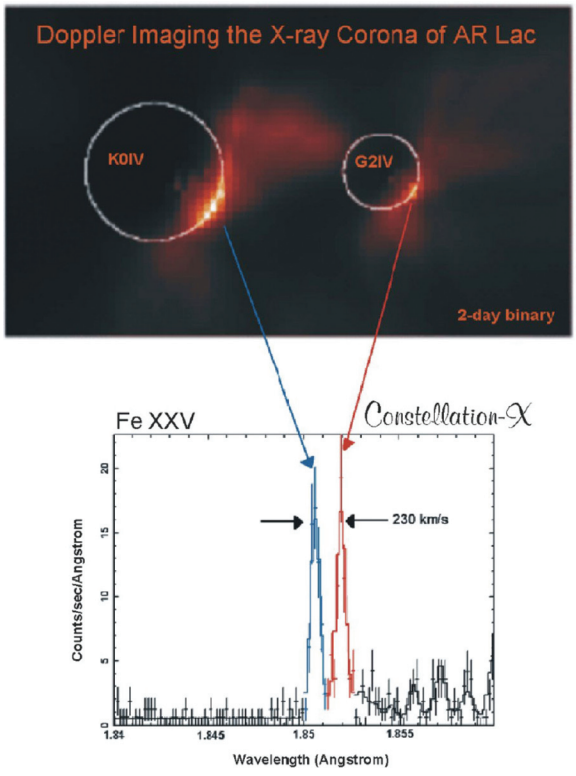

Figure 2 Left: Simulated XMS spectra in the region of the He-like Fe and Ar complexes for a 25ks observation of AD Leo. The simulations assumed that the plasma was heated by continuous flaring with upflows in the range of 0-200 km s^{-1}. Understanding flares occurring under these conditions (much more extreme than in the Sun) will help bridge the gap to the conditions around black hole accretion disks. Right: The top panel shows an eclipse-mapping spatial deconvolution of the coronae of the RS CVn binary AR Lac as derived from a long EXOSAT exposure. The lower panel shows a simulated 20 ks Constellation-X observation of AR Lac, assuming that the exposure was centered on orbital quadrature when the velocity separation of the two stars in this binary system is at its maximum value of 230 km s^{-1}. For simplicity, it is assumed that each star contributes equally to the total X-ray emission. The strong Fe XXV λ 1.85 resonance line is clearly split into two components due to the differential Doppler shifts of the two stars. (Figure courtesy of Steve Drake.)

pose a hazard to both manned and unmanned spacecraft, and understanding them is important for predictive and preventative measures. However, magnetic reconnection, flares and coronal mass ejections remain quite poorly understood: What we know is based on what has been learned from the Sun, yet even current models fail to match some salient aspects of solar flares (Doschek 1990; Feldman 1990). In particular, blushifted emission expected from upflowing evaporation of the chromosphere (see Figure 2) heated by protons and electrons accelerated in the reconnection event is inadequate to explain the flare emission and sometimes appears prematurely at flare onset. The temporal relationship between hard X-rays (due to the accelerated particles) and soft X-rays (due to chromospheric evaporation) is often not satisfied either, in that soft X-rays can commence *before* the hard X-ray burst.

Time series analyses of EUV and X-ray observations of active stars have provided evidence that plasma at temperatures $\geq 4 \times 10^6$ K arises purely from flares, analogous to the idea of "nanoflare" theories of solar coronal heating (Parker 1988; Guedel 1997; Audard et al. 2000; Kashyap et al. 2002). Constellation-X will provide a sensitive test of flare heating through both Doppler shifts and photon arrival times. A Constellation-X XMS effective area of 6,000 cm^2 at *E* 3–6.5 keV and resolving power of $E/\Delta E > 1{,}000$ brings within reach Doppler diagnostics in H-like and He-like S (λ4.73, 5.04), Ar (λ 3.95, 3.73) and Fe (λ1.85). A simulation of a 25 ks XMS observation of the nearby flare star AD Leo (dM3e; d = 4.7pc) is illustrated in Figure 2.

Another major Constellation-X breakthrough in the study of stellar flares will be the enormous improvement in photometric precision of flare light curves and spectra, allowing direct measurement of coronal loop resonant frequencies themselves. (Mitra-Kraev et al. 2005) have recently detected oscillations in the X-ray emission from M-dwarf AT Mic by XMM-Newton (see Figure 3). Oscillations in solar loops are seen routinely (Schrijver et al. 2002; Wang et al. 2003; Mariska 2005) and arise from a resonance in the flare loop whereby the loop plasma is successively compressed and rarified. The observed period and its decay can be used to determine the magnetic loop length and magnetic field. Loop "wobble" velocities on the Sun have reached up to 200 km s^{-1}. Constellation-X detections of loop oscillations, both spectroscopically and photometrically, could provide unique measurements of these quantities in a wide range of stars, from accreting T Tauri stars to evolved giants. Resolving powers of 1000 are needed to make firm detections of line-of-sight velocity components of 100 km s^{-1}.

Detection of hard X-rays in stellar flares would define a major breakthrough for stellar physics. This emission is unequivocally related to impulsively accelerated electrons and ions that do not suffer from magnetic trapping (as radio-emitting electrons do). In the case of the Sun, hard X-rays and gamma rays have been the prime source for the study of energy release physics, particle acceleration in magnetic fields, and coronal heating. The different, and probably more extreme, magnetic configurations in magnetically active stars could lead to quite different acceleration histories and heating efficiencies in large flare events. Detection of hard X-ray components would thus open an entirely new avenue in the study of the energetics of hot, magnetized coronal plasma. For the Constellation-X HXT area of a few 10^3 cm^2, bright flares on nearby stars can be detected in only 100s.

5.1.4 Outflows and Shocks in Massive Stars

The ubiquity of rapidly expanding stellar winds from OB stars are one of the most unexpected and important discoveries of the early NASA space program (e.g. Snow & Morton 1976). Soft X-ray emission is understood in terms of shock instabilities in line-driven winds (Lucy & White 1980); however, the nature of the processes that lead to shocks and X-ray emission are still unclear. One possible geometry for the emission region postulates especially porous and fragmented stellar winds, allowing both blue and redshifted X-rays to penetrate through (e.g. Feldmeier et al. 2003); another suggests that X-rays arise in extended magnetic loops (Underhill 1979) within which both hot upflows and downflows are observed. XMS measurements of the profiles of emission lines such as Ar XVIII (λ3.73), Ca XX (λ3.02) or even Fe XXV (λ1.85) could provide important constraints, as the higher Z lines are likely emitted closer to the stellar surface and thus should become narrower within the fragmented wind scenario.

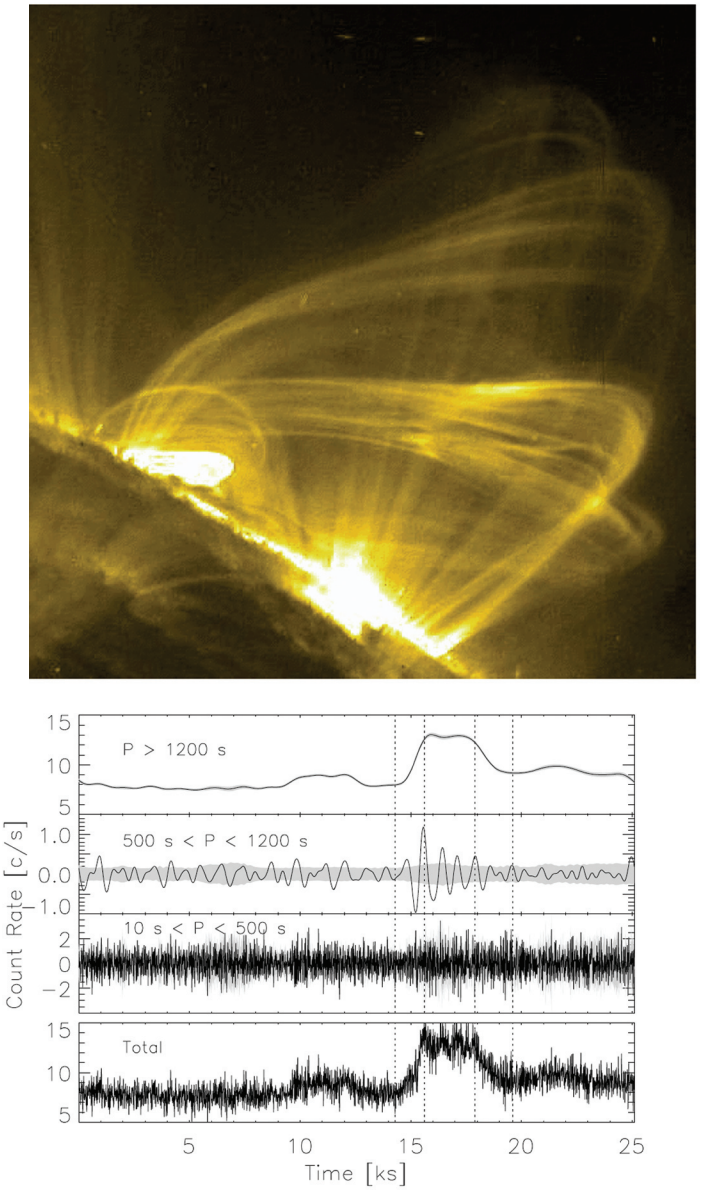

Figure 3 Top: Solar coronal loops undergoing transverse oscillations observed by TRACE (Schrijver et al. 2002). Analysis of loop oscillations by (Wang & Solanki 2004) indicates X-ray intensity variations have a pulse fraction as high as 13%. Bottom: An XMM-Newton lightcurve of a flare on AT Mic decomposed into three frequency bands: low (P > 1200 s) showing gross flare structure; medium (500 s < P < 1200 s) illustrating a coherent flare loop oscillation; and the high frequency (10 s < P < 500 s) noise component. The sum of these add up to the original data (lower panel). Loop oscillations provide direct diagnostics of magnetic field strength and loop length (Mitra-Kraev et al. 2005).

5.2 Supernova Remnants

The capabilities of Constellation-X will open a new window into the physics of supernova (SN) explosions through a dramatic improvement in the quality of the observations of young, ejecta-dominated supernova remnants (SNRs). The high spatial and spectral resolution of Constellation-X will enable determination of the composition, ionization state and velocity of the material throughout the SNR to build a complete model for the structure of the shocked ejecta and the ambient medium. This has an enormous potential to constrain both the physics of supernova explosions and the details of the pre-supernova evolution of the progenitor systems for both core collapse and thermonuclear supernovae. Constellation-X will also enhance our understanding of other aspects of supernova remnants, such as the acceleration of cosmic rays at shock fronts and pulsars and their wind nebulae.

5.2.1 Core Collapse

Constellation-X observations of core-collapse SNRs, will unveil new information about the core-collapse process by revealing the distribution and dynamics of nucleosynthesis products formed during the explosion, tracking the early evolution of SNRs, unveiling unshocked iron, and measuring the total mass of iron in SN ejecta.

A prime target for studies of core-collapse supernovae is the well-studied Cassiopeia A (Cas A), because it is the brightest X-ray remnant with emission dominated by silicon and iron ejecta. The X-ray emission from Cas A is spatially complex, showing structure on scales from the remnant's full ~ 3′ extent to knots and filaments ≤ 2″ in size (Hughes et al. 2000; Hwang et al. 2000). Ejecta radial velocities of up to ~2000 km s^{-1} have been measured on 20″ scales with XMM-Newton (Willingale et al. 2002). Hwang & Laming (2003) and Laming & Hwang (2003) demonstrated that the X-ray emission from Cas A's Si- and Fe-rich ejecta knots can be used to determine the ejecta density profile, explosion asymmetry, and mass coordinate of ejecta structures. All these studies have been done at CCD spectral resolution (R ≤ 100). Constellation-X will enable deeper investigations into the nature of the knots and other complex ejecta structures as its resolution approaches the goal of 5″.

The radioactive nucleus ^{44}Ti is closely connected with the explosive nucleosynthesis of Iron by complete Si burning (α-rich freeze-out). ^{44}Ti decays with a 60-day half-life to ^{44}Sc, then quickly to Ca. The Constellation-X calorimeter will reveal sites of ^{44}Ti production by mapping the inner-shell line radiation of ^{44}Sc at 4.086 and 4.090 keV. In addition Constellation-X will allow us to observe and study emission from less abundant species in the hot ejecta, including phosphorus, potassium, titanium and the rest of the iron group elements (vanadium, chromium, manganese, colbalt, and nickel). These elements in particular are sensitive to the poorly understood final mass cut between the ejecta and the forming neutron star (Woosley & Weaver 1995).

Another exciting target for core collapse studies is SN 1987A, which has given astronomers a unique opportunity to witness the birth of a supernova remnant. In recent years, its X-ray luminosity has increased rapidly as the forward shock crashes into the dense inner ring of circumstellar material (Park et al. 2004). The remnant may brighten 10- to 100-fold before Constellation-X launches (McCray, private communication 2004). The reverse shock has begun to propagate through the ejecta and is now being observed in high-velocity H-emission (Michael et al. 2003). In time heavier elements will begin to cross the reverse shock and reveal the radial structure of the ejecta. The estimated velocities of ejecta crossing the reverse shock range from 5,700 km s^{-1} to 6,700 km s^{-1} during the 5-year Constellation-X lifetime, while Iron ejecta are expected to reach lower velocities of ~4,400 km s^{-1} (McCray 1993).

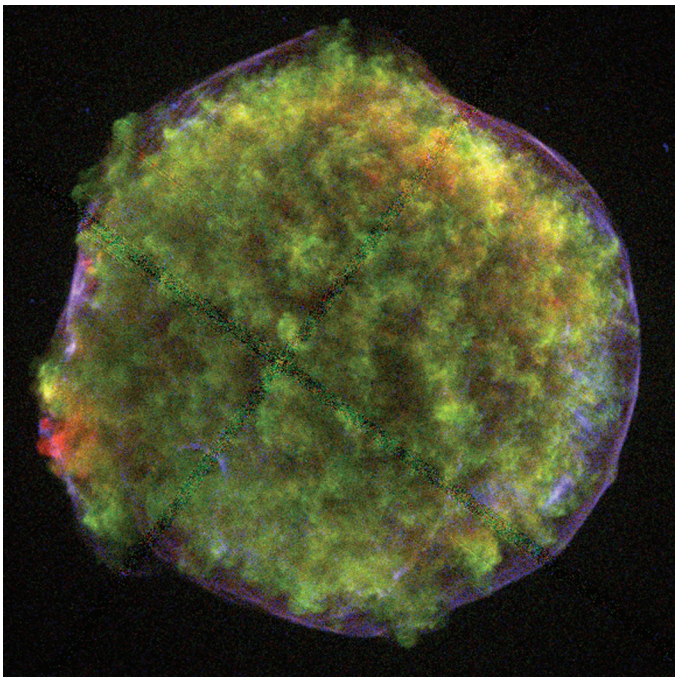

Figure 4: Chandra X-ray image of the Tycho supernova remnant showing iron-rich ejecta (red features), silicon-rich ejecta (green features), and featureless spectra from the forward shock (blue rims).

5.2.2 Thermonuclear Supernovae (SNe Ia) and their Remnants

One of the unsolved problems in SN research is the nature of Type Ia SNe (SN Ia) progenitor systems. One possible progenitor system is a C-O white dwarf accreting H/He-rich gas from a companion, in which case some circumstellar gas should be present when the SN explodes. Early Constellation-X observations of bright SN Ia (preferably before maximum optical brightness ~20 days after ignition) will constrain the progenitor's circumstellar environment. However, circumstellar material (CSM) in a normal SN Ia has yet to be detected. Currently, Chandra can reach a flux limit of ~10^{-15} ergs cm^2 s^{-1} (2–10 keV band) in 20 ks. Constellation-X will go an order of magnitude fainter, so will have 3× higher sensitivity to the CSM density. The precise limit depends nearly linearly on how soon after the explosion the SN is observed.

The cosmological importance of SNe Ia have inspired new surveys aimed at detecting early SNe Ia (2 days after the explosion) at distances comparable to the Virgo cluster (~16 Mpc; closer SNe Ia are very rare). Ongoing surveys are projected to discover 1 bright (mag 12-13) early SN Ia per year. Since time is of critical importance, Constellation-X must be able to observe a target of opportunity SN within 2 days.

Another issue for SN follow-up studies is the area of sky available for rapid slew. If Constellation-X's slew capability is limited to some fraction of the sky, then the number of targets it could potentially observe drops by that same fraction. With 20% sky coverage over the course of the 5-year mission, then Constellation-X would have a good chance of targeting one bright SN Ia over its lifetime. This level of sky coverage (20%) is the absolute minimum that would allow this science to be done.

Constellation-X studies on the structure of the shocked ejecta and ambient medium in Type Ia SNe will be instrumental to resolving the current debate over the

explosion mechanism and progenitor systems (see Badenes et al. 2003; Badenes & Bravo 2001). Using Chandra observations of the Tycho SNR as a benchmark (Figure 1), several requirements for Constellation-X arise. While an angular resolution of 10″–15″ is adequate for studying the clumpy ejecta emission (based on images and spectra from Hwang et al. 2002), better resolution would help distinguish forward shock emission from ejecta at the remnant's rim. The calorimeter's goal of 2-eV spectral resolution gives a resolution $R = E/\Delta E = 3{,}000$ at the iron Kα lines. In this region, ~10 bright lines are expected from individual charge states spread over a few hundred eV, so even if the velocity of the shocked ejecta in Tycho is ~3,000 km s^{-1}, the kinetic shifts and broadenings should be ~ 60 eV and line blending should not be a major issue.

5.2.3 *Probing Cosmic-Ray Acceleration in Supernova Remnants*

The presence of non-thermal X-ray emission in shell-type SNRs confirms that such remnants are the sites of high-energy particle acceleration that are part of the cosmic-ray spectrum. Assuming typical magnetic fields, the radio and X-ray properties of several young SNRs indicate the presence of electrons with energies of 10–50 TeV, which still falls far short of the "knee" in the cosmic-ray spectrum at an energy of ≥ 1,000 TeV. Moreover, while the total cosmic-ray energy density is dominated by ions, only the emission from electrons is directly observed in X-rays. Two key questions arise: What are the maximum energies available from particle acceleration in SNRs? Is there evidence for hadron acceleration in SNR shocks?

Hadron acceleration by SNR shocks can be identified through dynamical effects. For a given shock velocity, strong cosmic-ray acceleration will yield a lower-than-expected temperature than if the full shock energy heated the gas. Crucial X-ray measurements, then, are the temperature and velocity of the shocked gas. A large effective area and high spectral resolution are required to characterize gas in SNRs with primarily non-thermal X-ray emission (e.g. G347.3–0.5). The spectral resolution provided by the Constellation-X calorimeter will allow detection of thermal broadening, or a centroid shift, associated with the expanding shock for velocities ≥ 600 km s^{-1}. Line ratios will establish the temperature of the X-ray emitting gas. Comparing the shock velocity with the electron temperature will reveal the fraction of shock energy used in particle acceleration, thus identifying the hadronic component of the particles.

5.2.4 *Pulsars and Their Wind Nebulae*

Pulsars are the most extreme form of matter short of black holes. Their ultra-high densities, rapid rotations, and strong magnetic fields carry imprints of their formation processes in core-collapse SN. As they age pulsars spin down, depositing vast amounts of energy into their surroundings through relativistic winds and, in some cases, jets. Key elements of their evolution-

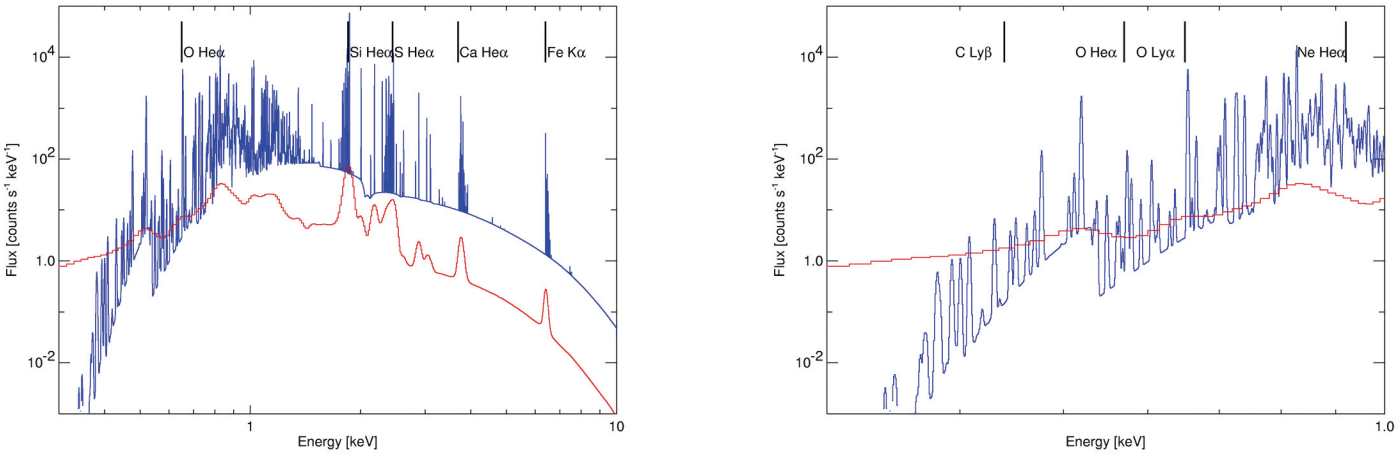

Figure 5: Simulated X-ray spectra, based on a model of Badenes et al. (2003), of the ejecta emission from Tycho's SNR convolved with the XMM EPIC-MOS (red) and Constellation-X XRS (blue) response functions. The left panel shows the entire band from 0.3–10 keV and the right panel shows an expanded view of the low energy region. Prominent line features from several abundant elements in the ejecta are noted.

ary history are revealed by these wind nebulae and the properties of the ejecta they sweep up.

Of particular importance are "naked" pulsar wind nebulae (PWNe) like the Crab Nebula and 3C 58 (see Figure 6), which exhibit little or no evidence of ejecta or material swept up by the SNR blast wave. This lack of observed thermal emission implies that they are expanding into extremely rarefied surroundings. However, ejecta must have formed in the explosion. Interestingly the size of the PWN (9.3 pc by 5.6 pc assuming a distance of 3.2 kpc) requires average expansion velocities of ≥ 10,000 km s^{-1}, while the highest velocities measured are of order 900 km s^{-1}. Identification of the higher-velocity gas is crucial to understand how this nebula has evolved. Based on Chandra observations, a 100-ks Constellation-X observation of the western region of 3C 58 will yield a surface brightness of 7 × 10^{-3} cts ks^{-1} $arcsec^{-2}$ in the Ne IX triplet. With Constellation-X's goal of 2-eV spectral resolution, velocities as low as ~ 600 km s^{-1} can be resolved which can easily be measured with roughly 100 counts in the line. This will allow the ejecta expansion to be measured on 10″–15″ scales. Using line ratios, the temperature and ionization state of the gas can also be determined and the density estimated. These measurements will establish the expansion profile of the ejecta, and provide constraints on the wind of the progenitor star.

5.2.4 Observatory Specifications

The most important instrumental performance characteristic for this subject area considered in its entirety is the point-spread function (PSF) of the telescope, which should meet the goal of 5″ or less. The most important studies that require this PSF value include the ejecta knots in Cas A, SNRs in the Magellanic Clouds and beyond. Some studies of larger SNRs (e.g., Tycho and SN1006) would yield valuable results with a PSF of 10″–15″, but a better PSF would result in better science.

Next in importance is spectral resolution, which for the non-dispersive device should be ~2 eV below 8 keV. At the oxygen K lines this corresponds to a velocity resolution of ~1000 km s^{-1}. The prime science is to measure velocities and line broadening as detailed in several studies above. The non-X-ray background needs to be kept at or below the level of the unresolved cosmic X-ray background.

The nominal effective area of the Constellation-X baseline is sufficient to study SNRs in M31 and M33; it would need to be increased significantly to study remnants in the more distant galaxies M81 and M101.

One requirement on the FOV of the high-resolution non-dispersive spectrometer is that it needs to be large enough that local background can be accurately subtracted from unresolved targets. From very simple general considerations it can be shown that one gets to 90% of the optimum signal-to-noise ratio when the area for background estimation is roughly 3× larger than the source extraction area. FOV should not be increased at the expense of effective area, since many studies can be done by raster scanning or mosaicking over a large extended target. This capability must be available to observers and it should be possible to execute such observations efficiently, i.e., with minimum setup or other overheads.

The high count rate capability requirement for SNRs is 3,000 cts s^{-1}, which corresponds to a 2.5′ square region of a bright portion of Cas A.

Event timing accuracy of 100μs for all instruments should be adequate for pulsar timing studies. For the hard X-ray telescope, extending the upper end of the energy band to beyond 78 keV would allow the study of nuclear transition lines from radioactive ^{44}Ti in young Galactic SNRs. Angular resolution of 1′ is probably acceptable for this instrument and it should have a FOV no less than that of the soft X-ray telescope.

5.3 Accreting Collapsed Objects

Sensitive spectroscopic observations of the X-ray emission from compact stellar objects (neutron stars, white dwarfs, and black holes) can provide the most direct experimental constraints on an array of important topics in astrophysics. High-resolution spectroscopy provides, among other things, a probe into stellar structure and evolution, stellar nucleosynthesis, the chemical evolution of our Galaxy, the physics of the densest states of matter, energy conversion in accretion flows, and the structure of space-time in the vicinity of black holes.

The study of X-ray emitting compact stellar remnants has evolved dramatically over the last few years, with spectroscopic observations from Chandra and XMM

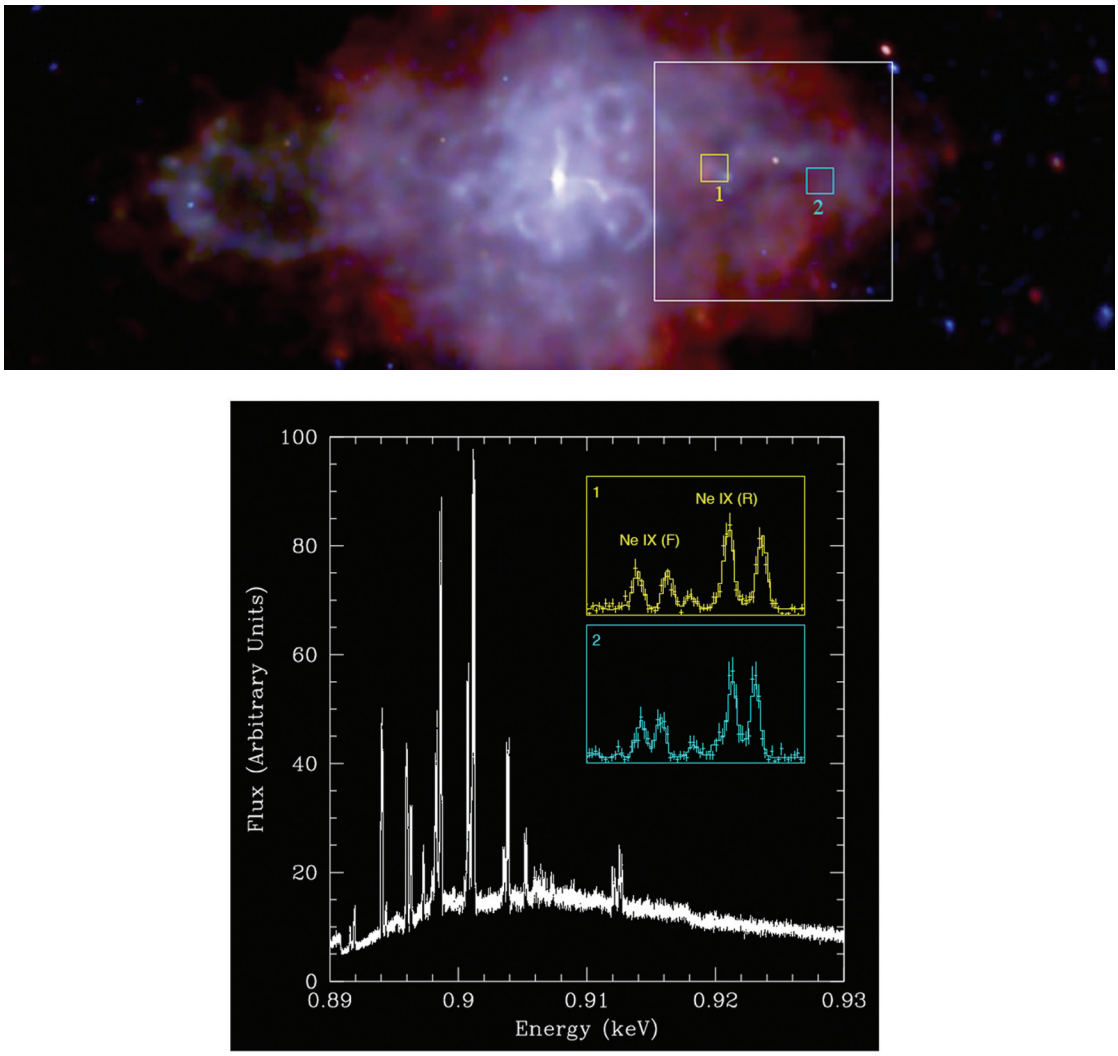

Figure 6: (top): Chandra image of 3C 58 with the Constellation-X calorimeter field of view (white) and two 15″× 15″ extraction regions indicated. (bottom): Simulated spectra of the entire region (white) and the Ne IX (helium-like) K line complex from the two smaller regions (yellow and cyan, corresponding to the colored extraction regions). The two-component spectrum observed with Chandra is assumed, with a power law accompanied by a thermal spectrum assumed to originate in a shell. The expansion velocity of the shell is assumed to be 900 km s^{-1}, as observed in optical filaments. The Doppler-shifted features from the front and back shells are clearly separated, and the variation in the projected velocity with radius is also evident as a smaller separation between the lines in the western-most (cyan)

and detections of coherent millisecond variability in X-ray bursts with the Rossi X-ray Timing Explorer (RXTE).

5.3.1 Using Neutron Stars as Probes of Fundamental Physics

Accreting neutron stars in X-ray binary systems provide the opportunity to explore important aspects of fundamental physics under extreme conditions that are not achieved anywhere else in the observable Universe. The extreme conditions in the deep interiors of neutron stars enable us to probe the highest densities known in the Universe, and test aspects of Einstein's theory of General Relativity when the gravitational field is very strong. The mass and radius of a neutron star depend directly on the physics of the interactions between fundamental particles: protons, neutrons and their constituent quarks. The theory of such interactions, Quantum Chromodynamics (QCD), is extremely complex and not yet sufficiently constrained to accurately predict the state of matter at such extreme densities. One way to

constrain the theory is with precise measurements of both the masses and radii of neutron stars. (Thorsett & Chakrabarty 1999; Orosz & Kuulkers 1999; Nice, Splayer & Stairs 2004).

While accurate masses for neutron stars have been obtained from careful observations of young neutron star pulsars in binary systems by observing spectral lines produced from elements (like iron) in the atmospheres of accreting neutron stars, Constellation-X can determine both the masses and radii of such neutron stars. In these accreting systems the continuous supply of metals will yield more prominent absorption lines than non-accreting neutron stars. Accretion of light elements will lead to thermonuclear X-ray bursts, brief but bright flashes of thermal X-rays shining through the neutron star atmosphere, that should produce spectral lines. In addition these older neutron stars may have gained enough mass to probe the mass-radius relation in a different regime than the young pulsars. This leads to the possibility of obtaining mass-versus-radius curves for neutron stars, telling us a great deal about the state of matter at extreme densities (Lattimer & Prakash 2001).

Careful study of the absorption spectrum leads to a direct measurement of the gravitational redshift at the surface of the star, which provides a measure of the mass-to-radius ratio but not a separate measure of the mass and the radius. By accurately measuring both the gravitational redshift and the line profile (due to rotational broadening), it is possible to determine both the mass and radius of the star.

Indeed, observations of the neutron star binary EXO 0748-676 made with XMM-Newton provide the first evidence for the presence of absorption lines during X-ray bursts (Cottam, Paerels & Mendez 2002). With its much larger collecting area, Constellation-X will be able to make much more sensitive searches for such lines, and will be able to better measure the energies and profiles of the lines (see Figure 7). Neutron star radii can also be determined from doppler broadening of the lines if the spin frequency is known. Modeling of the observed widths of the EXO 0748-676 absorption lines using the recently measured spin frequency shows they are consistent with a neutron star radius in the 9.5–15 km range (Villarreal & Strohmayer 2004). Constellation-X should be able to measure the radius to within a few percent by measuring the widths of the absorption lines with much greater precision than is possible with current data.

The shapes of surface absorption (or emission) lines from neutron stars can also tell us about fundamental aspects of Einstein's theory of General Relativity. Because the profiles of lines observed at infinity depend on the detailed trajectories of photons from different parts of the neutron star through the potential well, the profile shapes are sensitive to the precise magnitude of relativistic effects that affect those trajectories (Ozel & Psaltis 2003; Bhattacharyya, Miller & Lamb 2004). The most famous of those effects is the one associated with the relativistic 'dragging' of reference frames. By observing line features with the large collecting area and high spectral resolution of Constellation-X it may be possible to measure the amount of frame dragging for given spin and mass of the neutron star, and thus test General Relativity.

5.3.2 Accretion and Massive Stellar Wind Dynamics in High Mass X-ray Binaries

High-mass X-ray binaries (HMXBs) are composed of an early-type star and a compact object, either a neutron star or black hole. The companion star of a standard HMXB is an OB giant or supergiant; while a second, and more prevalent class, the Be-XRBs, harbors a rapidly spinning B-emission line star. Two HMXBs have been identified as black hole systems: Cyg X-1 and LMC X-3. As bright X-ray sources, HMXBs represent a unique phase of the binary evolution. In the evolutionary context, mass transfer plays the dominant role (Verbunt & van den Heuvel 1995).

In studying HMXBs, one pursues an understanding of the accretion of material onto compact objects—the conversion of gravitational potential energy into radiation—and the mass loss from early-type stars—the physics of the stellar wind that provides the accreting material (Liedahl et al. 2001). Both aspects of HMXB physics fall within the purview of X-ray spectroscopy. Recent Chandra observations have shown that high-resolution X-ray line spectra convey the spectral imprints of large-scale velocity fields. These spectra have provided detailed constraints on ionization distributions (and thus density fields) and by recording orbital-phase-resolved spectra, have clearly implied deviations from spherical outflow and deviations from smoothness (Paerels et al. 2000; Sako et al. 1999).

With Constellation-X, we can expect to increase the sample size by roughly an order of magnitude. With larger collecting area, orbital-phase-resolved spectra can be obtained with much better time resolution, therefore allowing us to study intrinsic spectral variability resulting from inhomogeneities in the stellar wind.

A central theme in X-ray spectroscopic studies of HMXBs is the assessment of the effects of the primary X-ray continuum on the physical state and dynamics of the wind (Stevens & Kallman 1990). In HMXBs we have access to ionization parameters ranging across four to five orders of magnitude, and temperatures and densities ranging across three orders of magnitude. The emission-line and absorption-line spectra are extremely rich. Note that the two line transfer processes in HMXB winds—resonant line scattering (which competes with recombination in producing X-ray lines; Wojdowski et al. 2003) and resonant Auger destruction, both of which profoundly constrain the structure and dynamics of HMXB accretion flows, require resolving powers of several hundred. The contribution from resonance line scattering of the X-ray continuum to the net line spectrum depends on the velocity gradient structure in the wind, thereby providing an indispensable diagnostic. In addition, P Cygni profile analysis imposes simultaneous constraints on the velocity field and the density field over the entire source volume.

5.3.3 Physics of Accreting White Dwarfs

Among the various classes of accreting compact binaries, cataclysmic variables (CVs)—semi-detached binaries composed of a low-mass secondary and an accreting white dwarf primary—are arguably the best laboratories in which to study accretion flows. Relative to neutron star binaries, white dwarf binaries have ~100 times lower velocities (v/c ~0.01). The relatively low velocities means that the lines are narrow ($\Delta E/E \sim 10^{-3}$), so that they stand out against the continuum and so provide detailed diagnostics of the plasma temperature, density, abundances, emission measure distribution, and velocity. The relatively low luminosities means that photoionization is not as important in CVs, the relatively low temperatures means (blackbody temperatures T_{bb}~10 eV and virial temperatures T_{vir}~10 keV) means that the plasmas in CVs produce X-ray spectra that are rich in emission lines with critical diagnostics at soft energies. Constellation-X will increase by a factor of ~100 the number of CVs for which we will be able to obtain detailed X-ray spectra. Among the numerous detailed studies possible with Constellation-X, we discuss three that are unique to CVs.

First, compared to stars, the X-ray emitting plasma in CVs is expected to be dense. In magnetic CVs, high densities are the result of the magnetic channeling of the accreting material onto small spots near the white dwarf magnetic poles, while in nonmagnetic CVs it is the result of accretion through a disk and boundary layer onto a narrow belt on the white dwarf surface.

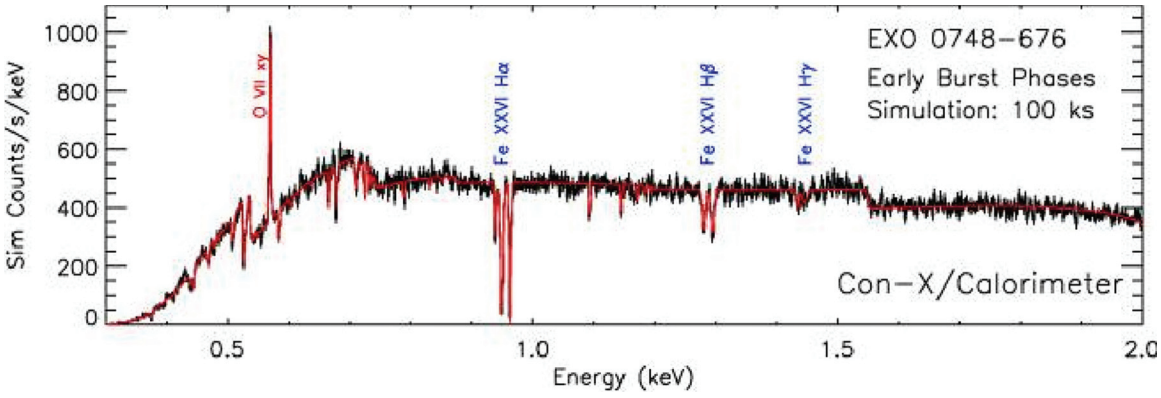

Figure 7: Simulated spectrum of the early phases of the X-ray bursts from the accreting neutron star EXO 0748-676 using the Constellation-X calorimeter. A 100 ks observation should result in 1 ks of burst time. The blue labeled lines are gravitationally red-shifted absorption lines from the neutron star atmosphere. The remaining spectral structure originates in the circumstellar material. The model was developed using the XMM-Newton data and theoretical calculations for the absorption line structure.

Mauche, Liedahl, and Fournier (2001, 2003) and Szkody et al. (2002) demonstrate the application of novel, high-density iron L density diagnostics to dense plasmas in EX Hya and U Gem. To apply these density diagnostics, it is necessary to resolve the Fe XVII 17.10 Å and 17.05 Å lines ($\Delta\lambda$ = 0.05 Å ; R ~ few times 350) and the Fe XXIII 11.74 A and the Fe XXII 11.77 Å lines ($\Delta\lambda$ = 0.03 Å ; R ~ few times 390). This is currently possible with the Chandra MEG ($\Delta\lambda$= 0.02 Å FWHM), but not with the XMM-Newton RGS ($\Delta\lambda$ ~ 0.07 Å FWHM). To apply the helium-like R density diagnostic for high Z elements, it is necessary to resolve the intercombination and forbidden lines, which in sulfur, argon, and iron are separated by 16, 19, and 31 eV.

A second area of CV science in which Constellation-X can make significant improvements is the study of systems in which the white dwarf is eclipsed by the secondary. Phase and eclipse ingress/egress-resolved spectroscopy has the potential to constrain the geometric as well as the thermal and density structure of the accretion flow. Currently, such studies are limited by counting statistics; the large effective area of Constellation-X will allow the first detailed studies of this kind.

Third, the unprecedented combination of energy resolution and sensitivity will for the first time permit the study of subtle but extremely powerful line transfer effects that offer probes of the physical conditions in CV plasmas. One example involves recombination iron lines in settings where opacity effects are important, for instance in the accretion column below the standoff shock above the surface of the white dwarf in magnetic CVs. Given the observed densities and the expected path lengths, the accretion column is expected to be optically thin to photoelectric absorption, thin to thick to Compton scattering, and thick to line scattering (Matt 1999, Terada et al. 2001), (see Figure 8).

5.3.4 Observatory Specifications

The scientific goals outlined above all require a spectral resolving power of order 1,000 across the 0.5-8 keV band. This spectral resolving power is of order that provided by the Chandra HETGS at energies below 1 keV; Constellation-X's increased effective area with respect to Chandra HETGS automatically ensures that spectroscopy that can currently be successfully performed with this instrument will be possible on sources ~20 to 50 times weaker than characteristic bright Galactic binaries. To perform phase-resolved spectroscopy of emission from bursting neutron stars (spin frequencies up to ~700 Hz have been seen) requires the capability to time-resolve photon arrival times well below a millisecond (eight phase bins in a 1/700 sec period results in a timing accuracy requirement of 1/5600 sec, or 0.16 msec). During an X-ray burst, the X-ray flux increases dramatically, and the observatory must be able to handle high count rates without loss of spectroscopic or timing resolution. (Note that this does not require that no information be lost on any photon; counting slower at full resolution is of course acceptable, because to first order that just increases the observation time.) The highest expected flux is ~1.0 counts s^{-1} cm^{-2}, which translates to count rates of ~7,000 counts s^{-1} in the microcalorimeter spectrometer, and ~650 counts s^{-1} in the grating spectrometer. The combination of the XMS and RGS in the baseline mission should meet the requirements imposed by these observations.

5.4 Solar System Studies

Suprisingly, given the low temperatures, a variety of high-energy processes are seen from all terrestrial planets, Jovian planets and minor bodies. Constellation-X can help advance our understanding of basic plasma and plasma-neutral processes within our solar system and, by implication, in extra-solar planetary systems.

5.4.1 Venus, Earth and Moon, and Mars

Most of the X-ray flux observed from Venus, Earth, Moon, and Mars is from fluorescent scattering of solar X-rays, either in the upper atmospheres of these planets or on the lunar surface. Following Chandra detection of Venusian and Martian X-rays in 2001 (Dennerl et al. 2002) simulations of Venusian X-ray emission predict pronounced brightening on the sunward limb (as was detected), and this limb brightening is sensitive to properties of the Venusian atmosphere above 110 km, thus presenting a way to monitor properties of the Venusian atmosphere. In contrast, the presence of Earth's pronounced magnetosphere provides an additional source of X-ray emission: When electrons, accelerated in the magnetosphere, strike the upper atmosphere, they may emit X-rays by bremsstrahlung. The X-ray intensity of this emission, which occurs at higher energies than fluorescence, is directly related to the

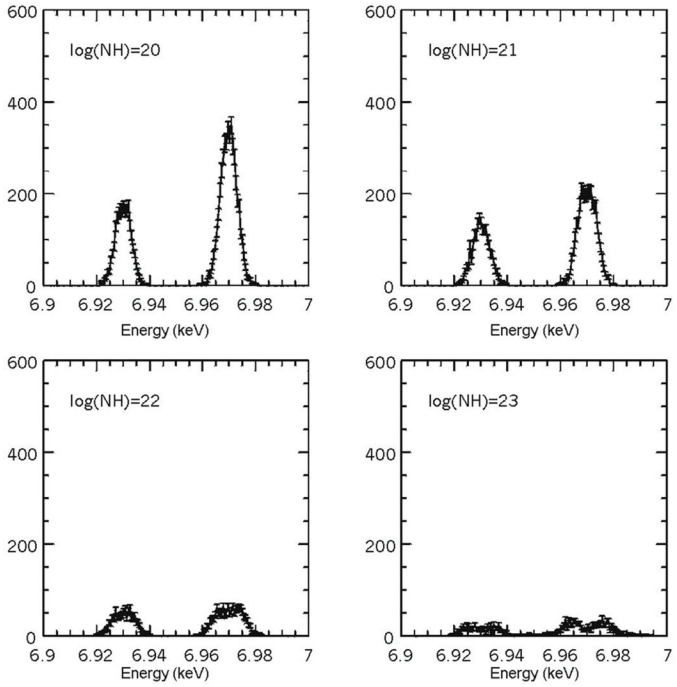

Figure 8: A simulated Constellation-X calorimeter observation of the line profiles of the Fe XXVI doublet for different column densities. While for low column densities, the matter is optically thin in the line center and the line shape is a Voigt profile, but for larger column densities, the matter becomes optically thick in the line centers and the lines become double-horn shaped. This spectroscopic signature provides a probe of the geometrical and physical conditions of the emitting plasma.

precipitated electron flux. The Martian X-ray properties observed were comparable to Venus due to their similar atmospheres and lack of strong magnetic fields.

Another source of X-ray emission observed from Mars exhibits properties similar to those seen in comets (see below) and the Moon's dark side. Chandra observations showed that this flux had spectral signatures resembling cometary X-ray spectra (Wargelin et al. 2004), suggesting X-ray emission from the geocorona, an extended cloud of hydrogen around the Earth. Chandra and XMM-Newton (Dennerl 2002) observations of Mars have revealed a faint, extended X-ray halo, displaying emission lines seen in cometary X-ray spectra. Understanding Mars' exosphere may aid in characterizing the X-ray properties of Earth's geocorona, subsequently revealing how this foreground emission could affect all X-ray observations.

5.4.2 The Jovian and Saturian systems

X-ray studies of Jupiter's auroral zones near the north and south poles, where the X-ray emission is most intense, offer a probe of Jupiter's magnetosphere (see the review by Bhardwaj and Gladstone 2000). Chandra and XMM-Newton data show that this auroral emission is due to the precipitation of highly ionized oxygen and either sulfur (favored by Chandra) or carbon (favored by XMM) into the polar regions (Horanyi et al. 1988; Cravens et al. 1995, 2003); the ionization states present and the line characteristics provide information on the electric fields present, thus probing the polar magnetosphere dynamics. Oscillations in the northern auroral flux observed in December 2000 (Gladstone et al. 2002) are likely associated with the energetic particle flux in the outer disk magnetosphere and with quasiperiodic radio bursts from Jupiter (McKibben, Simpson & Zhang 1993; MacDowall et al. 1993; Karanikola et al. 2004). More detailed observations of these oscillations and the conditions under which they appear would further constrain the dynamics of Jupiter's polar magnetosphere.

Chandra discovered faint X-ray emission from the Io plasma torus and Io, Europa, and possibly Ganymede (Elsner et al. 2002). While the origin of the X-ray emission from the torus in not clear, the emission from the Galilean moons is almost certainly due to bombardment of their surfaces by energetic hydrogen, oxygen, and sulfur atoms and ions.

Chandra observations of Saturn found variations in the averaged X-ray flux of a factor of ~4 over one week (Bhardwaj et al. 2005b) that appeared closely tied to the incident solar X-ray flux. In addition, on timescales of ~0.5 hour, an X-ray "flare" from Saturn was closely linked to the eruption of a solar X-ray flare. The same observations showed emission from the south polar cap and an emission line probably due to oxygen Ka fluorescence from the rings. These new objects are faint X-ray sources, and detailed investigation of their X-ray properties require the high-throughput and high-energy resolution provided by Constellation-X.

5.4.3 Comets

The 1996 discovery of strong X-ray emission from comet C/1996 B2 (Hyakutake) by ROSAT (Lisse et al. 1996) was surprising, since cometary atmospheres are known to be cold, with characteristic temperatures between 10 and 1,000 K. Chandra has found that the soft X-ray spectra from some comets is dominated by line emission, not by continuum. Solar wind minor ions readily undergo charge transfer (or exchange) reactions when they are within ~ 1 nm of a neutral atomic species. Model charge exchange X-ray spectra are in good agreement with the low resolution X-ray spectra from comets, and the line centers of the high-resolution spectra have been successfully predicted using charge exchange theory (Lisse et al. 1999, 2001; Krasnopolsky & Mumma 2001; Weaver et al. 2002).

The best spectrum available (Chandra ACIS-S) of cometary X-ray emission is limited in energy resolution and spatial quality. Due to the extended nature of comets, both Chandra and XMM data require complex interpretation, while suffering from low spectrometer throughput. The Constellation-X spectrometer will be sensitive to the forest of lines predicted by solar charge exchange models (e.g., OVIII, OVII, NVIII, NVI & CVII). Constellation-X will also offer sufficient resolution (as shown by Wegmann et al. 1998, and Kharchenko and Dalgarno 2000) to distinguish between emission due to solar wind charge transfer and bremsstrahlung.

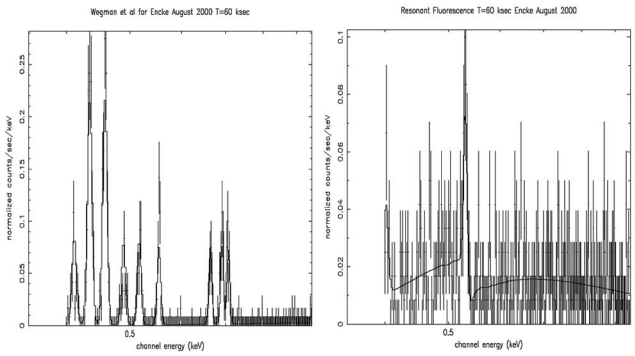

References

Chapter 1- Introduction

Brandt, W.N., and Hasinger, G., ARA&A, in press, 2005; (astro-ph/0501058)
Paerels, F. B.S., and Kahn, S.M., ARA&A, 41, 291-342, (2003)
Smith, R. K. et al. 2001, ApJ, 556, L91
Young, A.J. and Reynolds, C.S, in ApJ, 529, 101 (2000)

Chapter 2 - Black Hole Science

Abramowicz, M. A., & Kluzniak, W. 2001, A&A, 374, L19
Abramowicz, M. A., Kluzniak, W., McClintock, J. E., & Remillard, R. A. 2004, ApJ, 609, L63
Armitage & Reynolds, 2003, MNRAS, 341, 1041-1050
Baganoff, F. K. et al. 2001, Nature, 413, 45
Baganoff, F. K. et al. 2003, ApJ, 591, 891
Belanger, G. et al. 2005, ApJ, submitted
Bland-Hawthorn, J. & Cohen, M. 2003, ApJ, 582, 246
Blandford, R.D., Znajek, R.D., 1977, MNRAS, 179, 433
Bower, G. C., Falxke, H., Wright, M. C. H., & Backer, D. C., 2005, ApJ, 618, L29
Brandt, W. N. & Hanisger, G., 2005, (astro-ph/0501058)
Colbert, E. J. M., & Mushotzky, R. F. 1999, ApJ, 519, 89
Cropper, M., Soria, R., Mushotzky, R. F., Wu, K., Markwardt, C. B. & Pakull, M. 2004 MNRAS, 349, 39.
Dovciak, M., Karas, V., Yaqoob, T., 2004, ApJS, 153, 205
Eckart, A. et al. 2004, A&A, 427, 1
Fabian, A.C., et al., 2002, MNRAS, 331, L35
in't Zand, J. J. M., et al. 2002, A&A, 390, 597
Iwasawa, K., Miniutti, G., Fabian, A. C., 2004, MNRAS, 355, 1073
Madau, P., & Rees, M. J., 2001, ApJ, 551, L27
Markowitz, A. G. et al. 2003, ApJ, 593, 96.
Mauerhan, J. C. et al. 2005, ApJ, accepted, (astro-ph/0503124)
McClintock, J. E. & Remillard, R. A. 2004, to appear in "Compact Stellar X-ray Sources," eds. W.H.G. Lewin and M. van der Klis, Cambridge University Press, (astro-ph/0306213)
Miller, M. C., & Hamilton, D. P., 2002, ApJ, 576, 894
Miller, J. M. et al., 2002, ApJ, 578, 348
Miller, J. M. et al. 2004, ApJ, 606, L131.
Miller, J. M. & Homan, J. 2005, ApJ, 618, L107.
Miller, J. M., Fabian, A. C., & Miller, M. C., 2004, ApJ, 614, L117
Miniutti, G., Fabian, A. C., & Miller, J. M. 2004, MNRAS, 351, 466
Murakami, H. et al. 2001, ApJ, 550, 297
Portegies-Zwart, S. F., et al., 2004, MNRAS, 355, 413
Pounds, K. et al., 2003, MNRAS, 345, 705
Reeves, J. N., et al., 2003, ApJ, 593, L65
Remillard, R. A., Morgan, E. H., McClintock, J. E., Bailyn, C. D., & Orisz, J. A. 1999, ApJ, 522, 397.
Remillard, R. A., Muno, M. P., McClintock, J. E., & Orosz, J. A. 2002, ApJ, 580, 1030.
Reynolds, C. S. & Nowak, M. A. 2003, Physics Reports, 377, 389
Strohmayer, T. E. 2001, ApJ, 552, L49.
Strohmayer, T. E. & Mushotzky, R. F. 2003, ApJ, 586, L61.
Tanaka, Y., et al., 1995, Nature, 375, 659
Totani, T. et al. 2005, ApJ, 621, L9
White, S., 2004, Proceedings of KITP Conference: Galaxy Intergalactic Medium Interactions (October 2004)
Wilms J., et al., 2001, MNRAS, 328, L27
Young & Reynolds, 2000, ApJ, 529, 101
Yusef-Zadeh, F. et al. 2002, ApJ, 570, 665
Yusef-Zadeh, F. & Königl, A. 2004, (astro-ph/0403201)
Yusef-Zadeh, F. et al. 2005, (astro-ph/0502260)

Chapter 3 - Dark Energy, Dark Matter and Cosmology

Allen, S. W., Schmidt, R. W., Ebeling, H., Fabian, A. C., and van Speybroeck, L., 2004, MNRAS, 353, 457
Allen, S. W., Schmidt R. W., & Fabian A. C. 2002, MNRAS, 334, L11
Arabadjis, J. S., Bautz, M. W., & Garmire, G. P. 2002, ApJ, 572, 66
Baumgartner, W., et al. 2004, in preparation
Bautz, M. W., & Arabadjis, J. S. 2004, in Carnegie Observatories Astrophysics Series, Vol. 3, edited by J. S. Mulchaey, A. Dressler, & A. Oemler
Buote, David A.; Lewis, Aaron D.; Brighenti, Fabrizio; Mathews, William G., 2003, ApJ, 595, 151
Carroll, S., 2005, S&T, 109, no. 3, 32
Cen, R. & Ostriker, J.P. 1999, ApJ, 519, L109
Davè, R. et al. 2001, ApJ, 552, 473
David, L. P., 2000, ApJ, 529, 682
Donahue, M. & Voit, G.M., 2004, Carnegie Observatories Astrophysics Series, Vol. 3, Edited by J.S. Mulchaey, A. Dressler, and A. Oemler, , p. 144
Ettori, S., Fabian A. C., 1999, MNRAS, 305, 834
Ettori, S., et al., 2004, MNRAS, 354, 111
Evrard, A. E. 2004, in Carnegie Observatories Astrophysics Series, Vol. 3: Clusters of Galaxies, edited by. J. S. Mulchaey, A. Dressler, & A. Oemler
Fabian, A. C. & Nulsen, P. E. J. 1977, MNRAS, 180, 479
Fang, T., Bryan, G., & Canizares, C. 2002, ApJ, 564, 605
Fang, T., et al. 2002, ApJ, 572, L127
Fang, T., Sembach, K., & Canizares, C. 2003, ApJ, 586, L49
Finoguenov, A.; Burkert, A.; Böhringer, H, 2003, ApJ, 594,136
Fox, D. C., Pen, U.-L., 2002, ApJ, 574, 38
Gnedin, N.Y., & Ostriker, J.P. 1997, ApJ, 486, 581
Hashimoto, Yasuhiro; Barcons, X.; Böhringer, H.; Fabian, A. C., Hasinger, G.; Mainieri, V.; Brunner, H. 2004, A&A, 417, 819
Jones, L. R., et al. 2004, in Carnegie Observatories Astrophysics Series, Vol. 3, edited by J. S. Mulchaey, A. Dressler & A. Oemler
Kaiser, C. R., & Binney, J. 2003, MNRAS, 338, 837
Komatsu, E., Seljak, U. 2001, MNRAS, 327, 1353
Krolik, J. H., Raymond, J. C., 1988, ApJ, 335, 39
Lewis, A. D., Buote, D. A., & Stocke, J. T. 2003, ApJ, 586, 135
Loken, C., Norman, M. L., Nelson, E., Burns, J., Bryan, G.L., & Motl, P. 2002, ApJ, 579, 571
Markevitch, M. 1998, ApJ, 504, 27
McKernan et al. 2004, ApJ, 617, 232, ApJ
Molendi, S., & Pizzolato, F. 2001, ApJ, 560, 194
Monar, S. M., Haiman, Z., Birkinshaw, M., Mushotzky, R. F., 2004, ApJ, 601, 22
Mushotzky, R. F., Serlemitsos, P. J., Boldt, E. A., Holt, S. S., & Smith, B. W. 1978, ApJ, 225, 21
Navarro, J. F., Frenk, C. S., White, S. D. M. 1997, ApJ, 490, 493 (NFW)
Nicastro, F., et al. 2002, ApJ, 573, 157

Nicastro, F., et al. 2005a, Nature, 433, 495
Nicastro et al. 2005b, ApJ, in press (astro-ph/0504187)
Peterson, J. R., Kahn, S. M., Paerels, F. B. S., Kaastra, J. S., Tamura, T., Bleeker, J. A. M., Ferrigno, C. & Jernigan, J. G., 2003, ApJ, 590, 207
Peterson, J. R. et al. 2001, A&A, 365, L104
Peterson, J. R., Kahn, S. M., Paerels, F. B. S., Kaastra, J. S., Tamura, T., Bleeker, M., Ferrigno, C., & Jernigan, J. 2003, ApJ, in press (astro-ph/0210662)
Pratt, G. W., Arnaud, M. 2002, A&A, 394, 375
Renzini, A. 2004, in Carnegie Observatories Astrophysics Series, Vol. 3: Clusters of Galaxies, edited by J. S. Mulchaey, A. Dressler & A. Oemler
Rosati, P. et al., 2004, AJ, 127, 230
Sarazin, C. L. 1986, Rev. Mod. Phys., 58, 1
Sarazin, C. L., 1989, ApJ, 345, 12
Shen, S., White, S.D.M., Mo, H.J., Voges, W., Kauffman, G., & Tremonti, C. 2005, MNRAS, in press
Shull, J.M., Tumlinson, J., & Giroux, M.L. 2003, ApJ, 594, L107
Springel, D., Proc. of IAUS 222 (Cambridge Univeristy Press), 2004, p. 260
Tozzi, P., Rosati, P., Ettori S., Borgani S., Mainieri V., Norman, C., 2003, ApJ, 593, 705
White, S. D. M., Frenk, C. S., 1991, ApJ, 379, 52
Voit, G. M. & Bryan, G. L., 2001 Nature, 414, 425

Chapter 4 - Cosmic Feedback, The Growth of Structure

Adelberger, K., et. al, 2003, ApJ, 584, 45.
Alexander, D.M., Brandt, W.N., Hornschemeier, A.E., Garmire, G.P., Schneider, D.P., Bauer, F.E., & Griffiths, R.E., 2001, AJ, 122, 2156
Alexander, D.M., et al., 2005, Nature, 434, 738
Avillez, M.A., 1999, "Stromlo Workshop on High Velocity Clouds", Edited by B.K. Gibson & M.E Putman, ASP Conference Series, 166, 103.
Barger, A. J., Cowie, L. L., Capak, P., Alexander, D. M., Bauer, F. E., Fernandez, E., Brandt, W. N., Garmire, G. P., & Hornschemeier, A. E. 2003, AJ, 126, 632
Barger, A.J., Cowie, L.L., Mushotzky, Yang, Y., Wang, W. H., Steffen, A. T. & Capak, P., 2005, AJ, 129, 578
Barger, A.J, et al. 2005, AJ, in press (astro-ph/0410527)
Bauer, F. E., Alexander, D. M., Brandt, W. N., Scheneider, D. P., Treister E., Hornschemeier A. E. Garmire G. P. 2004, AJ, 128, 2048
Becker, W. & Aschenbach, B. 2002, MPE Report 278, p. 63
Belmont, R. et al. 2005, submitted to Nature.
Benson, A.J., et. al , 2000, MNRAS, 314, 557.
Brandt, W.N., et al. 2005, astro-ph/0411355
Bregman, J.N., 1980, ApJ., 236, 577.
Chartas, G., Brandt, W. N., & Gallagher, S. C., 2003, ApJ, 595, 85
Chevalier, R., Clegg, A., 1985, Nature, 317, 44
Cowie, L.L., Barger, A.J., Bautz, M.W., Brandt, W. N., & Garmire, G.P. 2003, ApJ, 584, L57
Dave, R. et al. 2001, ApJ, 552, 473
De Lucia, G., Kauffmann, G., & White, S.D.M. 2004, MNRAS, 349, 1101
Di Matteo, T., Springel, V. & Hernquist, L. 2005, Nature, 443, 604
Dogiel, V. A. et al. 2005, ApJ, 581, 1061
Dwek, E. 1997, ApJ, 484, 779
Fabian, A. C., Sanders, J. S., Allen, S. W., Crawford, C. S., Iwasawa, K., Johnstone, R. M., Schmidt, R. W., Taylor, G. B. 2003, MNRAS, 344, L43
Fabian, A.C. 1999, MNRAS, 308, L39
Figer, D. F. et al. 2004, ApJ, 601, 319
Ghavamian, P., Raymond, J. C., Smith, R. C., & Hartigan, Kaastra, J. S., Mewe, R., Liedahl, D. A., Komossa, S., & Brinkman, A. C. 2000, A&A, 354, L83
Kaspi, S. et al. 2002, ApJ, 574, 643
King, A.R. & Pounds, K.A. 2003, MNRAS, 345, 657
Kobulnicky, H.A., 1998, Abundance Profiles: Diagnostic Tools for Galaxy History, ASP Conf. Ser. Vol. 147, 108
Krivonos, R. et al. 2005, ApJ, in press (astro-ph/0409093)
Law, C. & Yusef-Zadeh, F. 2004, ApJ, 611, 858
Lehnert, M., Heckman, T., 1995, ApJS, 95, 99
Mainieri, V., Bergeron, J., Hasinger, G., Lehmann, I., Rosati, P., Schmidt, M., Szokoly, G., & Della Ceca, R. 2002, A & A, 393, 425
Marconi, A., Risaliti, G., Gilli, R., Hunt, L.K., Maiolino, R., & Salvati, M. 2004, MNRAS, 351, 169
Muno, M. P. et al. 2004a, ApJ, 613, 323
Muno, M. P. et al. 2004b, ApJ, 613, 1179
Murray, N., Chiang, J., Grossman, S.A., & Voit, G.M. 1995, ApJ, 451, 498
Norman, C.A., Ikeuchi, S., 1989, ApJ, 345, 372.
Ogle, P. M., Marshall, H. L., Lee, J. C., & Canizares, C. R., 2000, ApJ, 545, 81
Park, S. et al. 2005, ApJ submitted
Peterson et al. 2001, A&A, 365, L104
Proga, D., Stone, J.M., & Kallman, T.R. 2000, ApJ, 543,686
Reynolds, C.S. & Nowak, M.A. 2003, Phys. Rep., 377, 389
Sako, Masao, Kahn, Steven M., Paerels, F., & Liedahl, D. A., 2000, ApJ, 543, L115
Shore, S. N. & La Rosa, T. N. 1999, ApJ, 521, 587
Silk, J. & Rees, M.J. 1998, A&A, 331, L1
Sobolewska, M.A., Siemiginowska, A., & Zycki, P.T. 2004, ApJ, 608, 80
Sommer-Larsen, J., et. al., 2003, ApJS, 284, 693.
Strateva, I. et al. 2005, AJ, in press (astro-ph/0503009)
Streblyanska, A., Hansiger, G., Finoguenov, A., Barcons, X., Mateos, S. & Fabian, A.C., 2005, A&A, 432, 395
Strickland, D., et. al 2004a, ApJS, 151, 193.
Strickland, D., et. al 2004b, ApJ, 606, 829.
Strickland, D., Stevens, I., 2000, MNRAS, 314, 511
Tamura et al. 2001, A&A, 365, L87
Toft, S., et. al, 2002, MNRAS, 335, 799
Tremonti, C., et. al, 2004, ApJ, 613, 898
Ueda, Y., Akiyama, M., Ohta, K., & Miyaji, T. 2003, ApJ, 598, 886
Vignali, C., Brandt, W.N., & Schneider, D.P. 2003, AJ, 125, 433
Wang Q. D. 2004 (astro-ph/0410035)
Weisskopf, M. C., O'Dell, S. L., Paerels, F., Elsner, R. F., Becker, W., Tennant, A. F., & Swartz, D. A. 2004, ApJ, 601, 1050
White, S., 2004, Proceedings of KITP Conference: Galaxy Intergalactic Medium Interactions
Wilkes, B.J., Schmidt, G.D., Cutri, R.M., Ghosh, H., Hines, D.C., Nelson, B., & Smith, P.S. 2002, ApJ, 564, L65
Worsley , M. A. et al., 2005 MNRAS, 357, 1281
Yusef-Zadeh, F. et al. 2002, ApJ, 570, 665
Yusef-Zadeh, F. & Königl, A. 2004, (astro-ph/0403201)
Yusef-Zadeh, F. et al. 2005, (astro-ph/0502260)
Zdziarski, A.A. & Gierlinski, M. 2004, Progress of Theoretical Physics Supplement, 155, 99

Zubko V., Dwek, E., & Arendt, R. G. 2004, ApJS, 152, 211

Chapter 5 - Life Cycles of Matter

Audard, M. Gudel, M. Drake, J. J., Kashyap, V. L. 2000, ApJ 541, 396
Badenes, C., & Bravo, E. 2001, ApJ, 556, L41
Badenes, C., Bravo, E., Borkowski, K. J., and Domnguez, I. 2003, ApJ, 593, 358
Bhardwaj, A., Gladstone, G. R., 2000, Rev. Geophys., 38, 295
Bhardwaj, A., et al., 2005b, in preparation
Bhattacharyya, S., Miller, M.C., & Lamb, F.K. 2004, ApJ, submitted (astro-ph/0412107)
Cottam, J., Paerels, F., & Mendez, M. 2002, Nature, 420, 51.
Cravens, T. E., Howell, E., Waite, J. H., and Gladstone, G. R. 1995 J. Geophys. Res., 100, 17,153
Cravens, T. E., et al.; 2003, J. Geophys. Res., 108
Dennerl, K., Burwitz, V., Englhauser, J., Lisse, C.M., Wolk, S. 2002, A&A, 386, 319
Dennerl, K., 2002, A&A, 394, 1119
Doschek, G.A. 1990, ApJS, 73, 117
Elsner, R. F., et al., 2002, ApJ. 572, 1077
Favata, F., Micela, G., Silva, B., Sciortino, S., Tsujimoto, M., 2005, A&A, 433, 1047
Feigelson, E. 2003, in IAUS, 219, 217
Feldman, U. 1990, ApJ, 364, 322
Feldmeier, A., Oskinova, L., & Hamann, W.-R. 2003, A&A, 403, 217
Ghavamian, P., Raymond, J. C., Smith, R. C., & Hartigan, P., 2001, ApJ, 547, 995
Gladstone, G. R., et al., 2002, Nature, 415, 1000
Glassgold, A.E., Feigelson, E.D., Montmerle, T., & Wolk, S., 2004, in Workshop on Chondrites and the Protoplanetary Disk, ASP Conf. Series, 9026
Guedel, M. 1997, ApJ, 480, 121
Horanyi, M., Cravens, T. E., and Waite, J. H. 1988, J. Geophys. Res., 93, 7251
Hughes, J. P., Rakowski, C. E., Burrows, D. N., & Slane, P. O. 2000, ApJ, 528, L109
Hughes, J. P., Rakowski, C. E., & Decourchelle, A. 2000, ApJ, 543, L61
Hwang, U., Decourchelle, A., Holt, S. S., & Petre, R. 2002, ApJ, 581, 1101
Hwang, U., Holt, S. S., & Petre, R. 2000, ApJ, 537, L119
Hwang, U., & Laming, J. M. 2003, ApJ, 597, 362
Imanishi, K., Koyama, K., & Tsuboi, Y. 2001, ApJ, 557, 747
Karanikola, I., Athanasiou, M., Anagnostopoulos, G. C., Pavlos, G. P., Preka-Papadema, P., 2004, Planet Space Sci., 52, 543
Kashyap, V. L., Drake, J. J., Gudel, M., Audard, M. 2002, ApJ, 580, 1118
Kastner, J. H., Huenemoerder, D. P., Schulz, N. S., & Canizares, C. R. 2002, ApJ, 567, 434
Kharchenko, V., Dalgarno, A., 2000, J. Geophys. Res., 105, 18351
Krasnopolsky, V. A., Mumma, M. J., 2001, ApJ, 549, 629
Laming, J. M., & Hwang, U. 2003, ApJ, 597, 347
Lattimer, J.M. & Prakash, M. 2001, ApJ, 550, 426.
Liedahl, D.A., Wojdowski, P.S., Jimenez-Garate, M.A., & Sako, M. 2001, in ASP Conference Series, Vol. 247, edited by G. Ferland & D. Savin (San Francisco: Astronomical Society of the Pacific), p. 417.
Lisse, C. M., et al. 1996, Science, 274, 205
Lisse, C. M., et al. 1999, Icarus, 141, 316
Lisse, C. M., et al. 2001, Science, 292, 1343
Lucy, L.B. & White, R.L. 1980, ApJ, 241, 300
MacDowall, R. J., et al., 1993, Planet. Space Sci., 41, 1059
Mariska, J.T. 2005, ApJL 620, L67
Matt, G. 1999, ASP Conf. Ser. 157: Annapolis Workshop on Magnetic Cataclysmic Variables, 299.
Mauche, C.W., Liedahl, D.A., & Fournier, K.B. 2001, ApJ, 560, 992
Mauche, C.W., Liedahl, D.A., & Fournier, K.B. 2003, ApJ, 588, L101
McCray, R. 1993, ARA&A, 31, 175
McKibben, R. B., Simpson, J. A., Zhang, M. 1993, Planet Space Sci., 41, 1041
Michael, E., et al. 2003, ApJ, 593, 809
Mitra-Kraev, U., Harra, L.K., Williams, D.R., & Kraev, E. 2005, (astro-ph/0503384)
Nice, D.J., Splaver, E.M., & Stairs, I.H. 2004, IAU Symposium, 218, 49
Orosz, J.A. & Kuulkers, E. 1999, MNRAS, 305, 132
Ozel, F. & Psaltis, D. 2003, ApJ, 482, L31
Paerels, F., Cottam, J., Sako, M., Liedahl, D.A., Brinkman, A.C., van der Meer, R.L.J., Kaastra, J.S., and Predehl, P. 2000, ApJ, 533, L135
Park, S., Zhekov, S. A., Burrows, D. N., Garmire, G. P., & McCray, R. 2004, ApJ, 610, 275
Parker, E. N. 1988, ApJ, 330, 474
Sako, M., Liedahl, D.A., Paerels, F., & Kahn, S.M. 1999, ApJ, 525, 921
Schmitt, J.H.M.M., Robrade, J., Ness, J.-U., Favata, F., & Schrijver, C.J., Aschwanden, M.J., & Title, A.M. 2002, Sol Phy 206, 69
Snow, T.P. & Morton, D.C. 1976, ApJS, 32, 429
Stelzer, B. & Schmitt, J.H.M.M. 2004, A&A, 418, 687
Stevens, I.R., & Kallman, T.R. 1990, ApJ, 365, 321.
Szkody, P., et al. 2002, ApJ, 574, 942.
Terada, Y., et al. 2001, MNRAD, 328, 112.
Thorsett, S.E. & Chakrabarty, D. 1999, ApJ, 512, 288.
Tsujimoto, M., Feigelson, E.D., Grosso, N., Micela, G., Tsuboi, Y., Favata, F., Shang, H., & Kastner, J.H. 2004, (astro-ph/0412608)
Underhill, A.B. 1979, ApJ, 234, 528
Verbunt, F., & van den Heuvel, E.P.J. 1995, in X-Ray Binaries, edited by W.H.G. Lewin, J. van Paradijs, and E.P.J. van den Heuvel (Cambridge University Press)
Villarreal, A.R., & Strohmayer, T.E, 2004, ApJ, 614, L121.
Wang, T.J. & Solanki, S.K. 2004, A&A, 421, L33
Wang, T.J., Solanki, S.K., Curdt, W., Innes, D.E., Dammasch, I.E., & Kliem, B. 2003, A&A, 406, 1105
Wargelin, B.J., et al., 2004, ApJ, 607, 596
Weaver et al., 2002, ApJ, 576, 95
Wegmann, R., Schmidt, H. U., Lisse, C. M., Dennerl, K., Englhauser, J., 1998, Planet. Space Sci., 46, 603
Willingale, R., Bleeker, J. A. M., van der Heyden, K. J., Kaastra, J. S., & Vink, J. 2002, A&A, 381, 1039
Wojdowski, P.S., Liedahl, D.A., Sako, M., Kahn, S.M., & Paerels, F. 2003, ApJ, 582, 959.
Woosley, S. E., & Weaver, T. A. 1995, ApJS, 101, 181

Acronyms

AGN	Active Galactic Nuclei
ASCA	Japanese/U.S. X-ray Mission (1993 - 2000)
ASTRO-E2	Astro-E2 is a joint NASA /JAXA X-ray mission due for launch summer 2005
CV	Cataclysmic Variable
CXRB	Cosmic X-ray Background
DE	Dark Energy
ESA	European Space Agency
FWHM	Full-width Half Max
HETG	Chandra's High Energy Transmission Grating
HEW	Half Energy Width
HMXB	High-Mass X-ray Binary
HPD	Half Power Diameter
HXT	Hard X-ray Telescope on Constellation-X
ICM	Intracluster Medium
IGM	Intergalactic Medium
IMBH	Intermediate-Mass Black Hole
INTEGRAL	Intergalactic Gamma Ray Astrophysics Laboratory (ESA/Russia/NASA)
JAXA	Japanese Aerospace Exploration Agency
LETG	Chandra's Low Energy Transmission Grating
LISA	Laser Interferometer Space Antenna
LSF	Line Spread Function (indicates detector spectral resolution)
PSF	Point Spread Function (indicates telescope angular resolution)
QPO	Quasi-Periodic Oscillation
QCD	Quantum Chromodynamics
RGS	Reflection Grating Spectrometer on XMM
ROSAT	German/U.S. X-ray Observatory Rötgensatellit (1990 - 1999)
RXTE	Rossi X-ray Timing Explorer (1995 - present)
SN	Supernova
SNR	Supernova Remnant
TES	Transition-Edge Sensor Calorimeter
ULX	Ultra-Luminous X-ray Source
XMM	The ESA/NASA X-ray Multi-Mirror Mission (1999 - present)

Constellation - X

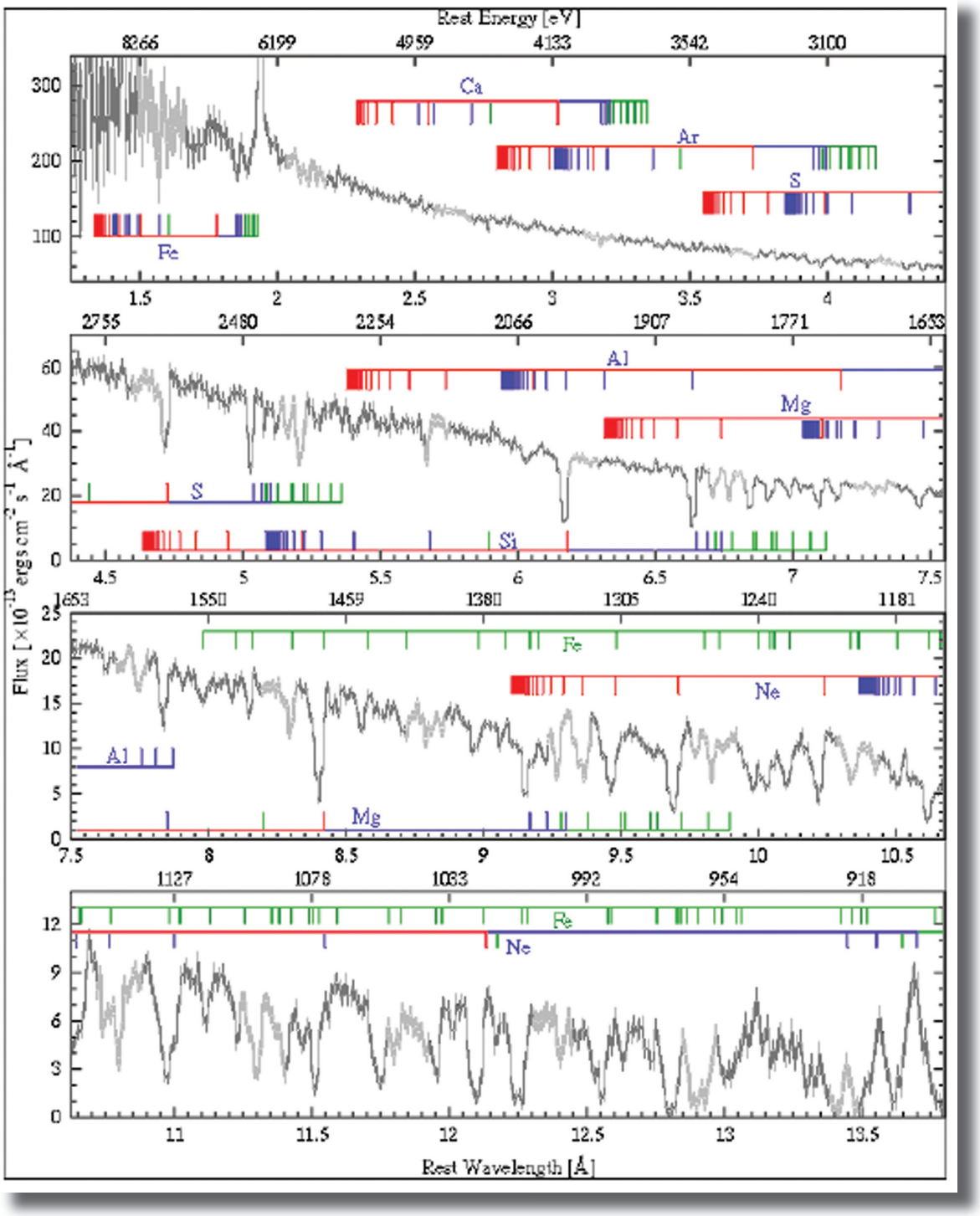

Chandra HETG spectrum of the Seyfert galaxy NGC 3783. This 900 ks observation demonstrates a complex velocity structure that will easily be observed with Constellation-X in 50-100 ks observations. (Kaspi et al. 2002)